



**Universidade de
Aveiro**

2014/2015

Departamento de Química

**João Paulo Duarte
Calixto**

**Concentração de biomarcadores tumorais utilizando
sistemas aquosos bifásicos**

**Concentration of tumor biomarkers using aqueous
biphasic systems**



**João Paulo Duarte
Calixto**

**Concentração de biomarcadores tumorais utilizando
sistemas aquosos bifásicos
Concentration of tumor biomarkers using aqueous
biphasic systems**

Dissertação apresentada à Universidade de Aveiro para cumprimento dos requisitos necessários à obtenção do grau de Mestre em Bioquímica, ramo de Bioquímica Clínica, realizada sob a orientação científica da Doutora Mara Guadalupe Freire Martins, Investigadora Coordenadora do Departamento de Química, CICECO, da Universidade de Aveiro, e co-orientação do Professor Doutor João Manuel da Costa Araújo e Pereira Coutinho, Professor Catedrático do Departamento de Química da Universidade de Aveiro.

*Aos meus pais, o suporte do meu bem-estar e ao meu irmão, a minha
maior referência...*

O júri

presidente

Prof. Dr. Pedro Miguel Dimas Neves Domingues
Professor Auxiliar com Agregação do Departamento de Química da
Universidade de Aveiro

Dr^a. Mara Guadalupe Freire Martins
Investigadora Coordenadora do Departamento de Química, CICECO, da
Universidade de Aveiro

Dr^a. Ana Catarina Almeida Sousa
Estagiária de Pós-Doutoramento do Centro de Investigação em Ciências da
Saúde, CICS-UBI, da Universidade da Beira Interior

Agradecimentos

Gostaria de começar esta fase de agradecimentos por agradecer aos meus orientadores, a Dr^a Mara Freire e o Professor João Coutinho, pelo excelente acompanhamento e pela força, otimismo e entusiasmo que me inculcaram desde o início.

Gostaria igualmente de agradecer ao Path e a todos os seus elementos por tudo o que me ensinaram e por terem feito de mim um de vós. Obrigado, em especial a ti, Matheus Pereira, por tudo o que de fantástico fizeste por mim. Pela paciência, pelo apoio, pelos conselhos ou mesmo por não me dares trabalho às sextas para eu poder sair às quintas à noite, muito obrigado. Se esta tese existe, isso deve-se muito a ti.

Obrigado a todos os professores, não só da Universidade de Aveiro, mas também do Colégio Dr. Luís Pereira da Costa, por todos os conhecimentos que me transmitiram e por serem um suporte base da nossa sociedade que nem sempre é devidamente reconhecido.

Obrigado a todos os colegas da equipa de Bioquímica e da AAUAv e ao meu treinador.

Obrigado a todos os amigos e colegas de curso que comigo trilharam e que fizeram destes 5 anos, os 5 melhores anos da minha vida. Torna-se difícil e injusto individualizar, no entanto, Henrique, Rafa, Daniel, Joel, Diogo, Rafa, Tiago, André, João Pedro, David, Mauro, Diana e Margarida, muito obrigado!

Obrigado a todos os meus familiares, por se preocuparem e serem atenciosos e por me irem perguntando, ao longo destes 5 anos, “Então como está Aveiro?” ou “Isso da Bioquímica serve para o quê?”.

Um agradecimento especial aos meus avós, às minhas tias Isabel e Alcinda Calixto e aos meus primos Alexandre Calixto dos Santos e Diana Calixto Gil.

Por fim, muito obrigado às 3 pessoas mais importantes da minha vida: o meu pai, a minha mãe e o meu irmão. Ao meu pai, Antero Calixto, obrigado por seres o meu maior fã, obrigado por todos os conselhos, por me dares, com a mãe, todas as condições para concluir o meu percurso académico e por fazeres de mim o homem que sou hoje. À minha mãe, Fernanda Calixto, obrigado por todo o carinho e atenção nos momentos mais difíceis, obrigado por me acordares devagarinho ao Domingo quando fico a dormir até à hora do almoço, obrigado pelas remessas semanais de tupperwares e por me teres ensinado todas aquelas pequenas coisas “da casa” que nestes 5 anos me deram muito jeito. Ao meu irmão, Cláudio Calixto, obrigado acima de tudo por seres a minha maior referência e a pessoa mais importante da minha vida. Obrigado por me teres ajudado a crescer, por tudo que fazes por mim e por estares sempre do meu lado. Todos temos um ídolo, alguém que tentamos seguir e para o qual olhamos “para cima” em sinal de respeito e admiração. O meu ídolo, desde a minha infância, és tu!

Neste momento, a dor da nostalgia acaba por me atraiçoar o coração, no entanto, o que de fantástico vivi, e a sensação de que, se tivesse a oportunidade de voltar atrás eu faria exatamente tudo do mesmo modo, acaba por ser superior e dá-me força para continuar.

Obrigado, do fundo do coração, a todos os que comigo percorreram este caminho!

Palavras-chave

Cancro da próstata, marcadores tumorais, antigénio prostático específico, sistemas aquosos bifásicos, técnica de concentração, líquidos iónicos

Resumo

De acordo com dados disponibilizados pela Organização Mundial de Saúde, cerca de 8,2 milhões de pessoas morrem anualmente com cancro. A elevada taxa de mortalidade associada ao cancro resulta da maioria dos pacientes não efetuar exames de rotina e porque a manifestação dos sintomas, na maioria dos casos, acontece quando o paciente já se encontra numa fase avançada da doença. Atualmente, o cancro da próstata representa a segunda maior causa de morte entre indivíduos do sexo masculino em todo o mundo. Tendo em conta que não existe cura para casos avançados de cancro da próstata, a estratégia passa por um diagnóstico precoce que permita aumentar a taxa de sucesso dos tratamentos. O antigénio prostático específico (PSA) é um biomarcador importante do cancro da próstata que pode ser detetado em fluidos biológicos, nomeadamente sangue, urina e sémen. No entanto, os kits comerciais disponíveis utilizam amostras de sangue e os métodos analíticos normalmente utilizados na sua deteção e quantificação requerem pessoal especializado, equipamento específico e um processamento extensivo das amostras, resultando em processos com um elevado custo associado. Assim, o objetivo deste mestrado passou por desenvolver um método simples, eficiente e menos dispendioso para a extração e concentração de PSA a partir de amostras de urina utilizando sistemas aquosos bifásicos (SAB) constituídos por líquidos iónicos.

Numa fase inicial, determinaram-se os diagramas de fases de um conjunto de sistemas aquosos bifásicos constituídos por um sal orgânico e por líquidos iónicos. Em seguida, avaliou-se a capacidade dos mesmos para a extração do PSA. Os resultados obtidos demonstram que, nos sistemas em estudo, o antigénio prostático específico é totalmente extraído para a fase rica em líquido iónico num único passo. Por fim, averiguou-se a aplicabilidade dos SAB estudados para a concentração do PSA a partir de soluções aquosas e de urina. A baixa concentração deste biomarcador na urina (cl clinicamente significativo abaixo de 150 ng/mL) dificulta a sua deteção através de técnicas analíticas convencionais. Os resultados obtidos demonstraram que é possível extrair e concentrar PSA até 250 vezes, numa única etapa, sendo este detetável através de técnicas menos dispendiosas.

keywords

Prostate cancer, cancer biomarkers, prostate specific antigen, aqueous biphasic systems, concentration technique, ionic liquids

abstract

According to the World Health Organization, around 8.2 million people die each year with cancer. Most patients do not perform routine diagnoses and the symptoms, in most situations, occur when the patient is already at an advanced stage of the disease, consequently resulting in a high cancer mortality. Currently, prostate cancer is the second leading cause of death among males worldwide. In Portugal, this is the most diagnosed type of cancer and the third that causes more deaths. Taking into account that there is no cure for advanced stages of prostate cancer, the main strategy comprises an early diagnosis to increase the successful rate of the treatment. The prostate specific antigen (PSA) is an important biomarker of prostate cancer that can be detected in biological fluids, including blood, urine and semen. However, the commercial kits available are addressed for blood samples and the commonly used analytical methods for their detection and quantification requires specialized staff, specific equipment and extensive sample processing, resulting in an expensive process. Thus, the aim of this MSc thesis consisted on the development of a simple, efficient and less expensive method for the extraction and concentration of PSA from urine samples using aqueous biphasic systems (ABS) composed of ionic liquids.

Initially, the phase diagrams of a set of aqueous biphasic systems composed of an organic salt and ionic liquids were determined. Then, their ability to extract PSA was ascertained. The obtained results reveal that in the tested systems the prostate specific antigen is completely extracted to the ionic-liquid-rich phase in a single step. Subsequently, the applicability of the investigated ABS for the concentration of PSA was addressed, either from aqueous solutions or urine samples. The low concentration of this biomarker in urine (clinically significant below 150 ng/mL) usually hinders its detection by conventional analytical techniques. The obtained results showed that it is possible to extract and concentrate PSA, up to 250 times in a single-step, so that it can be identified and quantified using less expensive techniques.

Contents

1.	General introduction.....	1
1.1.	Scopes and objectives	3
1.2.	Cancer update overview.....	5
1.2.1.	Epidemiology	5
1.2.2.	Carcinogenesis: molecular changes and risk factors.....	6
1.3.	Cancer biomarkers	11
1.4.	Prostate cancer	16
1.4.1.	Etiology	16
1.4.2.	Signals, symptoms and diagnosis.....	16
1.5.	Prostate-specific antigen as a prostate cancer biomarker	17
1.5.1.	Prostate cancer screening, stage and grade	18
1.5.2.	Monitoring therapy and disease recurrence	20
1.5.3.	Molecular characteristics	20
1.5.3.1.	Biosynthesis structure	20
1.5.3.2.	Structure and physicochemical properties	21
1.5.3.3.	Physiological role of PSA in prostate and in external tissues.....	22
1.5.3.4.	Molecular derivatives of PSA and their role in diagnosis	23
1.5.3.5.	Stability of total and free PSA	24
1.6.	Analytical methods for the quantification of PSA.....	25
1.7.	Aqueous biphasic systems (ABS) for the extraction and concentration of proteins	28
1.7.1.	Phase diagrams.....	28
1.7.2.	Ionic liquids as phase-forming components of ABS.....	29
2.	Extraction of PSA using phosphonium-based ILs + salt ABS.....	35
2.1.	Introduction.....	36
2.2.	Experimental Section	38
2.2.1.	Chemicals.....	38
2.2.2.	Experimental Procedure	38
2.2.2.1.	Synthesis and characterization of the Good's buffers ionic liquids.....	38
2.2.2.2.	Phase diagrams and tie-lines (TLs).....	39
2.2.2.3.	Partition of PSA	41
2.3.	Results and discussion	42

2.3.1. Characterization of the synthesized ionic liquids	42
2.3.2. Phase Diagrams and Tie-lines	45
2.3.3. Partition of PSA	50
2.4. Conclusions.....	52
3. Concentration of PSA using model IL-based ABS.....	55
3.1. Introduction.....	56
3.2. Experimental section.....	56
3.2.1. Chemicals	56
3.2.2. Experimental procedure	57
3.2.2.1. Lever-arm Rule	57
3.2.2.2. Concentration factors of PSA	57
3.2.2.3. Size-exclusion HPLC (SE-HPLC).....	58
3.3. Results and discussion	58
3.3.1. Concentration factors of PSA.....	58
3.4. Conclusions.....	61
4. Concentration of PSA from human fluids using optimized IL-based ABS.....	64
4.1. Introduction.....	65
4.2. Experimental Section	66
4.2.1. Chemicals	66
4.2.2. Experimental procedure	66
4.2.2.1. Size-exclusion HPLC (SE-HPLC).....	66
4.2.2.2. Sodium dodecyl sulphate polyacrylamide gel electrophoresis (SDS-PAGE) ...	67
4.3. Results and discussion	67
4.3.1. Concentration of PSA from human urine samples.....	67
4.4. Conclusions.....	70
5. Final remarks and future work	73
6. References	76
Appendix A	87
<i>BLItz® Pro system calibration curve</i>	87
Appendix B.....	89
<i>Experimental binodal data</i>	89
Appendix C.....	98
<i>Experimental data for CF</i>	98

List of tables

Table 1.1. Categories of cancer types according to their source (15).	7
Table 1.2. Cancer biomarkers identified in biological fluids or tissues in cancer diagnosis, stage, response to treatment and prognosis (47).	13
Table 1.3. PSA values of reference for men with 40-79 years old in blood (66).	19
Table 1.4. Risk stratification of CaP patients according to PSA levels, Gleason grade and Clinical stage (69).	19
Table 1.5. Comparison of literature methods for the purification/concentration/quantification of PSA isoforms from different human matrices.	26
Table 1.6. Chemical structures of phosphonium-based ionic liquids (114).	31
Table 1.7. Chemical structures of GBs: MES: 2-(N-morpholino)ethanesulfonic acid; TES: 2-[[1,3-dihydroxy-2-(hydroxymethyl)propan-2-yl]amino]ethanesulfonic acid; HEPES: 4-(2-hydroxyethyl)-1-piperazineethanesulfonic acid; CHES: N-cyclohexyl-2-aminoethanesulfonic acid; Tricine: N-2(2-Hydroxy-1,1-bis(hydroxymethyl)ethyl)glycine.	33
Table 2.1. Chemical structures and molecular weight (g/mol) of the synthesized GB-ILs ([P ₄₄₄₄][MES], [P ₄₄₄₄][TES], [P ₄₄₄₄][HEPES], [P ₄₄₄₄][CHES], [P ₄₄₄₄][Tricine]).	44
Table 2.2. Correlation parameters used to describe the experimental binodal data by Eq. 1 and respective standard deviations (σ) and correlation coefficients (R^2).	47
Table 2.3. Data for the tie-lines (TLs) and tie-line lengths (TLLs). Initial mixture compositions are represented as [Salt] _M and [IL] _M , whereas [Salt] _{Salt} and [IL] _{Salt} are the compositions of IL and salt at the IL-rich phase, respectively, and <i>vice-versa</i>	48
Table 2.4. Extraction efficiency of PSA ($EE_{PSA}\%$) at 25° C in the ABS composed of ILs and K ₃ C ₆ H ₅ O ₇	50
Table 3.1. Concentration factors (initial compositions of the mixtures in <i>Appendix C</i>) in the ABS composed of [P ₄₄₄₄][GB] + K ₃ C ₆ H ₅ O ₇ + water. ✓: achieved <i>CF</i> ; ✗: not achieved <i>CF</i>	60
Table 3.2. Concentration factor of 250-fold achieved for PSA at the IL-rich phase for the systems composed of GB-IL + K ₃ C ₆ H ₅ O ₇ + PSA. ✓: achieved <i>CF</i> ; ✗: not achieved <i>CF</i> . .	60

Table B.1.1. Experimental weight fraction data for the binodal curve of the systems composed of [P ₄₄₄₄][GB] (1) + K ₃ C ₆ H ₅ O ₇ (2) at (25 ± 1) °C.....	90
Table B.1.2 Experimental weight fraction data for the binodal curve of the systems composed of [P ₄₄₄₄][GB] (1) + K ₃ C ₆ H ₅ O ₇ (2) at (25 ± 1) °C.....	95
Table C.1.2. Experimental data for CF of the systems composed of [P ₄₄₄₄][GB] + K ₃ C ₆ H ₅ O ₇ + water at (25 ± 1) °C.....	99

List of figures

Figure 1.1. Bars-plot of new cancer cases and deaths of worldwide population in 2012 (numbers in millions of new cancer cases/deaths) (12).....	5
Figure 1.2. Number of new cancer cases in Portuguese population (males) in 2012 (dark-blue), and predictions to 2015 (blue) and 2030 (light-blue). Numbers for the 5 most common types of cancer in Portugal (13).....	6
Figure 1.3. Schematic representation of PSA processing in epithelial cells of the prostate. Adapted from (75).	21
Figure 1.4. 3D representation of PSA using light-assisted molecular immobilization technology (78).....	22
Figure 1.5. Different fPSA precursor forms (bPSA, proPSA and intact unclipped PSA) and PSA complexes (PSA-ACT, PSA-API and PSA-A2M) (5).....	24
Figure 1.6. Phase diagram of an ABS: TCB = binodal curve; C = critical point; TB = tie-line; T = composition of the top phase; B = composition of the bottom phase; X, Y and Z = mixture compositions at the biphasic region. Adapted from (108).	29
Figure 2.1. GB-ILs synthesis. An equimolar excess of the aqueous solution of buffer was added to [P ₄₄₄₄]OH solution (A). The mixture was dried at 50-60 °C under reduced pressure in a <i>Carrousel</i> 6 plus reaction station (B). A mixture of acetonitrile and methanol (1:1, v:v) was added to the viscous liquid and then vigorously stirred at room temperature for 1 h (Fig. 2.1. C). The solvent mixture was evaporated and the GB-IL was dried in vacuum (10 Pa) for 3 days at room temperature (D).....	39
Figure 2.2. Blitz [®] PRO System and Super Streptavidin Biosensors.	41
Figure 2.3. Macroscopic appearance of the synthesized Good's Buffer ionic liquids at 25°C. From the left to the right: [P ₄₄₄₄][MES], [P ₄₄₄₄][TES], [P ₄₄₄₄][CHES], [P ₄₄₄₄][HEPES], [P ₄₄₄₄][Tricine].....	43
Figure 2.4. Phase diagrams for the systems composed of IL + K ₃ C ₆ H ₅ O ₇ + H ₂ O at 25°C and atmospheric pressure (in wt%) with the corresponding binodal data adjusted by Eq. 1: [P ₄₄₄₄][Tricine] (■); [P ₄₄₄₄][HEPES] (▲); [P ₄₄₄₄][TES] (●); [P ₄₄₄₄][MES] (■);[P ₄₄₄₄][CHES] (◆);.....	45
Figure 2.5. Phase diagrams and TLs (■) and adjusted binodal data using Eq. 1 (-), at 25°C and atmospheric pressure, for the ternary systems composed of K ₃ C ₆ H ₅ O ₇ + water +	

[P ₄₄₄₄][MES] (■); [P ₄₄₄₄][CHES] (◆); [P ₄₄₄₄][HEPES] (▲); [P ₄₄₄₄][Tricine] (■); [P ₄₄₄₄][TES] (●).....	49
Figure 2.6 PSA secondary structure (1) and their active site (2) (using the Discovery Studio software).....	51
Figure 3.1. Different compositions along the same TL obtained by applying the lever-arm rule which allow to obtain different <i>CF</i> for the ABS composed of K ₃ C ₆ H ₅ O ₇ + [P ₄₄₄₄][CHES] + water.....	59
Figure 3.2. HPLC spectra of bottom (left) and top (right) phases for the systems composed of GB-IL + K ₃ C ₆ H ₅ O ₇ + water/PSA. A spectrum of pure PSA in water (<i>C</i> = 50 ng/L) is also provided as an insert for terms of comparison.	61
Figure 4.1. ABS composed of [P ₄₄₄₄][CHES] + salt + human urine (150 ng/mL of PSA added). ABS after being vigorously stirred (on the left) and after being centrifuged for 10 min and left in equilibrium for 15 min (on the right).....	68
Figure 4.2. SE-HPLC profile of pure PSA in aqueous solution, human urine and in the top and bottom phases of an ABS composed of [P ₄₄₄₄][CHES] + salt + human urine (150 ng/mL of PSA added).....	69
Figure 4.3. SDS-PAGE analyses. A: Molecular Wweight marker; B: Pure human serum; C: Pure human urine.....	70
Figure A.1. Calibration curve for PSA in aqueous solution.....	88
Figure C.1.3. Experimental data for <i>CF</i> of the systems composed of [P ₄₄₄₄][GB] + K ₃ C ₆ H ₅ O ₇ + water at (25 ± 1) °C.....	100

List of symbols

wt% – weight fraction percentage;

σ – standard deviation;

Abs – absorbance (dimensionless);

M_w – molecular weight ($\text{g}\cdot\text{mol}^{-1}$);

R^2 – correlation coefficient (dimensionless);

α – ratio between the top weight and the total weight of the mixture (dimensionless);

$[IL]$ – concentration of ionic liquid (wt% or $\text{mol}\cdot\text{kg}^{-1}$);

$[IL]_{IL}$ – concentration of ionic liquid in the ionic-liquid-rich phase (wt%);

$[IL]_{\text{Salt}}$ – concentration of ionic liquid in the salt-rich phase (wt%);

$[IL]_{\text{M}}$ – concentration of ionic liquid in the initial mixture (wt%);

$[Salt]$ – concentration of salt (wt% or $\text{mol}\cdot\text{kg}^{-1}$);

$[Salt]_{IL}$ – concentration of salt in the ionic-liquid-rich phase (wt%);

$[Salt]_{\text{Salt}}$ – concentration of salt in the salt-rich phase (wt%);

$[Salt]_{\text{M}}$ – concentration of salt in the initial mixture (wt%);

$[Salt]$ – concentration of salt (wt% or $\text{mol}\cdot\text{kg}^{-1}$);

$EE_{\text{PSA}}\%$ – percentage extraction efficiency of PSA (%);

CF_{PSA} – PSA concentration factor;

w_{IL} – weight of the IL-rich phase;

w_{Salt} – weight of the salt-rich phase.

ACRONYMS

A2M – alpha-2-macroglobulin;
ABS – aqueous biphasic systems;
ACT – alpha-1-antichymotrypsin;
API – alpha-1-protease inhibitor
B – bottom phase;
BPH – benign prostate hyperplasia;
BPSA – benign PSA;
BSA – bovine serum albumin
C – critical point;
CaP – prostate cancer;
CHES – N-cyclohexyl-2-aminoethanesulfonic acid;
CML – chronic myelogenous leukemia;
DNA – deoxyribonucleic acid;
DRE – digital rectal examination;
ELISA – enzyme-linked immunosorbent assay;
ER – endoplasmic reticulum;
FDA – Food and Drug Administration;
fPSA – free PSA;
GBs – Good’s buffers;
HEPES – N-cyclohexyl-2-aminoethanesulfonic acid;
HPLC – High-performance liquid chromatography;
IGF – insulin-like growth factor;
IGFBP – insulin-like growth factor binding protein;
iPSA – intact PSA;
 $K_3C_6H_5O_7$ – potassium citrate;
MES – 2-(N-morpholino)ethanesulfonic acid;
PAP – prostatic acid phosphatase.

pI – isoelectric point;
proPSA – precursor isoforms of PSA;
PSA – prostate specific antigen;
RNA – ribonucleic acid;
ROS – reactive oxygen species;
SPE – solid-phase extraction;
SPR – surface plasmon resonance technology;
T – top phase;
TL – tie-line;
tPSA – total PSA;
TRIFA – immunochemiluminescent;
TRUS – transrectal ultrasound;
TS – tumor suppressor;
[P₄₄₄₄][CHES] – tetrabutylphosphonium 2-(cyclohexylamino)ethanesulfonate;
[P₄₄₄₄][HEPES] – tetrabutylphosphonium 2-[4-(2-hydroxyethyl)piperazin-1-yl]ethanesulfonate;
[P₄₄₄₄][MES] – tetrabutylphosphonium 2-(N-morpholino)ethanesulfonate;
[P₄₄₄₄][TES] – tetrabutylphosphonium 2-[[1,3-dihydroxy-2-(hydroxymethyl)propan-2-yl]amino]ethanesulfonate;
[P₄₄₄₄][Tricine] – tetrabutylphosphonium N-2(2-Hydroxy-1,1-bis(hydroxymethyl)ethyl)glycine.

1. General introduction

1.1. Scopes and objectives

Prostate cancer is the second more common type of cancer, and represents 15% of the cancer-related diseases in males (1). Despite the efforts in the search of new and effective therapies, up to now, none of the known therapies is entirely effective when the diagnosis is carried out at an advanced stage, emphasizing thus the importance of early detection as a powerful way to increase the curative successful rate (2). Prostate cancer is usually identified through biopsy, a procedure that is still known as the diagnostic “gold strand”. However, associated with this procedure, there are several and serious side effects, like febrile urinary tract infection (UTI), urosepsis, bleeding and hematuria. In addition, this procedure is also connected to 15%-20% of false negative results (3). Therefore, it is of crucial importance to find non-invasive diagnostic tools that could replace the commonly used biopsy. The identification and quantification of cancer biomarkers in human serum and urine is a potential alternative and has received a significant attention in the past few years (4). For instance, the identification and quantification of the prostate specific antigen (PSA) is the most widely used assay to detect prostate cancer at earlier stages bypassing unnecessary biopsies and reducing the number of patients where metastatic disease is found (5).

Currently, there are diverse companies (6) that offer several commercial kits for the PSA quantification in blood samples, but some of them require the use of immunoassay-qualified antibodies, specific and expensive equipment and highly skilled technical operators – time-consuming and expensive immunoassays (7,8). Thus, the main objective of this work comprises the development of an alternative technique for the extraction and concentration of PSA from human urine using a liquid-liquid extraction procedure. This procedure should allow the concentration of PSA up to levels capable of being detected by more accessible and less expensive equipment, such as high-performance liquid chromatography (HPLC). To achieve this goal, aqueous biphasic systems (ABS) composed of water, ionic liquids (ILs) and organic salts were investigated. In the past decade, a large effort has been dedicated to IL-based ABS since these systems have demonstrated superior extraction efficiencies and selectivities when compared to the more traditional polymer-based ABS (9). Moreover, moderately toxic imidazolium-based ILs with no buffering capacity have been the most studied class of phase-forming components of IL-based ABS (10). The control of the pH of the aqueous medium is highly

relevant when working with the extraction and concentration of proteins (such as PSA) since they can denature and precipitate, leading therefore to non-accurate results. To overcome these drawbacks, ILs comprising anions derived from Good's buffers, which have shown to have self-buffering characteristics (11), in combination with biodegradable organic salts, were investigated in this work.

This work starts with a brief statistical analysis on the cancer incidence and mortality, followed by a small introduction to carcinogenesis, where the role of mutations, tumor suppressor genes and oncogenes are highlighted with special emphasis on prostate cancer (CaP). The molecular characteristics of PSA (a prostate cancer biomarker) and its derivatives are then presented and reviewed. Further, the common methods for PSA quantification from human fluids, and IL-based ABS as a liquid-liquid extraction technique, are introduced and described. Finally, this work ends with the experimental results achieved using IL-based ABS for the extraction and concentration of PSA from human urine samples and respective discussion. Outstanding complete extractions and concentration factors up to 250-fold were obtained in a single-step, allowing thus the use of HPLC as a less expensive technique for the quantification of PSA levels in human fluids.

1.2. Cancer update overview

1.2.1. Epidemiology

Cancer is the major death cause in the world with an estimated 14.1 million new cases and 8.2 million deaths in 2012 and, according to projections for 2030, the number of new cases will increase 68% (up to 23.6 million) (12). More than 80 billion € are spent each year in USA to deal with cancer healthcare (13). Therefore, more investment in cancer early detection assays and in new therapies in order to increase the lifespan of patients, as well as to decrease medical costs of advanced cases of disease, are urgent requirements. Lung, female breast, bowel and prostate cancers are the most common solid neoplasms (Fig. 1.1.). Portugal has a rate of 246.21 *per* 100,000 individuals which means an incidence of 49,174 cancer new cases *per* year, resulting in an overall number of 25,758 deaths in 2012 (14).

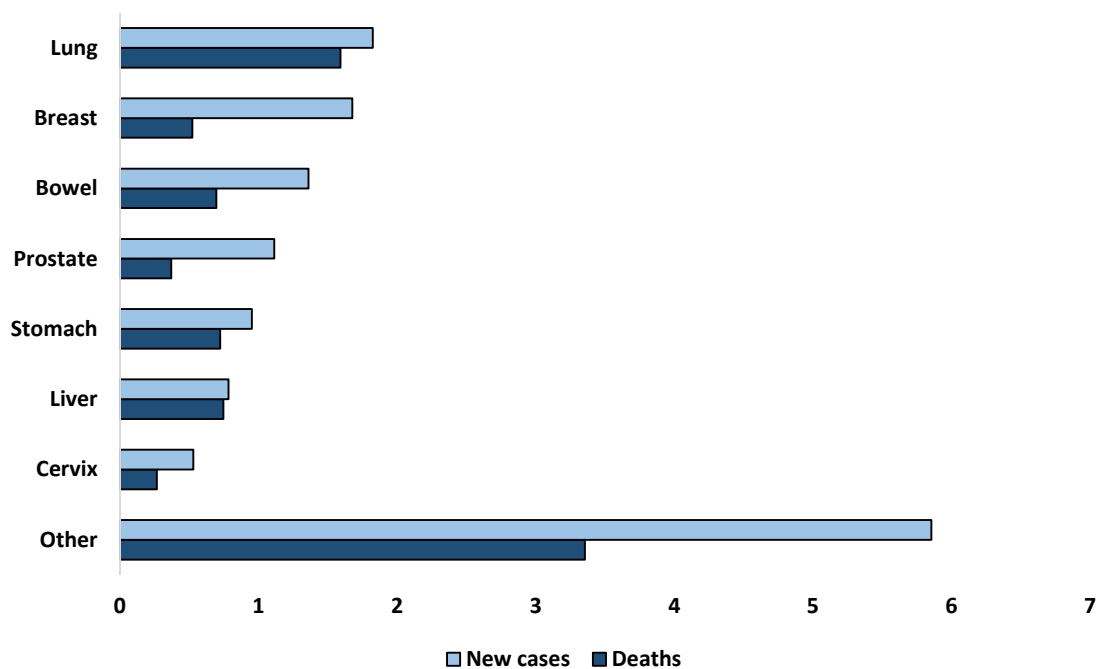


Figure 1.1. Bars-plot of new cancer cases and deaths of worldwide population in 2012 (numbers in millions of new cancer cases/deaths) (12).

Prostate cancer (CaP) is the second most common diagnosed cancer in males with more than 1.11 million new cases worldwide and almost 40% of them – 417,000 – were

diagnosed in Europe, meaning that the CaP incidence is not equally distributed around the world (1). However, CaP mortality is equally distributed around the world (15). Thus, cancer incidence is not equally distributed but mortality is. In Portugal, for instance, CaP is the third most common cancer-related cause of death (1582 deaths) and the most diagnosed cancer (6622 cases). The number of new cases has been increasing in the past few years and there are some alarming reports that predict a rise of more than 30% in new CaP cases to 2030 (Fig. 1.2.) (1,14).

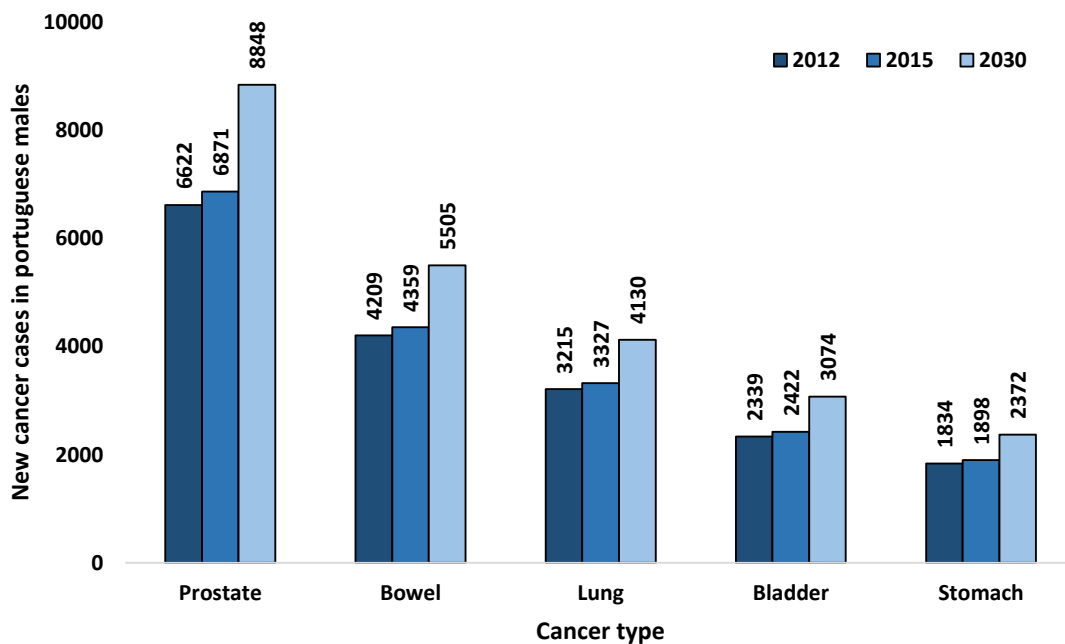


Figure 1.2. Number of new cancer cases in Portuguese population (males) in 2012 (dark-blue), and predictions to 2015 (blue) and 2030 (light-blue). Numbers for the 5 most common types of cancer in Portugal (13).

1.2.2. Carcinogenesis: molecular changes and risk factors

Cancer is the word used to describe a group of diseases in which abnormal cells tend to divide. In this multistep process, cells can suffer severe behavioral and metabolic alterations and ultimately invade distant tissues and form metastases *via* blood and lymphatic systems (16). Cancer types can be divided into 5 categories according to their source (Table 1.1.). These include carcinoma, sarcoma, leukemia, lymphoma, myeloma and central nervous system cancers.

Table 1.1. Categories of cancer types according to their source ((17)15).

Cancer type	Source
Carcinoma	Cancer begins in the skin or in tissues around internal organs. Carcinoma is subdivided into adenocarcinoma (starts in glandular cells), basal cell carcinoma (begins in the lower part of the epidermis), squamous cell carcinoma (begins in squamous cells) and transitional cell carcinoma (occurs mainly in the organs of the urinary system).
Sarcoma	Cancer begins in connective or supportive tissues, like cartilage, fat, bone and blood vessels.
Leukemia	Bone marrow produces a large number of abnormal blood cells that enter into the bloodstream.
Lymphoma	Develops in glands or nodes of the lymphatic system. Lymphomas are classified into Hodgkin lymphoma and non-Hodgkin lymphoma.
Myeloma	Cancer that originates in plasma cells of the bone marrow. The plasma cells produce some of the proteins found in blood.
Mixed types	The type components may be within one category or from different categories, such as adenosquamous carcinoma, mixed mesodermal tumor and teratocarcinoma.

The process by which cells lead to cancer is called carcinogenesis and is a multifactorial process that involves 3 major steps (18). The first step comprises the initiation, in which due to genotypical and phenotypical changes that arise spontaneously or are induced by exposure to a carcinogen, normal cells become more likely to malign evolution. A cell that suffers such changes is called an initiated cell and suffers mutations that induce proliferation but not differentiation. Thereby, the proliferating initiated cells have less time to be repaired by the DNA repair system and the injury becomes permanent and irreversible; so, the cellular genome undergoes mutations that favor the neoplastic development of the affected cells (19). The cellular genes involved in this step are the proto-oncogenes. They are groups of genes that when mutated cause normal cells to become cancerous. However, they are not discarded by evolutionary processes because they have important roles, such as the encoding of proteins that stimulate cellular division, inhibition of cellular differentiation and are involved in signal transduction. Proto-oncogenes have, as usual in all other genes, a regulatory region that regulates the gene expression, and a structural region that encodes the amino acid sequence of a protein.

Mutations in any of these regions can activate a proto-oncogene, creating an oncogene (20). There are several types of known oncogenes, such as RAS, MYC, ERK, TRK or WNT. Another oncogene type is the Bcr-Abl gene, found on the Philadelphia chromosome (21). This oncogene is a known example of an oncogenic chromosomal translocation wherein a piece of chromosome 22 end with the BCR genes broken, and then suffers fusion with a fragment of chromosome 9 that carries the ABL-1 gene, yielding thus the Philadelphia chromosome with the BCR-ABL fused gene. This oncogene is translated into tyrosine kinase receptors that are involved in cell cycle regulation and stimulation of cell division, leading to uncontrolled cell division which can cause chronic myelogenous leukemia (CML) and other types of leukemia (21).

The second step of carcinogenesis is promotion. After initiation, a cell can remain latent for weeks, months or years until and unless it is stimulated to undergo further proliferation, disturbing the cellular balance. Promoter compounds act at this stage only in the activated cells, inducing cell proliferation of susceptible tissues, helping to fix mutations, increasing alterations in genetic expression and causing changes in cellular growth control. This causes the onset of new oncogenes and disruption of the tumor suppressor genes action, leading to neoplastic transformation and development (22,23). Tumor Suppressor (TS) genes are a group of genes that regulate cell proliferation by checking the cell cycle progression, are involved in DNA repair processes preventing the accumulation of mutations in cancer-related genes and stimulate cell death when an injury is detected, and so, they are known as negative growth regulators (24). One of the most studied TS genes is p53, which is a protein encoded by the *TP53* gene and has an important role in cellular and genomic equilibrium – reason for “The guardian of the genome” label. Mutations in this gene were found in at least 50% of human cancers. This TS gene regulates the cells cycle in the G1-S checkpoint, induces cell differentiation and promotes apoptosis. In a normal cell, when DNA damage is detected, p53 binds to DNA and stops the cell cycle. This happens because p21, a protein whose transcription is activated by p53, binds to cdk-cyclin complex inhibiting its kinase activity which causes a delay in G1 checkpoint and enabling the DNA repair mechanisms to act. If DNA is repaired, p53 promotes its differentiation and multiplication. If the cell cannot be repaired, p53 gives information to be eliminated by apoptotic processes. Therefore, when p53 is mutated, it can lose its function causing suppression of apoptosis, promoting cell division and hindering the differentiation of the cells. There are another important types of TS genes, like RB1, APC, BRCA1/2, among others (25).

The last step in carcinogenesis is the progression, a step where pre-neoplastic lesions and/or benign neoplasms turn into malign lesions. Progression is characterized by irreversibility, because once in this condition, cells are compromised into the malign development. The acquired genetic instability causes undifferentiated cells to proliferate faster while the well differentiated and slow growth cells die. There are also some biochemical, metabolic and morphological changes, as well as the appearance of new cell clones with genetic heterogeneity with a high capacity to proliferate and metastasize, which will induce the formation of a tumor mass (26,27).

There are few theories regarding the explanation of how cancer starts and what causes its development; the most widely accepted is the “two hit” hypothesis, based on the mechanisms of retinoblastoma, proposed by Alfred Knudson in 1971 (28). In an initial stage of retinal cancer, retinoblasts do not differentiate into retinal photoreceptors cells and nerve cells, and continue to proliferate forming tumors in retina able to metastasize to other parts of the body. Knudson (28) studied 48 patients with retinoblastoma for 20 years, and tabulated the patient age, family history, gender, and if the tumor occurs in one or in both eyes. With the obtained data and knowing that retinoblastoma is caused by a recessive mutation, the researcher verified that bilateral hereditary retinoblastoma occurred at a younger age while unilateral nonhereditary retinoblastoma is somehow delayed (28). Based on these findings, the researcher concluded that two mutations or “two hits” are required, one in each copy of a TS gene (today called RB1) (28). In hereditary cases, patients get one mutation and need to acquire only one to develop retinoblastoma in a process known as loss of heterozygosity. In what concerns to non-hereditary cases, patients have to acquire 2 mutations during their life to develop this type of cancer, what explains why nonhereditary retinoblastoma is developed latter. This is one of the most accepted theories for cancer-related researches; however, it is not 100% correct because it only takes into account mutations in TS genes (28,29).

Family history seems to be one of the most important factors which can lead to cancer (28). In general, 5-10% of all cancers are hereditary (30). One of the most common syndromes is the hereditary non-polyposis colorectal cancer (HNPCC) or Lynch syndrome. This syndrome is mostly related with endometrial cancer but it is also associated with ovary, stomach, pancreas, kidney and brain cancers. In HNPCC, genes involved in the DNA repair mechanism are mutated leading to cancer development (31).

Aging is another predisposing factor in carcinogenesis. During aging, DNA strand-break occurs in tissues and there is the accumulation of DNA adducts, assumed to

be caused by an imbalance between cellular pro-oxidants and antioxidants. In cellular metabolic processes, free radicals and reactive species of oxygen (ROS) are produced. These cellular antioxidants are accumulated over the years and damage macromolecules and organelle functions due to their high reactivity (32). Inflammation is also an important factor in oncogenesis. With aging, cellular damage increases, and in order to fix this damage, cells tend to produce cytokines, such as the tumor necrosis factor (TNF)- α , interleukin (IL)-1, IL-6, interferon (IF)- γ and C-reactive protein (CRP), resulting in a state known as low-grade chronic inflammation. The rising in cytokines concentration affect angiogenesis what may enhance cell proliferation (33). Finally, epigenetic alterations are also connected to cancer. These are genome modifications during cell division that do not involve changes in the DNA sequence, have a hereditary character, are able to modify gene expression and affect all tissues and cells throughout life (34). DNA methylation at CpG islands is a common epigenetic alteration. CpG islands are short regions of 0.5-4 kb in length rich in CpG and are located in promoter regions of half the genes in mammalian genome, including TS genes (35). Usually, they are un-methylated; yet, in cancer, hypermethylation occurs blocking the action of the genes involved in cells cycle regulation, resulting in their uncontrollable proliferation and cancer development (36). Histone modifications, such as ubiquitylation, methylation, acetylation and phosphorylation are other epigenetic alterations more usual with aging. They affect the chromatin structure leading to deregulated expression of important genes in cancer progression (34).

The human's diet also affects the probability of cancer development. Some studies indicated that a longer and planned low-fat dietary pattern can decrease the probability of developing cancer (37,38). A fiber-rich diet is also associated with a lower risk of colon cancer (39). Excessive consumption of alcohol has been proved to be associated with the development of head, neck, esophageal, liver, breast and colorectal cancers. For instance, ethanol in alcoholic drinks is metabolized to acetaldehyde that damages genetic material and proteins (40). There are still some carcinogenic compounds added to food or produced during its preparation. One of them is acrylamide, present in foods heated above 120 °C, such as potato chips, and that was found to have a positive association with renal cancer (41). Heterocyclic amines (HCs) and polycyclic aromatic hydrocarbons (PAHs), produced when amino acids, sugars and creatinine of the meat are directly exposed to fire, particularly when they are grilled or barbecued, were also found to be mutagenic (43). Moreover, pesticides used in food products can persist in environment and

bioaccumulate in the body, and thus be responsible for some type of cancer, and in particular of pancreatic and breast cancers (42).

People lifestyle is another important factor in the probability of developing cancer. Overexposure to UV sunlight radiations leads to gene mutations, oxidative stress and inflammatory responses. In addition, UV radiations cause direct mutations in the TS gene p53, and are responsible for cancers like melanoma and basal cell carcinoma (44). Cigarette smoke, either as active or as a passive smoker, is also a carcinogenic inductor. More than 7000 chemicals are found in cigarettes and at least 69 of them were identified as carcinogenic, including nitrosamines, radioactive elements and PAHs, and whose action is responsible for the oral, esophageal, lung and pancreatic cancers (45). In summary, a balanced diet combined with frequent physical activities are fundamental in cancer prevention, particularly for breast, endometrial and colon cancers (46).

Viral infections caused by *Helicobacter pylori* and *Human papillomaviruses* can also promote carcinogenesis. *Helicobacter pylori* is a food and water contaminant capable of suppressing immune responses and causing gastric cancer (47). *Human papillomaviruses* are a group of sexually transmitted viruses responsible for the largest majority of cervical, vulvar and vaginal cancers (48).

1.3. Cancer biomarkers

One of the most revolutionary advances in oncologic diagnoses and related therapies was the detection and role of cancer biomarkers. According to the National Cancer Institute, a biomarker is a “biological molecule found in blood, other body fluids or tissues that is a sign of a normal or abnormal process, or of a condition or disease” and “may be to see how well the body responds to a treatment for a disease or condition” (49). Biomarkers can be produced by cancer cells or produced by the human body in response to cancer (Table 1.2.). Usually, most biomarkers are proteins but, more recently, additional biomarkers such as DNA, metabolites or RNA transcripts have been identified (4).

The “ideal” tumorous biomarker does not exist. In fact, it is difficult to find a 100% reliable biomarker especially in early detection and diagnosis. Their lack of specificity, and the fact that some markers are normally produced by the body and their action as cancer biomarkers is associated to concentration levels in body fluids, leads to some controversy in what regards the cut-off values established for biomarkers as an indication of cancer (50). Thus, an ideal biomarker, should be easy to identify in recurrent

screenings, should be able to diagnosis cancer in an early-stage, and should allow the evaluation of the prognosis status. Moreover, their identification and quantification should be consistent and accurate, and by non-invasive, cheap, and easily accessible methods (4,51). In general, the PSA quantification by blood tests is still the most reliable screening of prostate cancer (5).

Table 1.2. Cancer biomarkers identified in biological fluids or tissues in cancer diagnosis, stage, response to treatment and prognosis (51).

Tumorous biomarker	Biological fluids or tissues	Cancer type	Utility
Alpha-Fetoprotein (AFP)	Blood	Liver, germ cells tumors	Liver cancer diagnosis and response to treatment; Stage, prognosis and response of germ cell tumors.
Beta-2-microglobulina (B2M)	Blood, urine or cerebrospinal fluid	Multiple myeloma, chronic lymphocytic leukemia	Prognosis and to follow the individual response to treatment.
Beta-human chorionic gonadotrofin (Beta-hCG)	Urine or blood	Choriocarcinoma, testicular cancer	Identification of stage, prognosis, and response to treatment.
BCR-ABL fusion gene	Blood and/or bone marrow	Chronic myeloid leukemia	Diagnosis and to monitor the disease status.
Bladder tumor antigen (BTA)	Urine	Bladder	Confirm diagnosis; used with NMP22 to test cancer recurrence.

CA15-3/CA27.29	Blood	Breast cancer	To assess therapy results and disease recurrence.
CA19-9	Blood	Pancreas, gallbladder, bile duct, stomach	To assess therapy results.
CA-125	Blood	Ovaries	Diagnosis, assessment of response to treatment, and evaluation of recurrence.
Calcitonin	Blood	Medullary thyroid	Diagnosis, assessment of response to treatment, and evaluation of recurrence.
Carcinoembryonic antigen (CEA)	Blood	Colorectal cancer and breast cancer	To check if cancer has spread; Assessment of response to treatment and evaluation of recurrence.
CD20	Blood	Non-Hodgkin lymphoma	To check if a targeted therapy is appropriate.
Chromogranin A (CgA)	Blood	Neuroendocrine tumors	Diagnosis, assessment of response to treatment, and evaluation of recurrence.
Cytokeratin fragments 21-1	Blood	Lung	Evaluation of recurrence.

Immunoglobulins	Blood and urine	Multiple myeloma and Waldenström macroglobulinemia	Diagnosis, assessment of response to treatment, and evaluation of recurrence.
Lactate dehydrogenase	Blood	Germ cell tumors	To assess the cancer stage, prognosis, and response to treatment.
Prostate-specific antigen (PSA)	Blood and urine	Prostate	Diagnosis, assessment of response to treatment, and evaluation of recurrence.
Prostatic acid phosphatase (PAP)	Blood	Prostate, lung, multiple myeloma	Diagnosis.

1.4. Prostate cancer

1.4.1. Etiology

Prostate cancer (CaP) is one of the most common males' cancers in the world (1). The vast majority of prostatic tumors are adenocarcinomas with origin in prostatic epithelium. CaP is a multifactorial disease, where there is a relation between aging and environmental, physiological and molecular factors. Advanced age and its associated oxidative stress, low grade-chronical inflammation and epigenetic alterations are the most significant risk factors with an important role in tumor initiation (52). Around 60% of tumors are diagnosed in men with more than 65 years old, and 97% in men with more than 50 years old (1). Exposure to UV radiation, diet, alcohol consumption, family history, ethnicity and hormones are additional factors involved in the development of CaP. African or American men with more than 65 years and with a first-line familiar who had this type of cancer are those with a higher risk in CaP development (52).

In what concerns the molecular changes, some important mechanisms should be highlighted. The Wnt signaling pathway is a major signaling pathway involved in invasiveness of prostate tumor cells. Her-2/neu (ERBB2) is a proto-oncogene involved in, among others, prostate cancer. When active it is important in the differentiation and cells growth of tumor wherein high levels of Her-2/neu are related with metastatic prostate cancer. Phosphoinositide-3 Kinase/AKT (PI3K) is a mediator of several oncogenic signaling pathways and it is activated by receptor tyrosine kinases yielding secondary messengers promoters of cellular proliferation and survival. Due to somatic mutations, PI3K can be hyperactivated promoting the prostate cancer progression (53). Nowadays, there are no effective therapies for CaP if the tumor already spread the limits of the organ. Therefore, efforts and investments in the CaP early detection are critical requirements to increase the curative successful rate (14).

1.4.2. Signals, symptoms and diagnosis

Prostate cancer, as many other cancer types, can be effectively treated with surgery and radiation if detected at an early stage. However, a relevant percentage of patients is only diagnosed after demonstrating symptoms like haematuria, urinary obstruction, polyuria, among others. In more severe cases, when the tumor reaches the lymph nodes or bones, oedema and pain are major symptoms (54). At this stage, the treatments typically used are no longer efficient and the 5-year relative survival rate

decreases (2). This fact puts on evidence the screening importance attempting an early detection of CaP and the need to perform diagnostic tests even in the absence of signals and symptoms of the disease, which is in fact the biggest challenge in CaP diagnosis.

Digital rectal examination (DRE), measurement of the serum total PSA and transrectal ultrasound (TRUS) guided biopsies are the usual methods to detect CaP. If DRE and PSA as initial tests indicate the presence of the disease, TRUS guided biopsy is further carried out to confirm the diagnosis. Despite being widely used, these tests display however some disadvantages. The PSA cut-off test is not consensual because a serum PSA concentration above the threshold limit is not necessarily a result of CaP. Recent ejaculations, benign prostate hyperplasia (BPH) and urinary or prostatic infections can also increase PSA concentration. So, in the case of such over-diagnostics, unnecessary treatments, including prostatectomy and radiation therapy, will be conducted. DRE is a qualitative test and it is not possible to reach/evaluate the entire prostatic gland, especially in small tumors that have not reached yet the prostatic capsule. Finally, the TRUS guided biopsy is an invasive technique and does not allow distinguishing between CaP and BPH. Furthermore, there is a significant risk of infection and related consequences (fever, pain, hematuria and sepsis) (50,55).

1.5. Prostate-specific antigen as a prostate cancer biomarker

The first references to prostate cancer date from 1649 when Riolan described the enlargement of prostate as a clinical manifestation of a possible tumor and related it with the bladder obstruction (56). At this time, the diagnosis was done based only on the family history and physical examination (57). Only in 1938, PAP (prostatic acid phosphatase), the first prostate tumor biomarker, was proposed by Gutman (58). However, despite being one enzyme secreted by columnar epithelium secretory cells, it can be produced by other organs, blood components and several non-prostatic malignancies (Table 1.2.). Therefore, it is a non-specific biomarker. In addition, its concentration only significantly rises when the adenocarcinoma of prostate is metastasized, what makes of PAP an useless biomarker in CaP early detection (59,60).

Between 1960 and 1970, several researches were dedicated to the search of tumor specific antigens that could be useful in clinical diagnosis, with special focus in oncology (57). In 1960, Rubin Flocks reported some features of prostate antigens (61). The researcher showed that antibodies created against human prostate tissue were species- and tissues-specific; the antigens in benign and malignant tissue were similar and no specific

antigens could be isolated (62). In 1966, Mitsuwo Hara characterized a protein, “gamma-seminoprotein” (63), and in 1970, Tien Shun Li and Carl Beling reported some antigens in human semen (64). It is believed that both discoveries were related with PSA; nonetheless, the real “discovery” of PSA is attributed to Ming C. Wang and co-workers when they purified and characterized PSA from prostatic tissue (65). The research group revealed that PSA is only produced by prostatic tissue and is present in BPH and CaP (65). Once discovered its potential, the applications and use of PSA have been amplified. PSA was approved in 1987 by the Food and Drug Administration (FDA) to monitor the disease status in patients with prostate cancer (66). Latter, in 1994, the same organization approved the PSA blood test as an easy and inexpensive screening tool to be used in association with DRE to detect prostate cancer (67). A serum PSA measurement of ≥ 4.0 ng/mL is considered as a clinically relevant value where 25% of patients with values above this cut-off value had CaP (57), while urinary PSA has a cut-off value of 150 ng/mL (68). This cut-off value in urine demonstrated an impressive sensitivity of 92.5% to CaP diagnosis; however, due to the small number of cases analyzed, more studies have to be conducted to corroborate these results (69). The analysis of PSA in urine samples is also an important tool in distinguish amongst CaP and BPH, particularly when serum PSA is between 2.5 ng/mL and 10 ng/mL (68).

1.5.1. Prostate cancer screening, stage and grade

The PSA test is believed to be the best approach in the CaP early detection and probably the most used cancer blood test in medicine. A PSA value of ≥ 4.0 ng/mL in serum has been defined as abnormal and can indicate the presence of a prostatic tumor (70). FDA recommends an annual screening of CaP for men with 50 or more years old, and in African American men with more than 40 years old because ethnicity is a relevant factor. More than in other cancer types, age is a significant factor that influences the CaP development and PSA baseline values. Thus, urologists have to adjust the PSA cut-off levels according to age. Table 1.3. presents the reference PSA values in blood for men with 40-79 years old (1,71).

Table 1.3. PSA values of reference for men with 40-79 years old in blood (66).

Age / (years old)	Reference Values / (ng/mL)
40 - 49	0 - 2.5
50 - 59	0 - 3.5
60 - 69	0 - 4.5
70 - 79	0 - 6.5

Values of PSA between 4.0 and 10.0 ng/mL in blood are considered suspicious and the test needs to be repeated. Also the patient needs to be supervised to check whether these values continue to rise, and if DRE also suggests the presence of a tumor, a TRUS guided biopsy has to be done to confirm diagnosis. For values above 10 ng/mL the test is repeated after several days for confirmation because there are some factors that can cause fluctuations in PSA concentrations, and a TRUS guided biopsy has to be carried out because for these values a patient already has a chance of 67% of CaP (72).

The knowledge of the PSA levels also allows to evaluate the grade of the prostatic tumor: the higher the PSA levels, the more advanced is the disease and the larger is the tumor (70). PSA levels when combined with the Gleason sum score and the clinical stage can be used as predictors of the patient prognosis (Table 1.4.).

The Gleason classification is a system used in the evaluation of men with CaP prognosis. This classification is made according to histological and cellular characteristics of the tumor and is the sum of histological patterns (from 1-well differentiated- to 5- poorly differentiated) from the two predominant cellular types in tumor giving a score that can vary from 2 to 10. Scores from 0-6 have a good prognosis, 7 have moderated prognosis and scores between 8 and 10 correspond to undifferentiated tumor and the ones with worst prognosis (73). In what concerns the clinical stage, this is done to primarily evaluate the physical characteristics of the tumor and varies from T0 (no evidence of tumor) to T4 (tumor has invaded nearby tissues).

Table 1.4. Risk stratification of CaP patients according to PSA levels, Gleason grade and Clinical stage (69).

Risk	PSA levels / (ng/mL)	Gleason grade	Clinical stage
Low	< 10 ng/mL	≤ 6	T1-T2a
Intermediate	10 - 20 ng/mL	7	T2b-T2c
High	> 20 ng/mL	8 - 10	T3-T4

1.5.2. Monitoring therapy and disease recurrence

The risk stratification according to PSA levels is extremely important in the identification of CaP patients. For suspicious PSA levels, the first action consists on an active surveillance. 3-monthly PSA measurements and a re-biopsy should be done at 1 year, and whether clinical manifestations continue to suggest the presence of a tumor, new clinical actions should be implemented. External beam radiotherapy (EBRT) is often performed, but radical prostatectomy is the most common procedure when PSA levels suggest that the tumor is only localized within the prostate (74).

After radical prostatectomy, the PSA blood test is also important to check whether treatment was successful or whether there are signals of disease recurrence. After a few weeks, PSA values should decrease to undetectable concentrations (half time PSA in serum is approximately 2.2-3.2 days (75)) due to the removal of prostate. If the PSA concentration increases, there are evidences that the prostate was not totally removed or that the biomarker is being produced by metastases of the original tumor (74).

The PSA blood test has been extremely useful in early diagnosis of CaP leading to a significant increase of tumors detection at local stages, thus resulting in a decline of the mortality rate. However, there are some drawbacks associated to the PSA blood test. PSA can also be produced by other types of tumors, by prostate enlargement and inflammation or even by recent sexual activity leading to false positive results and unnecessary surgeries (50,55). In order to overcome these drawbacks, new tests with PSA have been developed to increase the diagnostic accuracy, including PSA density, free total PSA ratio and other molecular forms, such as free PSA, proPSA and BPSA (5).

1.5.3. Molecular characteristics

PSA is a serine protease which is part of kallikrein related peptidases (KLKs). KLKs are the largest cluster of peptidases in human genome and are located in a locus of chromosome 19q13.3-13.4 being responsible for the expression of 15 homologous serine proteases with an important role in several biological processes, such as reproduction, inflammation blood clotting and cancer. PSA is encoded by one of these genes, the KLK3 gene, whose expression is regulated by androgens (76).

1.5.3.1. Biosynthesis structure

PSA transcription and biosynthesis occur mainly in epithelial cells and periurethral glands in a process regulated by androgens. The KLK3 gene transcription

and translation yield an inactive proenzyme (pre-pro-PSA) with 261 residues. 17 of these are an amino acid leader sequence that is cleaved and works as a signal that directs pre-pro-PSA to the membrane on endoplasmic reticulum (ER). In ER, the originated pro-PSA (244 residues) has also a pro-peptide with 7 amino acids that is cleaved in N-terminals between the arginine at position 7 and isoleucine at position 8 in a process of zymogen activation that can be autocatalytic or catalyzed by trypsin like-peptidases (76). PSA is its active form (237 residues) and has 5 intrachain disulfide bounds, a single asparagine-linked oligosaccharide, a weight of 28-33 kDa, and is secreted into semen, being the most abundant protein in seminal fluid with a concentration between 0.5 and 2.0 mg/mL (Fig. 1.3.) (77). Once active, PSA can diffuse into circulation and be inactivated by the binding of protease inhibitors or by divalent inhibitors, particularly zinc. However, PSA can also become inactive due to proteolytic inactivation of the carboxy-terminals of the amino acid residues Lysine (Lys) 145 and/or Lys 182 and circulates in an unbounded state known as free PSA f(PSA) (78).

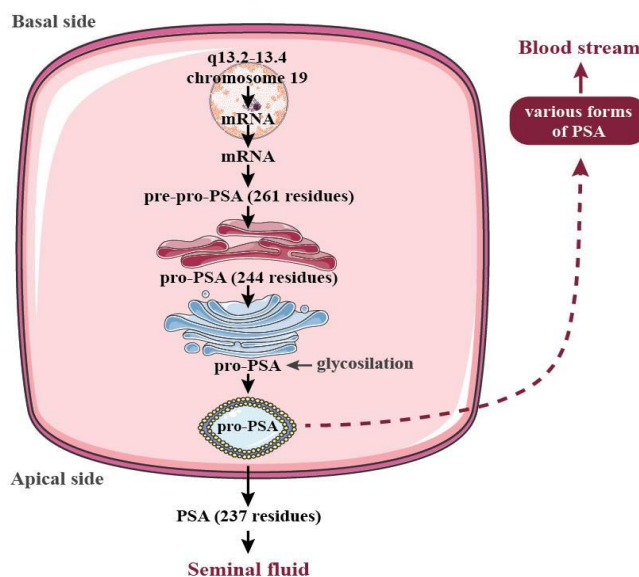


Figure 1.3. Schematic representation of PSA processing in epithelial cells of the prostate. Adapted from (75).

1.5.3.2. Structure and physicochemical properties

PSA is a serine protease glycoprotein with 28-33 kDa. PSA consists of a single polypeptide with 237 amino acids and a single N-linked sugar moiety at asparagine (Asn) 61 with two fucose linkages in the inner most of N-acetylglucosamine (GlcNAc) (79). PSA also has in its mature form a single carbohydrate unit at Asn45 with 5 disulfide

bonds which increases the total mass in 2-3 kDa. It was demonstrated that 92% of PSA is composed of peptides and 8% of carbohydrates, whose 4.84% is hexose, 2.87% is hexosamine and 0.25% is sialic acid (80). The protein consists of two 6-strand antiparallel β -barrels and three α -helices as depicted in Fig. 1.4..



Figure 1.4. 3D representation of PSA using light-assisted molecular immobilization technology (78).

The catalytic site (Serine (Ser) 195, Histidine (His) 57, and Aspartate (Asp) 102) is conserved and located in a cleft between two β -barrels. The sequence also contains the GWG motif, which is a typical pattern present in many proteins with proteolytic activity and the presence of the His-Asp-Ser triad and a catalytic domain similar to KLKs make it a serine protease. The GWG motif contains a Trp located in the β -barrel nearby the disulphide bond Cysteine (Cys)157-Cys 22 (81).

PSA has 5 isoenzymes, one with 5 antibody binding sites and an isoelectric point ranging between 6.7-7.2 (81). Trauma, stress or a tumor can rise the PSA serum levels but they are usually below 0.1 ng/L, depending on its production, distribution and elimination. fPSA forms are cleared from blood primarily in kidneys (half time of 12 hours). Complexed forms of PSA take more time to be eliminated (2.2-3.2 days) because they are larger and cannot be subjected to renal clearance (78).

1.5.3.3. Physiological role of PSA in prostate and in external tissues

PSA is a chymotrypsin-like protease with some properties that differentiate PSA from chymotrypsin and other serine proteases. The physiological function of PSA consists on liquefying seminal fluid after ejaculation in order to facilitate the sperm

transport in the vagina. Seminal fluid has gelified vesicles in coagulum shape and they are composed of seminogelins (SEMG1 and SEMG2), fibronectin, laminin and gelatin which are proteolytic degraded to liquefy sperm in a zinc-mediated process. In prostate, Zn^{2+} concentrations are high and the pH is alkaline, and the major role of zinc ions consists on inhibiting the proteolytic effect of PSA (78).

Typically, PSA biological effects are only confined to the interior of prostate glands where is predominantly in an active form. In blood, PSA is an intact and non-catalytic form due to internal cleavages or is covalently attached to α 1-antichymotrypsin (ACT) in levels from < 0.1 to 10^4 ng/mL. Levels above 10^2 ng/mL are found essentially in men with advanced prostate cancer (82). In CaP, the layer of basal cells and the basement membrane that surrounds prostate glands is disrupted and PSA can reach bloodstream and can influence neoplastic growth and metastases. PSA in bloodstream cleaves the insulin-like growth factor binding protein-3 (IGFBP-3), one of the major serum binding proteins for insulin-like growth factor-1 (IGF-1). IGF-1 is a risk factor for CaP and IGFBP-3 cleavages increases the IGF-1 availability increasing the proliferative effect of tumor cells (83). As mentioned, it has the capacity to cleave extracellular matrix glycoproteins, such as laminin and fibronectin, and also the urokinase-type plasminogen activator, that are involved in tumor invasion and metastases. Other studies suggested that PSA has an antiangiogenic effect and mitogen activity for osteoblasts transforming the growth factor-beta by proteolytic modulation of osteoblasts surface receptors (78).

1.5.3.4. Molecular derivatives of PSA and their role in diagnosis

Contrarily to initial findings, where PSA was considered a protein composed of 237 amino acids, it is now known that serum PSA can occur in two forms: (i) in a “complexed form” with protease inhibitors; or (ii) in a free unbounded form (fPSA), and as shown in Fig. 5. 65%-95% of PSA occurs linked to a protease inhibitor, ACT, in a PSA-ACT complex that is higher in CaP patients probably because of the loss of the prostate integrity (5,84).

In respect to fPSA, there are 3 distinct forms of inactive PSA. One of them, benign PSA (bPSA), is a clipped subform with 2 internal peptide bond cleavages at Lys 182 and Lys 145 and is associated with the transition zone of patients with nodular BPH (85). The second subform, inactive PSA, is “intact”, unclipped PSA (iPSA), that is similar to native PSA but with some structural changes that make it inactive. The third PSA form is proPSA (pPSA). pPSA comprises a 7 amino acid N-terminal pro leader peptide, [-7]

proPSA, that can be cleaved to form enzymatically active PSA. [-7]proPSA can also be truncated by proteolytic cleavage to [-4]proPSA, [-5]proPSA and [-2]proPSA. [-2]proPSA is of particular interest because it is not cleaved further and it accumulates in cancer tissues so it can have a diagnostic utility especially in the 2.5-4 ng/mL range (5). [-2]proPSA is also important in the prediction of CaP aggressiveness because it is a parameter of prostate health index, phi ($phi = \frac{[-2]proPSA}{fPSA} \times \sqrt{PSA}$), which is three times more specific than PSA (86).

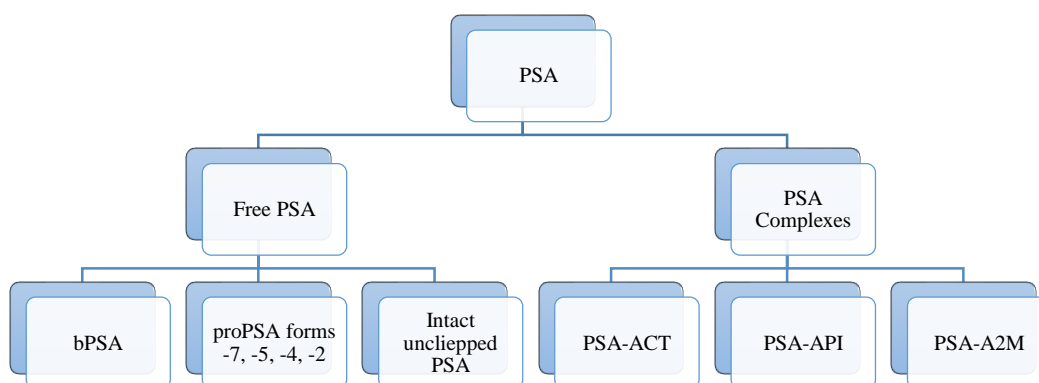


Figure 1.5. Different fPSA precursor forms (bPSA, proPSA and intact unclipped PSA) and PSA complexes (PSA-ACT, PSA-API and PSA-A2M) (5).

Some efforts have been done to refine and to improve the measurements of PSA levels aiming at gathering a more accurate diagnosis. The fPSA to tPSA ratio, usually known as %fPSA, has shown clinical relevance, and with a better performance of PSA and tPSA while differentiating between CaP and BPH when PSA values are in the grey zone (4-10 ng/mL) and DRE results are negative (82,87).

1.5.3.5. Stability of total and free PSA

The stability of PSA, important in clinical tests, is influenced by pH and temperature, particularly for fPSA isoforms. Biological samples containing PSA should be stored at 4°C and analyzed within 8 hours after collection or at -70°C and at pH of 5.5 for latter analysis. At these conditions, PSA can be stored for 9 months with only 5% loss (88). tPSa is more stable and studies have shown that it can be stored at 4°C for a week, at -20°C in a domestic freezer for a month and even at -80°C for 7 years (89,90).

1.6. Analytical methods for the quantification of PSA

Since the PSA discovery and purification by Ming C. Wang in 1979 (65) and after the knowledge of the PSA importance in the CaP early detection, diagnosis and monitoring, several tests to extract, concentrate and quantify PSA, fPSA, PSA-ACT and tPSA were developed and are now commercially available (7). The PSA purification/fractionation method with ammonium sulfate is usually followed by other separation methods, such as gel-filtration chromatography, affinity chromatography, high performance liquid chromatography (HPLC) and polyacrylamide gel electrophoresis (91). However, for clinical purposes, immunoassays are recommended (by FDA). These immunoassays require anti-PSA monoclonal antibodies that will specifically bound to PSA (91). There are various kinds of PSA immunoassays although the most widely used are the enzyme-linked immunosorbent assay (ELISA) (7), time-resolved immunofluorometric assay (TRIFA) (92), fluorescence microscopy (93), surface plasmon resonance technology (SPR) (94), and immunochromatography (95). Table 1.5. represents a review of literature of the immunoassays and column chromatography methods used for the extraction and quantification of different PSA isoforms.

Albeit these methods have some benefits and lead to high purification factors they still present major disadvantages. In particular, specific and highly expensive material and equipment are required, as well as highly qualified and trained technicians. Moreover, they are usually time-consuming. In fluorescence and electrochemical-based methods, the analyte to be quantified has to be dyed in order to amplify the respective signal and the sample can be lost during these preparation steps. In addition, the prolonged exposure of the fluorescence dye to excitation light sources can cause photo bleaching and quenching of signals leading to false negative results (96). ELISA is an expensive technique, because of the cost of antibodies required. It also has low reproducibility and the requirement of signal amplification using a biochemical reaction (96). Thus, it is clear that it is necessary a new method, more economically viable and simpler to concentrate and quantify PSA, and where aqueous biphasic systems (ABS) fit.

Table 1.5. Comparison of literature methods for the purification/concentration/quantification of PSA isoforms from different human matrices.

Purification/Concentration method	PSA Isoform	Matrix	PSA recovery / (%)	Ref.
Immunoassay				
Sandwich immunochromatography technology	tPSA	Blood	104.5	(95)
ELISA	tPSA	Serum	99.5	(7)
Sensitive rapid tandem bioluminescent enzyme immunoassay (BLIA)	PSA/ACT	Serum	85.6	(96)
Indirect Immunosorption	fPSA PSA/ACT	Serum	60	(97)
Imunofluometric assays (TRIFA)	fPSA	Serum	47.5	(92)
Column chromatography				
Thiophilic gel	fPSA	Seminal plasma	96	(98)
Ultrogel ACA44 column	fPSA	Serum	96	(99)
Column of immobilized monoclonal antibodies (commercial antibody fragment Vivapure anti-HSA kit)	free PSA PSA/ACT	Serum	95	(6)

Chip EIA	tpsa	Serum	88.9	(8)
Thiophilic gel	TPSA	Prostate tissue	87	(100)
Mixed polyclonal antibody and protein G column	fPSA; PSA/ACT	Serum	70	(6)
Affinity chromatography size-exclusion and ion exchange chromatography, anion-exchange chromatography	isoforms of PSA	Seminal plasma	55	(101)
Ammonium sulfate precipitation				
hydrophobic interaction chromatography, gel filtration and anion-exchange chromatography	isoforms of PSA	Seminal plasma	30	(102)
PSA microarray ASSAY	tpsa	Female plasma	30	(103)
Cibacron blue affinity-based depletion	fPSA; PSA/ACT	Serum	5	(6)

1.7. Aqueous biphasic systems (ABS) for the extraction and concentration of proteins

Aqueous biphasic systems (ABS) were discovered when agar and gelatin were mixed in water and two macroscopic and separated aqueous liquid phases were formed (104). However, the potential application of ABS to the extraction/separation of biomolecules, and as an alternative to traditional liquid-liquid extraction systems which use volatile and hazardous organic solvents, was only described by Albertson in 1955 (105). ABS, when compared to traditional liquid-liquid extraction techniques, are faster, more economic and allow the scale-up (106). In general, in an ABS, two aqueous solutions of structurally different compounds are separated into two coexisting phases above a given concentration, and where one of the aqueous phases will be enriched in one of the solutes and the other in the second one. ABS can be composed of polymers and salts and can be classified in polymer/polymer-, polymer/salt- and salt/salt-based systems (9). ABS have a high water content (up to 70-90%) being thus a biocompatible media for biologically active products.

ABS have already been used in the extraction and purification of cells, viruses, organelles, nucleic acids, lipids, amino acids, proteins, antibodies and enzymes (9,107). The extraction of proteins using ABS is governed by a complex phenomenon because inherent properties, such as the protein isoelectric point, surface hydrophobicity, molar mass, ionic strength, among others, influence the protein preferential partitioning. Short-range (van der Waals) and long-range molecular interactions between the biomolecule and the surrounding environment have been described as the major forces ruling the partitioning behavior among the coexisting phases (9). Kragl and co-workers (108) studied the phenomena governing the activity and extraction of proteins in ionic liquid media and the efficiency of extraction for myoglobin, trypsin, lysozyme and bovine serum albumin (BSA) under different conditions. There are several other important studies showing the potential of ABS for the extraction and purification of *Candida antarctica* lipase A (109), *Thermomyces lanuginosus* lipase (110), myoglobin and ovalbumin (111), among others.

1.7.1. Phase diagrams

ABS are ternary systems mainly composed of water and two other solutes. The respective phase diagrams are usually depicted in an orthogonal representation where the

water concentration is omitted and as depicted in Fig. 1.6. Each ABS has a characteristic phase diagram describing the conditions at which the biphasic mixture is formed and at which ternary compositions the extractions can be performed. Thus, the phase diagrams, under defined pH and temperature conditions, are useful to know the necessary concentrations of the phase-forming components required to form a two-phase system, and to know the compositions of the coexisting phases and volume or weight ratio of the phases. ABS are characterized by a binodal curve that represents the separation between the miscible and immiscible regions. The biphasic region is above the binodal curve and the monophasic region is below it (Fig. 1.6.) (9). The tie-line (TL) for a given mixture denotes the composition of the coexisting phases. Figure 1.6. shows an example of a ternary phase diagram of an ABS, and where the binodal curve, TCB, and three mixture compositions at the biphasic region, X, Y and Z, are depicted. The mixtures X, Y and Z are along the same tie-line (TL) meaning that all the initial mixtures will present the same top phase equilibrium composition (T_{IL} T_{Salt}) and the same bottom phase composition (B_{IL} B_{Salt}).

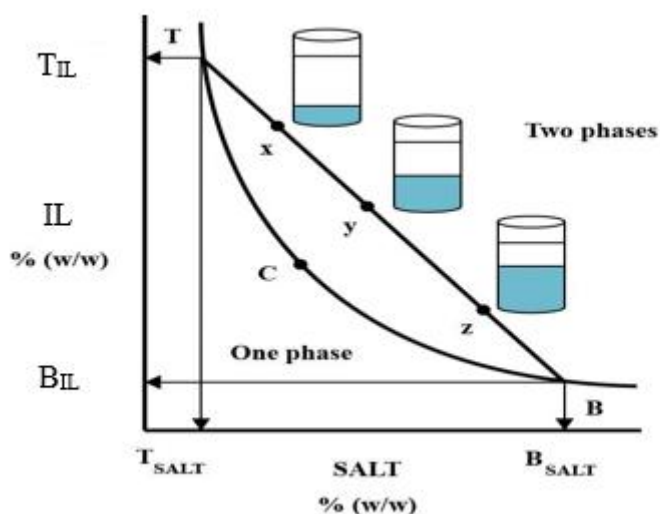


Figure 1.6. Phase diagram of an ABS: TCB = binodal curve; C = critical point; TB = tie-line; T = composition of the top phase; B = composition of the bottom phase; X, Y and Z = mixture compositions at the biphasic region. Adapted from (108).

1.7.2. Ionic liquids as phase-forming components of ABS

The first reported ionic liquid (IL) was synthesized by Paul Walden - ethylammonium nitrate, $(C_2H_5)NH_3NO_3$ – when the author was looking for new explosive

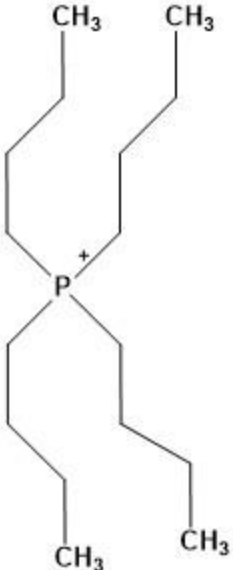
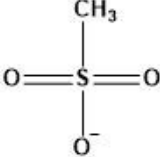
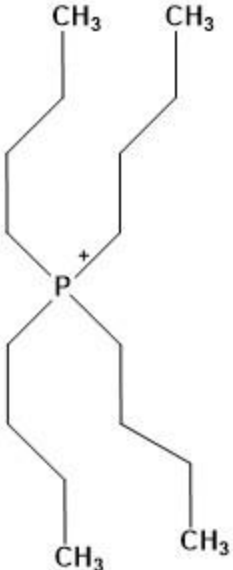
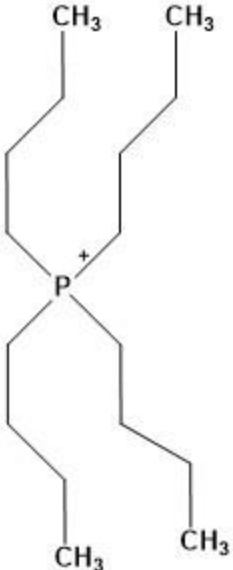
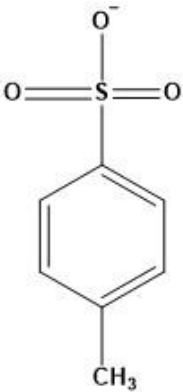
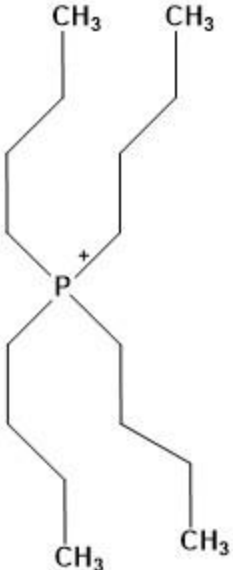
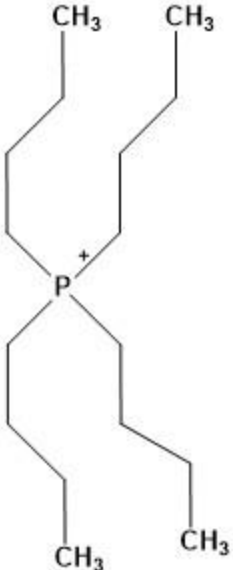
compounds (112). However, only in 1934, Charles Graenecher registered the first patent for an industrial application of ILs in the preparation of cellulose solutions (113). After these pioneering demonstrations, several patents were filled. Still, only with the appearance of air and water stable ILs, the research, development and new applications of novel ILs have significantly increased (107,108,114–116).

ILs are salts with a general melting temperature below 100 °C because they are constituted by large organic cations and usually an organic or inorganic anion. Due to large size of their ions, they do not easily form a crystalline structure and they are liquid at low temperatures (9). The ionic character associated to ILs is responsible for some of their remarkable features, namely a negligible vapor pressure, non-flammability, high thermal and chemical stabilities, and an enhanced solvation ability for organic, inorganic and organometallic compounds. Moreover, one of the main advantages of ILs is the fact that their physical state and their chemical properties can be adjusted by changing the cation and anion for a given application - “designer solvents”. This property promotes the possibility of adapting their properties, such as hydrophobicity and solution behavior, physical properties, and variable biodegradation ability or toxicological features (9).

The possibility of choosing the cation and the anion in ILs leads to a potential number of 10^6 different ILs. Today more than 1000 ILs were reported in the literature, and approximately 300 are commercially available (117). ILs are usually classified according to the cation and anion chemical structures, and cations such as imidazolium-, pyridinium-, pyrrolidinium-, ammonium-, sulfonium-, guanidinium- and phosphonium-based have been the most studied in the literature (117).

In this work, phosphonium-based ILs were investigated. The first reports of phosphonium-based ILs dates from the 70-80s, when Parshall (118) reported the synthesis of phosphonium-based ILs using stannate and germinate salts, and with the discovery of the tetrabutylphosphonium bromide as an ionic solvent by Knifton and co-workers (119). The four possible alkyl chain substituents on the phosphonium cation together with a multitude of available anions results in an enormous number of ionic liquids. Even so, tetrabutylphosphonium is the most studied phosphonium-based cation. Table 1.6. represents some of the most common associated anions and commercially available ILs.

Table 1.6. Chemical structures of phosphonium-based ionic liquids (114).

Phosphonium-based ILs	Cation	Anion	Molecular weight / (g/mol)
Tetrabutylphosphonium methanesulfonate			354.53
Tetrabutylphosphonium tetrafluoroborate		BF_4^-	346.24
Tetrabutylphosphonium <i>p</i> -toluenesulfonate			430.62
Tetrabutylphosphonium bromide		Br^-	339.33
Tetrabutylphosphonium chloride		Cl^-	294.88

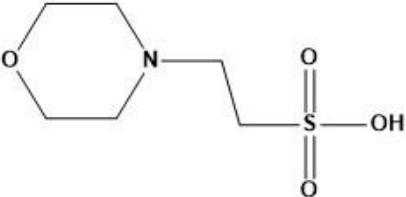
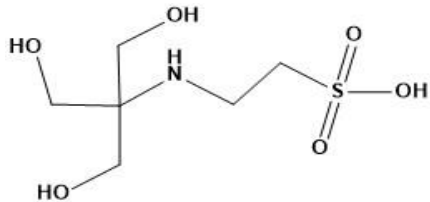
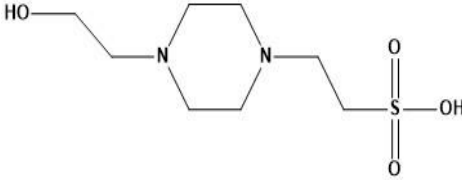
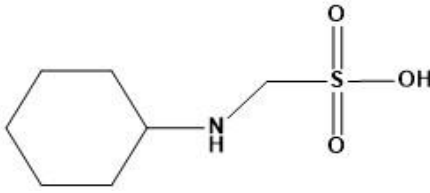
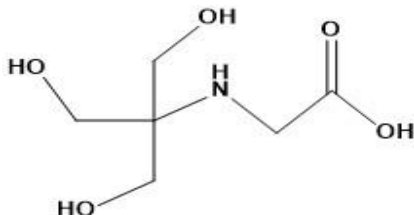
Phosphonium-based ILs have some advantages compared with nitrogen-based fluids, namely higher thermal and electrochemical stabilities - useful in processes that operate at temperatures higher than 100 °C (120). Phosphonium cations also lack acidic protons so they are stable under alkaline conditions (121). They are also less dense than water which might be beneficial in several setups involving the settling of aqueous layers. Taking into account these important characteristics, phosphonium-based ILs have been explored as phase transfer catalysts, in electrochemical media, as solvents, in high temperature poly-carbonate reactions and as exfoliation agents for montmorillonite clays (119).

Rogers and co-workers (118), in 2003, demonstrated that ILs can form ABS, using 1-butyl-3-methylimidazolium chloride, $[\text{C}_4\text{mim}]\text{Cl}$, and an inorganic salt, K_3PO_4 .

However, only in 2007, IL-based ABS were applied to the extraction of proteins by Du et al. (116). The authors extracted proteins from human body fluids with a system composed of $[C_4mim]Cl + K_2HPO_4$ (116). This first attempt opened a new path on the use of IL-based ABS to extract other proteins such as BSA, lysozyme, trypsin, myoglobin, horseradish peroxidase, cytochrome c, γ -globulins, haemoglobin, peroxidase and ovalbumin (9).

One of the main advantages of IL-based ABS, when compared to the more traditional polymer-based ABS conveys on the possibility of controlling their phases' polarities by an appropriate choice of the IL ions (9). Therefore, IL-based ABS can be properly selected aiming at extracting and concentrating, in a single-step, a multitude of proteins, and in particular PSA. However, since PSA is a protein, its stability is affected by the protons activity or by the pH of the medium (9). Most of the ILs investigated in IL-based ABS do not display self-buffering characteristics and the pH is attained by means of a buffered salt solution (usually phosphate-based salts) (123). In this context, ionic liquids derived from Good's buffers (GBs), with self-buffering characteristics, appear as a promising alternative. GBs are zwitterionic amino acid derivatives commonly used as biological buffers (124). They are chemically inert, do not interfere with the metal ion-protein binding, are non-toxic, are commercially available at low cost, their pK_a values range between 6.0 and 8.0, and have a high water solubility and low solubility in organic solvents (125). These GBs can thus be used as precursors of IL anions given rise to GB-ILs. The GBs MES, TES, HEPES, CHES and Tricine, presented in Table 1.7., were used in this work as anions of ILs and further employed as phase-forming components of ABS for the extraction and concentration of PSA. In particular, ABS formed by these phosphonium-based ILs and an organic salt (potassium citrate) were investigated. Initially, phosphonium-based ILs were synthesized, with tetrabutylphosphonium as the common cation, combined with 5 GB-derived anions to yield the ILs $[P_{4444}][MES]$, $[P_{4444}][TES]$, $[P_{4444}][HEPES]$, $[P_{4444}][CHES]$ and $[P_{4444}][Tricine]$, and characterized. Further, the respective ABS phase diagrams were determined at 25°C. Finally, these systems were evaluated as extraction and concentration techniques for PSA.

Table 1.7. Chemical structures of GBs: MES: 2-(N-morpholino)ethanesulfonic acid; TES: 2-[[1,3-dihydroxy-2-(hydroxymethyl)propan-2-yl]amino]ethanesulfonic acid; HEPES: 4-(2-hydroxyethyl)-1-piperazineethanesulfonic acid; CHES: N-cyclohexyl-2-aminoethanesulfonic acid; Tricine: N-2(2-Hydroxy-1,1-bis(hydroxymethyl)ethyl)glycine.

Good Buffer	Chemical Structure	Molecular weight / (g/mol)
MES		195.2
TES		229.2
HEPES		238.3
CHES		207.2
Tricine		179.1

One of the problems addressed in PSA analyses is its low concentration in human fluids, and in particular, in urine. Therefore, the main goal of this work is to reach concentration factors of PSA at the IL-rich phase detectable by more accessible equipment and less laborious techniques. For this purpose, it is necessary to test different initial concentrations of IL and organic salt, along the same tie-line, and to evaluate the extraction efficiencies and concentration factors experimentally achievable. The promising ABS were then tested with human urine by adding PSA at known concentrations.

2. Extraction of PSA using phosphonium- based ILs + salt ABS

2.1. Introduction

Proteins are a wide group of important biomolecules. They are present as enzymes, antibodies, hormones, transport and structural proteins, among others (126). Due to their admirable properties, there is an increasing interest in the production and extraction of proteins for a broad range of fields (127). Proteins are helpful in biochemical and medical research, for example as biomarkers of diseases (72), and in textile, food and pharmaceutical industries (127). In this context, many efforts have been carried out to optimize the extraction and purification procedures for proteins, because, due to their poor stability, changes in the microenvironment can cause their denaturation leading to protein unfolding and inactivation. It is therefore of critical relevance, in extractive procedures of proteins, to maintain their three-dimensional structure (127). Thereby, the efforts are directed to develop not just a biocompatible, but also cheaper, sustainable and one-step platform for the extraction and purification of proteins that can be easily scaled-up to an industrial level (123). Prostate specific antigen (PSA) is a glycoprotein of great interest in medical research as the gold-standard prostate cancer (CaP) biomarker (2). Values above 4 µg/L in human serum are considered suspicious and patients have to be subjected to more tests to confirm the diagnosis (70). However, the cut-off for serum PSA is below the detection limit of most quantification equipment and the conventional tests and techniques used for clinical analyses present serious drawbacks. As stated in Chapter 1.6., the commonly used tests and techniques to quantify PSA are immunoassays, such as ELISA (91), which requires the use of highly cost antibodies, and a large investment in time and resources - reason why these assays have to be performed in clinically specific laboratories. Moreover, in fluorescence and electrochemical-based methods, the analyte to be quantified has to be dyed to amplify the signal which can lead to sample lost in preparation steps. The prolonged exposure of the fluorescent dye to excitation light sources can also cause photo bleaching and quenching of the signals leading to false negative resources (96).

It is clear that a new platform for the one-step extraction and concentration of PSA, without changes in the protein 3D structure, and by a more economic and simple way, is a real need towards the use of less expensive and more accessible equipment for the PSA quantification in clinical laboratories. The commonly used protein purification methods include electrophoresis, ionic exchange and affinity chromatographies, and precipitation with salts or solvents, such as ammonium sulphate or ethanol (128,129).

Nevertheless, these methods, in addition to be high time and cost consuming, employ volatile organic compounds hazardous to human health and for the environment (130). All of these drawbacks can cause the loss of the 3D structure of proteins, reason for what the use of ABS with ILs has been emerged in recent years as an efficient and clean alternative over the traditional organic-water extraction systems (9). Moreover, the stability of proteins is strongly affected by the proton activity of the supporting solution and has an optimum pH that can be adjusted by the addition of a proper biological buffer. It is generally accepted that, at appropriate concentrations, hydrophilic ILs tend to dissociate in aqueous solutions, fully or partly, and into ions which form neutral or very weakly basic solutions (131). Therefore, the addition of a buffer into aqueous IL solutions, when dealing with protein stability, will not provide an adequate pH control since the ILs acidity or basicity can swamp the buffer effect (131). Taking into account the multitude of combinations between cations and anions in ILs, the synthesis of ILs with buffering characteristics seems to be the step to follow.

Norman Good and his research team (125) designed biological buffers (Good's buffers, GBs), zwitterionic amino acid derivatives, and these can be used as anion or cation precursors of ILs. It was suggested that these biological buffers act as protein structure stabilizers by a hydration phenomenon (131). These statements suggested the possibility of creating new self-buffering ILs with protein stabilization characteristics, and that were investigated in this work as phase-forming components of aqueous biphasic systems (ABS) for the extraction and concentration of PSA. As a first step, novel GB-ILs were synthesized and characterized. Their pH-profiles were already demonstrated and they act as adequate buffers in the 6-8 pH region (132). The GB-ILs adopted in this work are based on anions derived from N-(2-hydroxy-1,1-bis(hydroxymethyl)ethyl)glycine (Tricine), 2-[1,3-dihydroxy-2-(hydroxymethyl)propanyl]amino]ethanesulfonic acid (TES), N-cyclohexyl-2-aminoethanesulfonic acid (CHES), N-cyclohexyl-2-aminoethanesulfonic acid (HEPES), and 2-(N-morpholino)ethanesulfonic acid (MES), coupled with the common tetrabutylphosphonium ($[P_{4444}]^+$) cation. These GB-ILs were then used as constituents of ABS, combined with potassium citrate in aqueous media, as alternative extraction media for PSA. Initially, the ternary phase diagrams, tie-lines (TLs) and tie-line lengths (TLLs) were determined at 25°C. Then, these systems were investigated as liquid-liquid extraction platforms for PSA.

2.2. Experimental Section

2.2.1. Chemicals

The salt potassium citrate tribasic monohydrate ($K_3C_6H_5O_7 \cdot H_2O$, purity ≥ 99 wt%) was obtained from Sigma-Aldrich Chemical Co. (USA). PSA (purity ≥ 95 %) was obtained from Sigma-Aldrich Chemical Co.. Methanol (purity $> 99.9\%$) was obtained from Fisher Scientific. Acetonitrile (purity $> 99.7\%$) was supplied from Lab-Scan. The buffers required for the ILs synthesis, namely CHES (purity > 99 wt%), HEPES (purity > 99.5 wt%), MES (purity > 99 wt%), Tricine (purity > 99 wt%) and TES (purity > 99 wt%) were purchased from Sigma-Aldrich Chemical Co.. The cation precursor, $[P_{4444}][OH]$ (40 wt% in H_2O), was also supplied by Sigma-Aldrich Chemical Co.. Dimethyl sulfoxide (DMSO, purity > 99.9 wt%) and deuterium oxide (D_2O purity > 99.9 wt%) were obtained from Sigma-Aldrich Chemical Co.. Purified water passed through a reverse osmosis and a Milli-Q plus 185 water purifying system was used in all experiments. For quantification of PSA using the BLItz Pro System, Super Streptavidin biosensors acquired from VWR were used.

2.2.2. Experimental Procedure

2.2.2.1. Synthesis and characterization of the Good's buffers ionic liquids

The GB-ILs were synthesized *via* neutralization of the base with the appropriate acid. A slightly excess of an equimolar aqueous solution (1:1.1) of buffer was added dropwise to a tetrabutylphosphonium hydroxide solution. The mixture was stirred continuously for at least 12 h at room temperature (≈ 25 °C) (Fig. 2.1. A) to produce the ionic liquid and water as by-product. The mixture was then evaporated at 50-60 °C under reduced pressure and which gives rise to a viscous liquid (Fig. 2.1. B). A mixture of acetonitrile and methanol (1:1, v:v) was added to the viscous liquid and then vigorously stirred at room temperature for 1 h (Fig. 2.1. C). The solution was then filtered to remove any excess buffer. The solvent mixture was evaporated and the GB-IL product was dried in vacuum (10 Pa) for 3 days at room temperature (Fig. 2.1. D). The water content in each GB-IL was measured by Karl-Fischer (KF) titration, using a KF coulometer (Metrohm Ltd., model 831). The chemical structures of the GB-ILs were confirmed by 1H and ^{13}C NMR spectroscopy (Bruker AMX 300) operating at 300.13 and 75.47 MHz, respectively. Chemical shifts are expressed in δ (ppm) using tetramethylsilane (TMS) as internal

reference and D₂O as deuterated solvent. The ILs synthesized in this work showed high purity level without signs of decomposition.

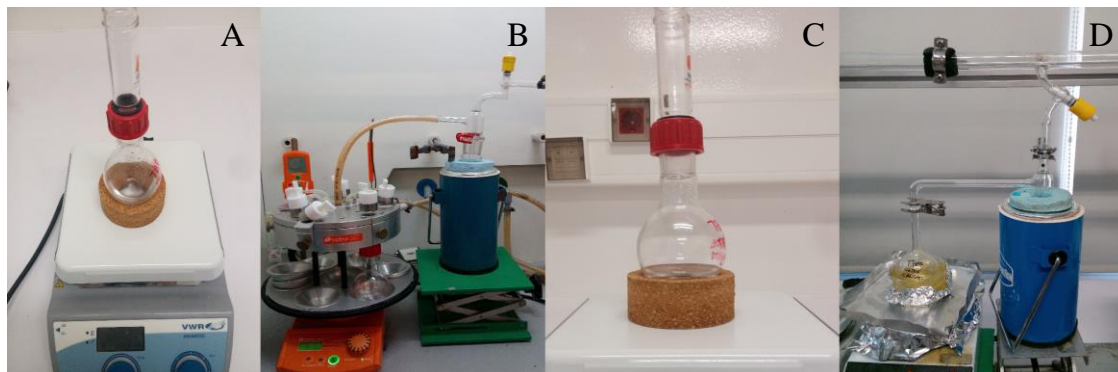


Figure 2.1. GB-ILs synthesis. An equimolar excess of the aqueous solution of buffer was added to [P₄₄₄₄]OH solution (A). The mixture was dried at 50-60 °C under reduced pressure in a *Carrousel 6 plus* reaction station (B). A mixture of acetonitrile and methanol (1:1, v:v) was added to the viscous liquid and then vigorously stirred at room temperature for 1 h (Fig. 2.1. C). The solvent mixture was evaporated and the GB-IL was dried in vacuum (10 Pa) for 3 days at room temperature (D).

2.2.2.2. Phase diagrams and tie-lines (TLs)

The binodal curve of each ABS was determined through the cloud point titration method at 25 (\pm 1) °C and atmospheric pressure. The experimental procedure adopted has been validated in previous reports (123,133). Repetitive drop-wise addition of the aqueous salt solution (K₃C₆H₅O₇ at 60 wt %) to the IL (*circa* 80 wt %) aqueous solution was carried out until the detection of a cloudy biphasic solution, followed by the drop-wise addition of water until the finding of the monophasic region. The opposite addition was also attempted aiming at gathering the maximum number of points to describe each binodal curve. This procedure was carried under constant stirring. Each mixture composition was determined by the weight quantification of all components added within an uncertainty of $\pm 10^{-4}$ g (using an analytical balance, Mettler Toledo Excellence XS205 DualRange).

The tie-lines (TLs) of each phase diagram, and at the mixtures compositions for which the extraction of PSA was carried out, were determined by a gravimetric method originally described by Merchuk et al. (134). The selected mixture, at the biphasic regime, was prepared by weighting the appropriate amounts of IL + salt + water and further vigorously stirred. Then, the mixture was submitted to centrifugation for 10 min at 5000

rpm and at controlled temperature of (25 ± 1) °C. After centrifugation, the sample was left in equilibrium for more 10 min at (25 ± 1) °C to guarantee the equilibration of the coexisting phases. After this period, each phase was carefully separated and weighted.

The experimental binodal curves were fitted using Eq. 1 (134),

$$[\text{IL}] = A \exp[(B[\text{Salt}]^{0.5}) - (C[\text{Salt}]^3)] \quad (1)$$

where $[\text{IL}]$ and $[\text{Salt}]$ are the IL and salt weight fractions percentages, respectively, and A , B and C are fitted constants obtained by least-squares regression.

Each individual TL was determined by a weight balance approach through the relationship between the top weight phase composition and the overall system composition. For the determination of TLs the following system of four equations (Eqs. 2 to 5) was used to estimate the concentration of IL and salt at each phase ($[\text{IL}]_{\text{IL}}$, $[\text{IL}]_{\text{Salt}}$, $[\text{Salt}]_{\text{Salt}}$ and $[\text{Salt}]_{\text{IL}}$) (134):

$$[\text{IL}]_{\text{IL}} = A \exp[(B[\text{Salt}]_{\text{Salt}}^{0.5}) - (C[\text{Salt}]_{\text{Salt}}^3)] \quad (2)$$

$$[\text{IL}]_{\text{Salt}} = A \exp[(B[\text{Salt}]_{\text{Salt}}^{0.5}) - (C[\text{Salt}]_{\text{Salt}}^3)] \quad (3)$$

$$[\text{IL}]_{\text{IL}} = \frac{[\text{IL}]_{\text{M}}}{\alpha} - \left(\frac{1-\alpha}{\alpha}\right) [\text{IL}]_{\text{Salt}} \quad (4)$$

$$[\text{Salt}]_{\text{IL}} = \frac{[\text{Salt}]_{\text{M}}}{\alpha} - \left(\frac{1-\alpha}{\alpha}\right) [\text{Salt}]_{\text{Salt}} \quad (5)$$

where the subscripts salt and IL designate the salt- and IL-rich phases, respectively, and M is the initial mixture composition. The parameter α is the ratio between the top weight and the total weight of the mixture. The solution of this system provides the concentration (wt %) of the IL and salt in the top and bottom phases, and thus the, TLs can be easily represented.

For the calculation of the tie-line length (TLL), Eq. 6 was applied.

$$\text{TLL} = \sqrt{([\text{Salt}]_{\text{IL}} - [\text{Salt}]_{\text{Salt}})^2 + ([\text{IL}]_{\text{IL}} - [\text{IL}]_{\text{Salt}})^2} \quad (6)$$

All the calculations considering the mass fraction or molality of the citrate-based salt were carried out discounting the complexed water. In all systems, the IL-rich phase

corresponds to the top phase while the bottom phase is mostly enriched in the organic salt.

2.2.2.3. Partition of PSA

The ternary mixtures compositions used in the partitioning experiments were chosen based on the phase diagrams determined in this work for each IL-salt-water system. Different mixture compositions (30 wt% salt + 30 wt% IL + 40 wt% H₂O and 30 wt% salt + 40 wt% IL + 30 wt% H₂O) were also studied to evaluate the effect of the concentration of the phase-forming components through the extraction of PSA. Aqueous solutions of PSA at concentrations of *circa* 50 ng.mL⁻¹ were used as the “water” added to each ABS. The used PSA concentration was chosen after optimization using BLItz[®] Pro system. Each mixture was vigorously stirred, centrifuged for 10 min, and left to equilibrate for more 10 min at (25 ± 1) °C to reach the PSA complete partitioning between the coexisting phases. After, a careful separation of the phases was performed and the amount of PSA in each phase was quantified using a BLItz[®] Pro system. The BLItz[®] Pro system is a highly precise and sensitive immunoassay tool to quantify specific proteins and which allows to infer on the protein stability. The BLItz[®] Pro system is based on the principle of antibody-antigen interactions. The Super Streptavidin Biosensors employed are coated with ultra-high density Streptavidin and allow the measurements of kinetic interactions (through the exploitation of the high affinity streptavidin-biotin interactions).



Figure 2.2. BlItz[®] PRO System and Super Streptavidin Biosensors.

The quantification of PSA in each phase was carried out by an external standard calibration method in the range of 1 to 100 ng.mL⁻¹ of protein. At least three independent

ABS were prepared and 2 samples of each phase were quantified using a calibration curve specifically determined for this purpose (*Appendix A*).

The percentage extraction efficiency of PSA, $EE_{\text{PSA}}\%$, is the percentage ratio between the amount of protein in the IL-rich aqueous phase to that in the total mixture, and is defined according to Eq. (7):

$$EE_{\text{PSA}}\% = \frac{w_{\text{PSA}}^{\text{IL}}}{w_{\text{PSA}}^{\text{IL}} + w_{\text{PSA}}^{\text{Salt}}} \times 100 \quad (7)$$

where $w_{\text{PSA}}^{\text{IL}}$ and $w_{\text{PSA}}^{\text{Salt}}$ are the total weight of protein in the IL-rich and in the salt-rich aqueous phases, respectively.

Computer proteomics is a growing area on the bioinformatics field typically used to study and predict the structural and functional organization of proteins. Nowadays, computer proteomics is performed based on thousands of databases, such as PROSITE, PFAM, BLAST, BLAST and UNIPROT (135). The Discovery Studio software, used in this work, allows the simulation of molecular mechanisms, antibodies modeling, and structure-, pharmacophore- and ligand based-designs, x-ray data processing and macromolecules design and analyses. In this work, Discovery studio was used for the macromolecule design and analysis with the purpose of performing sequence alignments and to generate the 3D structure model of PSA and, at the end, to study the macromolecule interactions with the phase-forming components of ABS.

2.3. Results and discussion

2.3.1. Characterization of the synthesized ionic liquids

The macroscopic appearance (Fig. 2.3.) and NMR characterization data for each GB-IL are described below. The chemical structures of the synthesized ILs are depicted in Table 2.1..



Figure 2.3. Macroscopic appearance of the synthesized Good's Buffer ionic liquids at 25°C. From the left to the right: [P₄₄₄₄][MES], [P₄₄₄₄][TES], [P₄₄₄₄][CHES], [P₄₄₄₄][HEPES], [P₄₄₄₄][Tricine].

[P₄₄₄₄][MES]: From the MES buffer (48.5 mmol), this compound was obtained as a white solid. Water content < 0.05 wt%. ¹H NMR (300 MHz, D₂O/TSP): 3.63 (t, 4H), 2.99 (t, 2H), , 2.72 (t, 2H), 2.50 (t, 4H), 2.02 (m, 8H), 1.27-1.42 (m, 16H), 0.78 (t,12H). ¹³C NMR (75.47 MHz, D₂O/TSP): 68.80, 55.44, 55.11, 50.02, 26.28, 20.80, 20.16, 15.44.

[P₄₄₄₄][TES]: From the TES buffer (45.1 mmol), this compound was obtained as a transparent viscous liquid. Water content < 0.05 wt%. ¹H NMR (300 MHz, D₂O/TSP): 3.31 (s, 6H), 2.82 (s, 2H), 2.57 (t, 2H), 2.10 (m, 8H), 1.29-1.49 (m,16H), 0.79 (t, 12H). ¹³C NMR (75.47 MHz, D₂O/TSP): 60.65, 57.63, 51.58, 37.69, 26.28, 20.83, 20.17, 15.46.

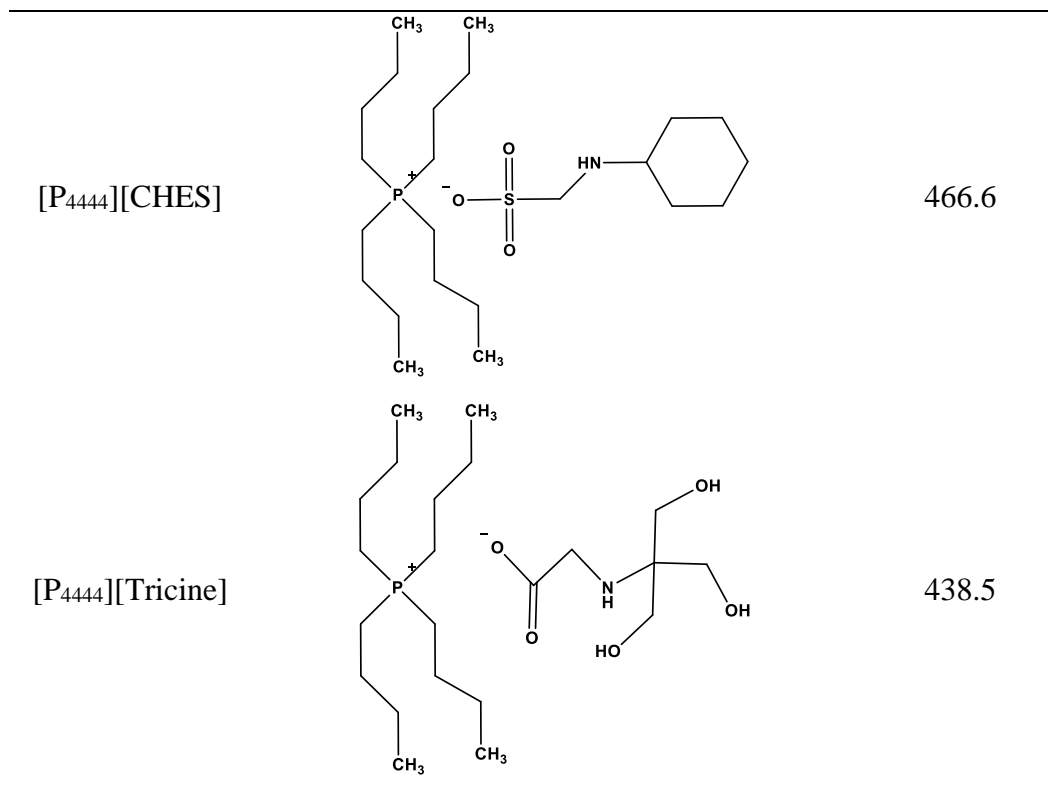
[P₄₄₄₄][CHES]: From the CHES buffer (47.2 mmol), this compound was obtained as a transparent viscous liquid. Water content <0.05 wt%. ¹H NMR (300 MHz, D₂O/TSP); ¹H NMR (300 MHz, D₂O/TSP); 2.95 (m, 2H), 2.38-2.47 (*m*, 1H), 2.02 (m, 8H), 1.28-1.45 (m, 16H,), 0.94 (m, 10H), 0.78 (t, 12H). ¹³C NMR (75.47 MHz, D₂O/TSP): 63.37, 63.09, 53.42, 39.56, 26.28, 26.08, 25.60, 20.30, 20.15, 15.43.

[P₄₄₄₄][HEPES]: From the HEPES buffer (44.3 mmol), this compound was obtained as a yellowish white solid. Water content < 0.05 wt%. ¹H NMR (300 MHz, D₂O/TSP): 3.59 (t,4H), 2.97 (t, 2H), 2.94 (t, 2H), 2.67 (t, 2H), 2.46 (t, 8H), 2.03 (m, 8H), 1.28-1.45 (m, 16H), 0.79 (t, 12H). ¹³C NMR (75.47 MHz, D₂O/TSP): 61.59, 60.87, 55.02, 54.78, 54.19, 50.39, 26.29, 20.80, 20.16, 15.44.

[P₄₄₄₄][Tricine]: From the Tricine buffer (50.3 mmol), this compound was obtained as white solid. Water content < 0.05 wt%. ¹H NMR (300 MHz, D₂O/TSP): 3.37 (s, 6H), 3.12 (s, 2H), 2.00 (m, 8H), 1.27-1.44 (m, 16H), 0.77 (t. 12H). ¹³C NMR (75.47 MHz, D₂O/TSP): 182.71, 63.12, 62.97, 47.68, 26.28, 20.79, 20.15, 15.42.

Table 2.1. Chemical structures and molecular weight (g/mol) of the synthesized GB-ILs ([P₄₄₄₄][MES], [P₄₄₄₄][TES], [P₄₄₄₄][HEPES], [P₄₄₄₄][CHES], [P₄₄₄₄][Tricine]).

GB-IL	Chemical Structure	Molecular weight / (g/mol)
[P ₄₄₄₄][MES]		454.6
[P ₄₄₄₄][TES]		488.6
[P ₄₄₄₄][HEPES]		497.7



2.3.2. Phase Diagrams and Tie-lines

The new phase-diagrams, at 25 °C and at atmospheric pressure, for the systems composed of water, K₃C₆H₅O₇ and [P₄₄₄₄][GB] ([P₄₄₄₄][Tricine], [P₄₄₄₄][CHES], [P₄₄₄₄][MES], [P₄₄₄₄][HEPES] and [P₄₄₄₄][TES]) are illustrated in Figure 2.4.

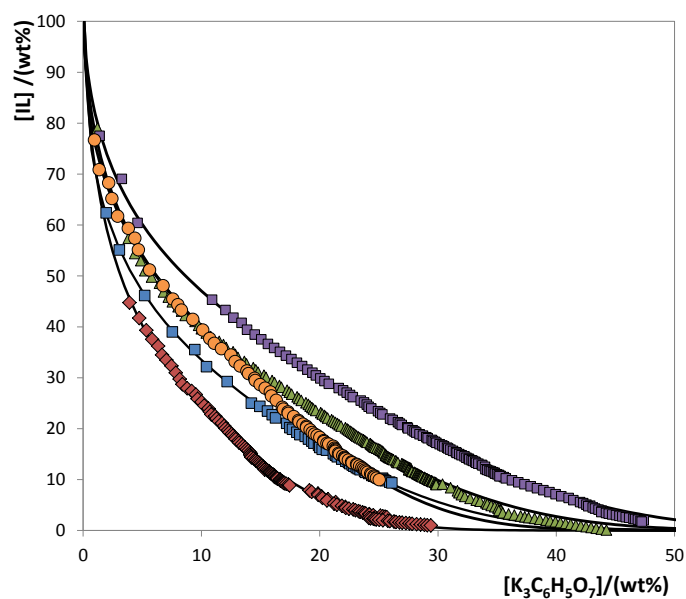


Figure 2.4. Phase diagrams for the systems composed of IL + K₃C₆H₅O₇ + H₂O at 25°C and atmospheric pressure (in wt%) with the corresponding binodal data adjusted by Eq. 1: [P₄₄₄₄][Tricine] (■); [P₄₄₄₄][HEPES] (▲); [P₄₄₄₄][TES] (●); [P₄₄₄₄][MES] (■); [P₄₄₄₄][CHES] (◆);

The experimental data are shown in weight fraction to allow a direct screening of the mixture compositions required to form two-phase systems able to carry out the PSA extraction and concentration. The detailed experimental data corresponding to the ternary phase diagrams determined in this work are presented in Appendix B.

In all ABS, the biphasic region is positioned above the solubility curve while the monophasic region is localized below. Diagrams with the largest area above the binodal curve have therefore a higher ability to form two phases, *i.e.*, the IL is more easily salted-out by the salt. Therefore, from Figure 2.4., and for instance at 10 wt% of $K_3C_6H_5O_7$, the ability of GB-ILs to create ABS follows the order: $[P_{4444}][CHES] > [P_{4444}][MES] > [P_{4444}][HEPES] \approx [P_{4444}][TES] > [P_{4444}][Tricine]$.

The formation of an ABS depends on the type of IL and its concentration, type of salt and its concentration, temperature, pH or pressure. The two-phases forming ability in each IL-based system is a result of complex and competing interactions occurring between the solutes and water or between the phase-forming components (9). Once the concentration of salt and IL, temperature, pressure and pH are maintained constants, the ABS formation is a result of the type of salt and IL, which means that the ABS studied reflect the competition between the salting-out ions and the IL ions for the formation of hydration complexes. The citrate-based salt is composed of a trivalent charged anion and is a strong salting-out species according to the Hofmeister series (136). Therefore, it has a high affinity for water, and thus, there is a preferential exclusion of the IL ions from the aqueous solution promoting the two-phases separation.

The ILs investigated are formed by a tetrabutylphosphonium ($[P_{4444}]^+$) cation and GB-derived anions. The cation is the same for all the investigated ILs and their effect cannot be appraised from the obtained phase diagrams. However, it was already demonstrated that $[P_{4444}]$ -based ILs display a high ability to promote the phase split when compared with ammonium-, pyridinium- and imidazolium-based ionic liquids (137). $[P_{4444}]$ -based salts have highly shielded charges, located mostly on the heteroatom surrounded by four alkyl chains, thus leading to a higher tendency towards their salting-out from aqueous media. On the other hand, the anions have a higher aptitude for creating hydration complexes because they are more polarizable and present more diffuse valence electronic distribution (138). This means that anions, when compared with cations, have

a more relevant influence in ABS formation and behavior. Anions with lower hydrogen-bond basicity values present lower ability to form coordinative hydrogen-bonds and to create hydration complexes, and therefore are more easily salted-out by conventional salts (138). The hydrogen-bond basicity values for the ILs used in this work have not been reported up to date; yet, relevant conclusions can be achieved using the octanol-water partition coefficients (K_{ow}) of each GB. The higher the value of $\log(K_{ow})$ the higher the affinity of the anion for the octanol-rich phase, meaning that it has a lower affinity for the water-rich phase and to be hydrated. In this context, higher $\log(K_{ow})$ values correspond to anions that are more easily separated by a salting-out phenomenon. As expected, the ILs composed of anions with $-OH$ groups and lower values of $\log(K_{ow})$ ([Tricine] $^-$: -5.25; [TES] $^-$: -4.48; [HEPES] $^-$: -3.11) (132) are those that correspond to ILs that are more distant from the axis in Figure 2.4.. Thus, these GB-ILs require higher amounts of salt for phase separation. On the other hand, GBs with no $-OH$ groups display higher $\log(K_{ow})$ values ([MES] $^-$: -2.48; [CHES] $^-$: -0.59) (132) reflecting their lower aptitude to hydrogen-bond with water and higher ability for liquid-liquid demixing in ABS.

For the studied systems, the experimental binodal data were further fitted by the empirical relationship described by Eq. 1. The regression parameters A , B and C , were estimated by the least-squares regression method, and their values and corresponding standard deviations (σ) are provided in Table 2.2. The respective correlations are also depicted in Figure 2.4 in combination with the experimental data. In general, good correlation coefficients were obtained for all systems, indicating that these fittings can be used to predict data in a given region of the phase diagram where no experimental results are available.

Table 2.2. Correlation parameters used to describe the experimental binodal data by Eq. 1 and respective standard deviations (σ) and correlation coefficients (R^2).

IL	$A \pm \sigma$	$B \pm \sigma$	$10^5 (C \pm \sigma)$	R^2
IL + $K_3C_6H_5O_7$ + water				
[P ₄₄₄₄][MES]	98.3 \pm 0.54	-0.327 \pm 0.022	3.96 \pm 0.06	0.9996
[P ₄₄₄₄][CHES]	111.9 \pm 2.49	-0.450 \pm 0.009	10.5 \pm 0.44	0.9929
[P ₄₄₄₄][HEPES]	105.1 \pm 1.19	-0.295 \pm 4.257	2.78 \pm 0.08	0.9978
[P ₄₄₄₄][Tricine]	105.1 \pm 5.10	-0.248 \pm 0.016	1.71 \pm 0.02	0.9992
[P ₄₄₄₄][TES]	99.6 \pm 0.51	-0.356 \pm 0.007	5.40 \pm 0.29	0.9971

The experimental TLs, along with their respective length (TLL), are reported in Table 2.3. The TLs obtained for each systems are depicted in Figure 2.6. In general, the TLs are closely parallel to each other.

Table 2.3. Data for the tie-lines (TLs) and tie-line lengths (TLLs). Initial mixture compositions are represented as [Salt]_M and [IL]_M, whereas [Salt]_{Salt} and [IL]_{Salt} are the compositions of IL and salt at the IL-rich phase, respectively, and *vice-versa*.

Weight fraction composition / (wt %)							
IL + K ₃ C ₆ H ₅ O ₇ + water							
IL	[IL] _{IL}	[salt] _{IL}	[IL] _M	[salt] _M	[IL] _{salt}	[salt] _{salt}	TLL
[P ₄₄₄₄][MES]	65.71	1.51	29.42	20.48	2.89	34.36	70.89
	90.81	0.06	29.36	30.33	0.37	44.12	100.60
	94.29	0.01	30.21	39.87	0.27·10 ⁻³	58.64	111.04
[P ₄₄₄₄][CHES]	67.45	1.26	29.70	19.83	0.11	34.38	75.04
	75.58	0.76	29.64	30.25	0.17·10 ⁻⁴	49.27	89.81
	93.56	0.16	30.11	39.95	0.18·10 ⁻⁸	58.83	110.44
[P ₄₄₄₄][HEPES]	57.51	4.14	29.89	20.14	6.59	33.63	57.80
	83.11	0.63	30.24	29.49	0.95	46.00	93.84
	90.97	0.24	29.72	40.13	0.03	59.46	108.52
[P ₄₄₄₄][Tricine]	52.11	7.75	30.08	24.73	4.42	44.50	60.20
	70.02	2.64	30.45	29.71	2.53	48.78	81.75
	94.31	0.19	29.78	40.11	0.54	58.20	110.26
[P ₄₄₄₄][TES]	50.61	5.97	30.28	19.70	0.39	39.87	60.59
	93.58	0.05	30.69	29.89	0.08	44.32	103.45
	96.00	0.02	30.43	39.48	0.11·10 ⁻³	57.80	112.05

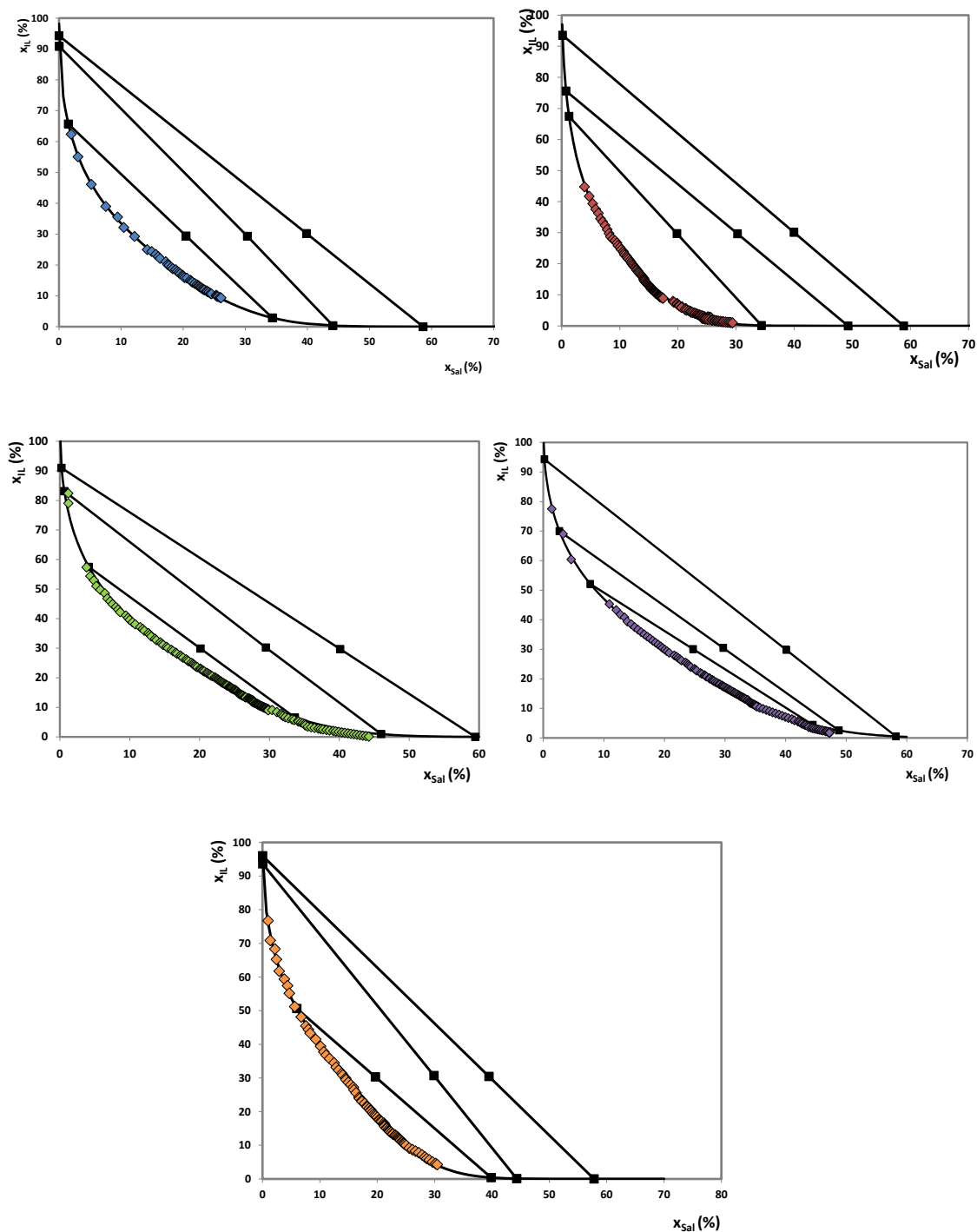


Figure 2.5. Phase diagrams and TLs (■) and adjusted binodal data using Eq. 1 (-), at 25°C and atmospheric pressure, for the ternary systems composed of $K_3C_6H_5O_7$ + water + [P₄₄₄₄][MES] (■); [P₄₄₄₄][CHES] (◆); [P₄₄₄₄][HEPES] (▲); [P₄₄₄₄][Tricine] (■); [P₄₄₄₄][TES] (●).

2.3.3. Partition of PSA

The driving forces that influence the proteins migration are still not clear, but have been described as mainly including electrostatic interactions between the negatively charged amino acids residues of the proteins surface and the cation of the ionic liquid (108,116) and hydrophobic interactions (139). However, hydrogen bonding, $\pi\cdots\pi$ interactions between the aromatic groups and dispersive-type interactions between the aliphatic groups also affect proteins extraction and partitioning and cannot be discarded.

The extraction efficiencies of PSA in ABS composed of [P₄₄₄₄][GB] + K₃C₆H₅O₇ at given mixture compositions are shown in Table 2.4. PSA was added to each system as an aqueous solution at a concentration *circa* 50 ng.mL⁻¹. The obtained results show that PSA is completely extracted to the top phase in all the studied systems since no PSA was found in the bottom phase. However, the results of the mass balance of protein reveal small losses of PSA, and between 1.27 – 5.16 % in the 30 wt% of IL + 30 wt% of salt, and between 5.05 – 10.73% in the 30 wt% of IL + 40 wt% of salt mixture compositions. As stated out before, PSA is a labile protein and may suffered some denaturation. However, these small losses are not significant after the concentration step that will be shown latter and for which PSA can be identified and quantified by HPLC.

Table 2.4. Extraction efficiency of PSA ($EE_{PSA}\%$) at 25° C in the ABS composed of ILs and K₃C₆H₅O₇.

IL	Weight fraction composition / (wt %)		$EE_{PSA}\%$	Loss of protein / (wt%)
	IL	Salt		
[P ₄₄₄₄][MES]	30.35 ± 0.15	30.84 ± 0.53	100	-4.71
[P ₄₄₄₄][CHES]	30.13 ± 0.25	30.54 ± 0.63	100	-1.27
[P ₄₄₄₄][HEPES]	30.16 ± 0.35	30.44 ± 0.29	100	-8.00
[P ₄₄₄₄][Tricine]	30.90 ± 0.28	30.70 ± 0.31	100	-9.74
[P ₄₄₄₄][TES]	29.95 ± 0.24	30.08 ± 0.69	100	-5.16
[P ₄₄₄₄][MES]	30.01 ± 0.04	40.03 ± 0.14	100	-5.87
[P ₄₄₄₄][CHES]	29.94 ± 0.13	40.12 ± 0.57	100	-5.05
[P ₄₄₄₄][HEPES]	30.09 ± 0.34	39.97 ± 0.27	100	-10.21
[P ₄₄₄₄][Tricine]	30.37 ± 0.17	39.98 ± 0.07	100	-10.73
[P ₄₄₄₄][TES]	30.63 ± 0.37	39.85 ± 0.17	100	-6.32

The driving forces in the PSA partitioning were investigated using the Discovery Studio software. Figure 2.6. depicts the PSA secondary structure (1) and their secondary structure with its active site highlighted with a red sphere (2).



Figure 2.6 PSA secondary structure (1) and their active site (2) (using the Discovery Studio software).

Figure 2.7. shows the surface of PSA and their sites for $\pi\cdots\pi$ (3), electrostatic (4), hydrophobic (5) and hydrogen-bonding interactions (6). It can be seen that hydrophobic interactions are the most predominant surface interactions especially in the PSA active site. These statements are in close agreement with the obtained data. Using the octanol-water partition coefficients ($\log(K_{ow})$) presented before, and by analyzing the loss of protein in each systems and displayed in Table 2.4., it is seen that ionic liquids with higher K_{ow} values, *i.e.*, more hydrophobic compounds and thus with stronger interactions with the hydrophobic active site of PSA, are those that lead to lower losses of protein (as observed with the [Tricine]-based IL).

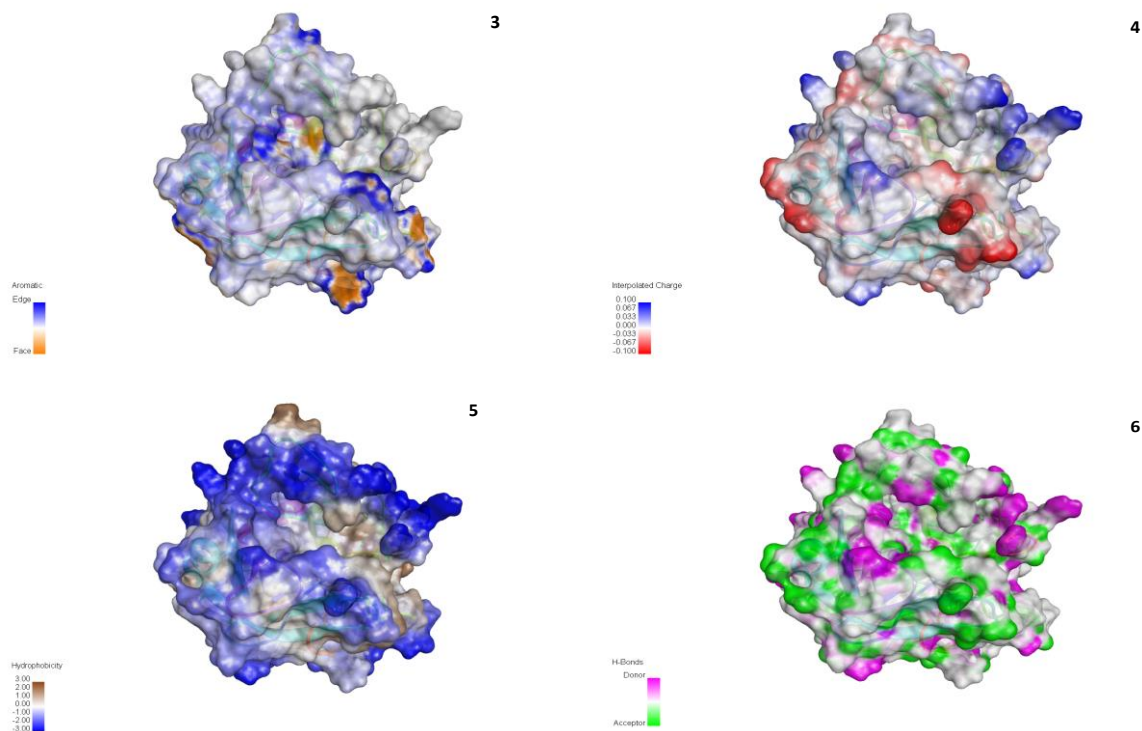


Figure 2.7. Discovery Studio analyses of the surface PSA interactions. (3) aromatic interactions; (4) electrostatic interactions; (5) hydrophobic interactions; (6) hydrogen-bonding interactions.

Few works have been reported with the use of GB-ILs for proteins extraction (131,140). Extraction efficiencies between 85-100% of BSA and antibodies were also achieved with ammonium- (131) and cholinium-based GB-ILs (140). However, in addition to the hydrophobic interactions, salting-out effects may also have a crucial impact in the complete extractions achieved in a single-step. The salt used is a strong salting-out species since it has a high-charge density anion with the capacity to create hydration complexes. Therefore, PSA can also be “excluded” from the salt-rich phase to the IL-rich phase, and as observed with previous systems were a strong salting-out species was used (131).

2.4. Conclusions

The obtained data can revolutionize the world of CaP early-stage diagnosis since this is the first work where 100% extraction efficiencies PSA for one of the aqueous phases were obtained. Up to now, no works have been published aiming the extraction of PSA with IL-based ABS, and only one work has been identified and which evaluated the PSA partition coefficient using polymer-based ABS (141). However, these published results are far from the complete extraction in a single-step (141). Therefore, the use of ILs certainly allows the one-step complete extractions of PSA. Once guaranteeing the 100%

of extraction of PSA for the top phase, this cancer biomarker can certainly be concentrated by reducing the amount of the top (IL-rich) phase while maintaining the mixture composition of the coexisting phases. The next section shows the results on the concentration of PSA so that it can be quantified by a more expedite equipment, such as HPLC.

3. Concentration of PSA using model IL-based ABS

3.1. Introduction

One of the major concerns addressed to the biomarkers analysis and their respective identification and/or quantification relies on their low concentration in body fluids. The quantification of PSA, as pointed out before, requires the use of immunoassays that can only be performed in specific clinical laboratories by skilled personnel (142). In addition, immunoassays require the use expensive antibodies and are time-consuming techniques (142). Moreover, different laboratories use antibodies from different sources which lead to significant dissimilarities in the results (142). Thus, it is difficult to establish large screening programs in urologic clinics and general medical practices based on immunoassays (142).

IL-based ABS represent a potential alternative for the commonly used techniques for PSA analysis in terms of compatibility, time and cost-consuming, as an easy-to-implement process and also as a concentration technique. It has been shown that IL-based ABS can be used to concentrate bisphenol A from biological fluids up to 100-times (143) and ethinylestradiol (EE2) from wastewaters up to 1000-times in a single-step. These results can be extrapolated to tumor biomarkers and can revolutionize the world of clinical analyses by the extraction and concentration of cancer biomarkers in human fluids allowing the use of more expedite and accessible equipment.

The cut-off value of PSA in urine is 150 ng/mL (144), and considering the detection limit of the HPLC used, concentration factors up to 175-fold are required. Nevertheless, and to guarantee no underestimated CaP diagnoses, concentration factors up to 250 were the main goal and were investigated herein.

3.2. Experimental section

3.2.1. Chemicals

The salt, ILs and water used in this section were described in Chapter 2. PSA (purity $\geq 95\%$) was obtained from Sigma-Aldrich Chemical Co.. For the HPLC analyses, sodium phosphate monobasic (NaH_2PO_4 , purity: 99 – 100.5 %), sodium phosphate dibasic heptahydrated ($\text{Na}_2\text{HPO}_4 \cdot 7\text{H}_2\text{O}$, purity: 98.2 – 102.0 %) and sodium chloride (NaCl) were acquired from Sigma–Aldrich and used.

3.2.2. Experimental procedure

3.2.2.1. Lever-arm Rule

The lever-arm rule was used to determine the weight percentages ratio of the coexisting phases in the respective phase diagrams. Several extractions were carried out at different compositions in the same TL which correspond to different concentration factors. Along the same TL, the composition of the phases is maintained while varying the weight or volume ratio between them. First, a fixed and long TL was selected, and a weight balance approach was used to determine the weight fraction of each phase-forming component ([P₄₄₄][GB] and K₃C₆H₅O₇) to be used in each extraction corresponding to a given concentration factor.

For each mixture, the salt and ionic liquid percentages were varied to obtain the desired concentration factor (CF , equation (8)),

$$CF = w_{H_2O} / w_{IL} \quad (8)$$

where w_{H_2O} and $w_{IL,phase}$ correspond to the weight of the aqueous solution containing PSA initially added to the system and the weight of the IL-rich phase in the biphasic mixture obtained.

3.2.2.2. Concentration factors of PSA

The ternary mixtures compositions used in partitioning experiments were chosen based on the phase diagrams determined and presented in Chapter 2.3.2.. Several ternary mixtures were prepared within the biphasic region with the theoretical weight percentages ratio of salt, IL and H₂O/PSA provided by the lever-arm rule for concentrations factors of 5, 20, 50, 100, 150, 200 and 250-fold. ABS were first prepared as a control without adding PSA, and once achieved the CF of 250-fold the extractions were performed adding an aqueous solution of PSA at a concentration of 150 ng/mL (the cut-off value found in urine (68)). Each mixture was vigorously stirred, centrifuged for 10 min and left to equilibrate for at least 10 min at $(25 \pm 1)^\circ C$.

The mixtures were carefully separated and weighted to check the predicted CF according to equation (8). PSA was then quantified in each phase by SE-HPLC.

3.2.2.3. Size-exclusion HPLC (SE-HPLC)

After a careful separation of the phases both of them were analyzed by SE-HPLC. A phosphate buffer solution (1000 mL) was prepared using 47 mL of a Solution A (27.8g NaH_2PO_4), 203 mL of a Solution B (53.65g $\text{Na}_2\text{HPO}_4 \cdot 7\text{H}_2\text{O}$) and 35g of NaCl. Each phase was diluted at a 1:9 (v:v) ratio in the phosphate buffer solution before injection. A Chromaster HPLC (VWR Hitachi) was used. The SE-HPLC was performed on an analytical column Shodex Protein KW- 802.5 (8 mm x 300 mm). A 100 mM phosphate buffer + NaCl 0.3 M was run isocratically with a flow rate of $0.5 \text{ mL} \cdot \text{min}^{-1}$. The column oven and autosampler temperatures were kept at 25°C and at 10°C , respectively. The injection volume was 25 μL . The wavelength was set at 280 nm using a DAD detector. The obtained chromatograms were treated and analyzed using the OriginPro8 software.

3.3. Results and discussion

3.3.1. Concentration factors of PSA

To optimize the procedure, several ABS without PSA were prepared at different compositions along the same TLL (Figure 3.1.) in order to reduce the IL-rich phase and to attain the required *CF*.

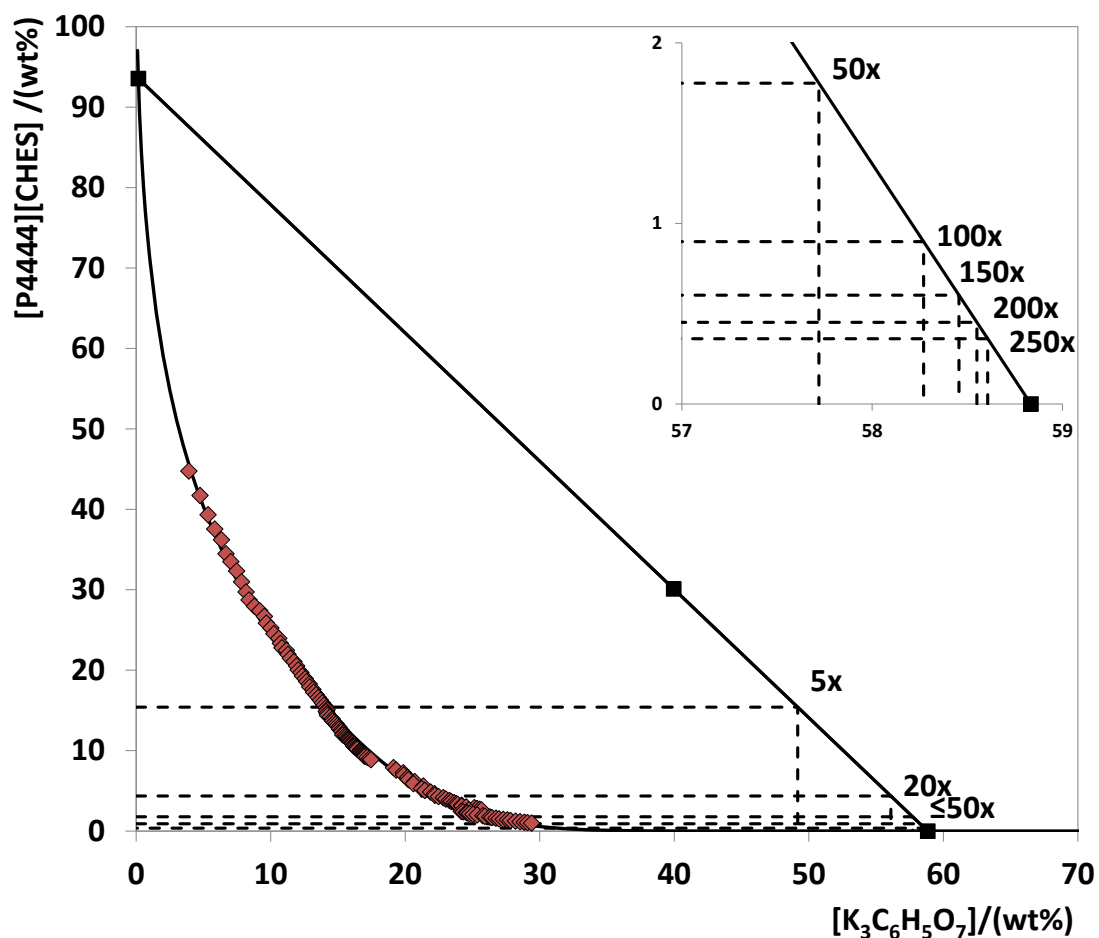


Figure 3.1. Different compositions along the same TL obtained by applying the lever-arm rule which allow to obtain different *CF* for the ABS composed of $K_3C_6H_5O_7 + [P_{4444}][CHES] + \text{water}$.

With the exception of $[P_{4444}][Tricine]$, concentration factors up to 250-fold were achieved for all the IL-based ABS investigated (Table 3.1). The representation of each system with the corresponding TLs and real CF are depicted in *Appendix C*. $[P_{4444}][Tricine]$ is the most hydrophilic GB-IL used in this work and, as shown in Chapter 2.3.2., the respective phase diagram is the farthest from the axis. Consequently, it has a smaller biphasic region and the theoretical information provided by the lever-arm rule is only valid up to concentration factors of 150-fold (*Appendix C*).

Table 3.1. Concentration factors (initial compositions of the mixtures in *Appendix C*) in the ABS composed of [P₄₄₄₄][GB] + K₃C₆H₅O₇ + water. ✓: achieved *CF*; ×: not achieved *CF*.

<i>CF</i>	[P ₄₄₄₄][CHES]	[P ₄₄₄₄][MES]	[P ₄₄₄₄][TES]	[P ₄₄₄₄][HEPES]	[P ₄₄₄₄][Tricine]
5	✓	✓	✓	✓	✓
20	✓	✓	✓	✓	✓
50	✓	✓	✓	✓	✓
100	✓	✓	✓	✓	✓
150	✓	✓	✓	✓	✓
200	✓	✓	✓	✓	×
250	✓	✓	✓	✓	×

After validating the *CF* achievable with each system, the procedure was then repeated by adding an aqueous solution of PSA (at 150 ng/mL) for the mixtures able to lead to a *CF* of 250. These mixture compositions allow to reduce the volume of the IL-rich phase down to a minimum capable of concentrate PSA in a factor of interest while allowing its detection and quantification by SE-HPLC.

As observed in the control experiments, *CF* of 250-fold were also achieved in the presence of PSA for all ABS, except for that composed by [P₄₄₄₄][Tricine] (*Appendix C*). The *CF* were confirmed by weighting both the IL-rich phase and the aqueous solutions containing PSA and by the application of Eq. (8).

Table 3.2. Concentration factor of 250-fold achieved for PSA at the IL-rich phase for the systems composed of GB-IL + K₃C₆H₅O₇ + PSA. ✓: achieved *CF*; ×: not achieved *CF*.

<i>CF</i>	[P ₄₄₄₄][CHES]	[P ₄₄₄₄][MES]	[P ₄₄₄₄][TES]	[P ₄₄₄₄][HEPES]	[P ₄₄₄₄][Tricine]
250	✓	✓	✓	✓	×

The obtained data suggest that PSA can be extracted and concentrated in a single-step up to 250-fold using a large variety of IL-GB ABS. However, in the concentration process it should be taking into account the protein stability and possible losses (which should be avoided).

Figure 3.2. shows the obtained HPLC spectra for the bottom (left) and the top (right) phases of the extractions performed for a CF of 250. For terms of comparison, the HPLC spectrum of an aqueous solution of pure PSA is also provided with the PSA peak appearing between 16 and 18 minutes under the operational conditions used.

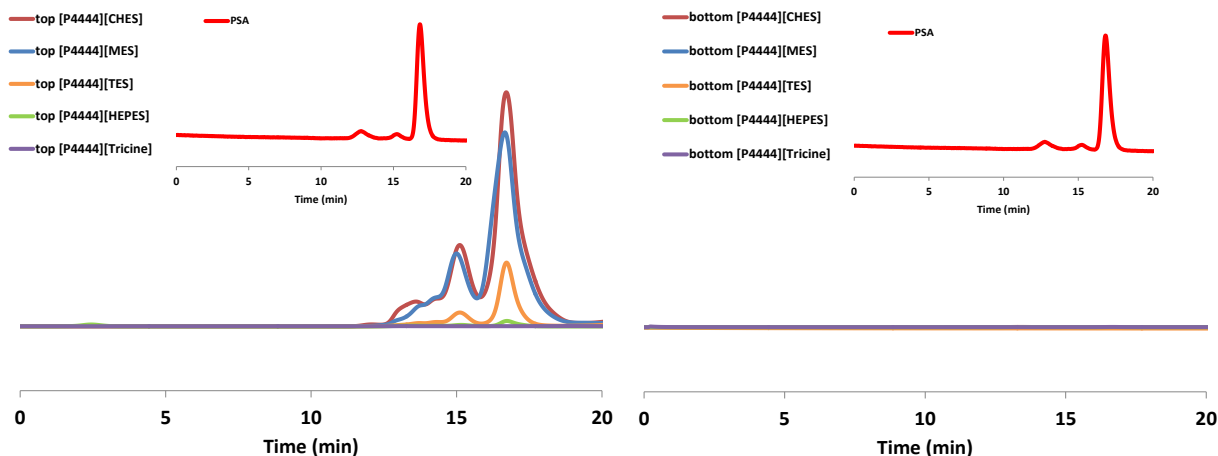


Figure 3.2. HPLC spectra of bottom (left) and top (right) phases for the systems composed of GB-IL + $K_3C_6H_5O_7$ + water/PSA. A spectrum of pure PSA in water ($C = 50$ ng/L) is also provided as an insert for terms of comparison.

The HPLC peak corresponding to PSA is not seen in the bottom phase of any extraction. These results are in agreement with those obtained in Chapter 2.3.3. where extraction efficiencies of 100% of PSA to the top phase have been achieved. On the other hand, the system composed of $[P_{4444}][Tricine]$ results in no peak of PSA detectable by HPLC since the CF of 250-fold was not achieved with this system. In addition, a tendency is clearly seen in the HPLC spectra: the peak intensity, and thus, the PSA concentration, decreases in the following order: $[P_{4444}][CHES] > [P_{4444}][MES] > [P_{4444}][TES] > [P_{4444}][HEPES] > [P_{4444}][Tricine]$. This trend is in close agreement with the PSA losses discussed before and that depend on the hydrophobic character of each IL. It is possible to see that the most intense peak corresponds to the more hydrophobic IL, $[P_{4444}][CHES]$, with the highest $\log(K_{ow})$ value.

3.4. Conclusions

Taking into account the theoretical concentration factors achieved and the results obtained *via* HPLC, PSA can be extracted and concentrated in a single step up to 250-fold and identified with less expensive equipment. The possibility of creating a kit

containing fixed amounts of IL and $K_3C_6H_5O_7$ in order to identify cancer biomarkers as a clinical/analytical strategy is closer now. Nevertheless, the reported results were attained using aqueous solutions of PSA and urine is a complex matrix where coexisting proteins, salts and other metabolites can eventually interfere with the process of extraction and concentration of PSA. The next chapter describes the application of the enhanced systems for the extraction and concentration of PSA from human urine samples.

4. Concentration of PSA from human fluids using optimized IL-based ABS

4.1. Introduction

Human body fluids include urine, blood, peritoneal fluid, cerebrospinal fluid (CSF), sweat, saliva, among others (145). They are remarkable sources of clinical markers and are considered potential tools for clinical diagnosis, stage and grade (145). For instance, cerebrospinal lysozyme can be useful in distinguish between bacterial and viral meningitis (146), while kappa free light chains and CSF in serum support the diagnosis of multiple sclerosis (147). The glycated hemoglobin test in blood is an important tool for diabetes diagnosis and also to predict the risk of cardiovascular diseases (148).

Human body fluids are also clinically relevant in the oncologic field. Several cancer biomarkers have been discovered in the past years in biological fluids (51). They are produced by cancer cells or in response to their presence, and are mainly proteins, such as alpha-Fetoprotein found in blood and used in the diagnosis of liver cancer (Table 1.2.). DNA, metabolites or RNA transcripts are also important tumor biomarkers as in the case of BCR-ABL fusion gene found in blood or in blood marrow used to monitor the status of chronic myeloid leukemia (Table 1.2.). The most acceptable biomarker of CaP is the prostate-specific antigen (PSA). PSA is a glycoprotein produced by epithelial cells of the prostatic gland and reach urine through prostatic ducts. PSA has a cut-off value ≥ 4.0 ng/mL in serum or ≥ 150 ng/mL in urine have been defined as abnormal and can indicate the presence of CaP (68,70). However, the methods used for the purification and quantification of PSA and other cancer biomarkers usually involve immunoassays and fluorescence- and electrochemical-based methods, which are expensive and time-consuming, have low reproducibility, and can lead to false negative results (96).

Albeit in this work GB-IL ABS have been tested with promising results leading to the single-step extraction and concentration of PSA up to 250-fold, the results were obtained with model ABS composed of GB-IL + salt + aqueous solutions of known concentrations of PSA. Urine is a complex matrix composed of a wide variety of salts, proteins and other metabolites (149). In this chapter, ABS composed of [P₄₄₄₄][CHES] (the most promising GB-IL) + salt + real urine were tested to check if the other components of urine interfere with the process of extraction and concentration of PSA, as well as with its identification and quantification.

4.2. Experimental Section

4.2.1. Chemicals

The salt, ILs and water used in this section were described in Chapter 2. PSA used is also described in chapter 2. The salts required for the HPLC analyses were described in Chapter 3.

The material required to perform the SDS-PAGE analysis comprise: tris(hydroxymethyl)aminomethane, PA from Pronalab; sodium dodecyl sulfate, SDS (> 98.5 wt % pure) and glycerol, 99.5 wt % pure, from Sigma-Aldrich; bromophenol blue and acid acetic, 99.8 wt % pure, from Merck; dithiothreitol, DTT (99 wt % pure), from Acros; and methanol, HPLC grade, from Fisher Scientific. The Amersham ECLGel Box, the Amersham ECL Running Buffer (10X), the Amersham ECL Gel 4-20 %, 10 wells, and the Full-Range Rainbow Molecular Weight Marker were acquired from GE Healthcare. The Coomassie Brilliant Blue G-250 was purchased from Sigma-Aldrich.

Urine was obtained from random healthy patients. The used urine was the first urine of the day.

4.2.2. Experimental procedure

4.2.2.1. Size-exclusion HPLC (SE-HPLC)

For the preparation of ABS with real urine, PSA (at 150 ng/mL) was firstly added to urine before its mixture with the salt and IL. Each mixture was vigorously stirred, centrifuged for 10 min, and left to equilibrate for 10 min at $(25 \pm 1)^\circ\text{C}$ to reach the PSA complete partitioning between the coexisting phases. The Falcon tubes used were than centrifuged for 10 min at 5000 rpm at $(25 \pm 1)^\circ\text{C}$. After a careful separation of the phases, both of them were analyzed by SE-HPLC. An aqueous solution of PSA (0.5 g/L) and pure urine were also analyzed. A phosphate buffer solution (1000 mL) was prepared using 47 mL of a Solution A (27.8g NaH_2PO_4), 203 mL of a Solution B (53.65g $\text{Na}_2\text{HPO}_4 \cdot 7\text{H}_2\text{O}$) and 35g of NaCl. Each phase was diluted at a 1:9 (v:v) ratio in the phosphate buffer solution before injection. The HPLC conditions used in this step were described in Chapter 3.

4.2.2.2. Sodium dodecyl sulphate polyacrylamide gel electrophoresis (SDS-PAGE)

The protein profile of urine was determined by SDS-PAGE. The urine samples were diluted in the order of 1:1 (v:v) in a dissociation sample buffer constituted by: 2.5 mL of 0.5 M Tris-HCl pH 6.8, 4.0 mL of 10 % (w:v) SDS solution, 2.0 mL of glycerol, 2.0 mg of bromophenol blue and 310 mg of dithiothreitol (DTT). This overall solution was heated at 95 °C for 5 min to reduce the disulphide linkages and to denature the proteins. This step allows to overcome some forms of the tertiary protein folding and to break up the quaternary proteins structure. Electrophoresis was run on polyacrylamide gels (stacking: 4 % and resolving: 20 %) with a running buffer consisting in 250 mM TrisHCl, 1.92 M glycine, 1 % SDS. The gels were stained with a solution of Coomassie Brilliant Blue G-250 0.1 % (w:v), methanol 50 % (v:v), acetic acid 7 % (v:v) and water 42.9 % (v:v), in an orbital shaker at a moderate speed overnight at room temperature. The destaining of the gel was done using a solution containing acetic acid 7 % (v:v), methanol 20 % (v:v) and water 73 % (v:v) in an orbital shaker at a moderate speed until remove all the excess of dye. SDS-PAGE Molecular Weight Standards, Marker molecular weight full-range (VWR), were used as protein standards.

4.3. Results and discussion

4.3.1. Concentration of PSA from human urine samples

In the previous chapter, it has been demonstrated that PSA can be concentrated up to 250-fold in ABS composed of [P₄₄₄₄][CHES], [P₄₄₄₄][MES], [P₄₄₄₄][HEPES] and [P₄₄₄₄][TES] + salt + aqueous solution containing PSA at a concentration of 150 ng/mL. However, HPLC analyses of the IL-rich phase revealed a tendency for obtaining higher peaks with the ABS composed of more hydrophobic GB-ILs, meaning less losses of protein. Taking into account these results, [P₄₄₄₄][CHES], the most promising GB-IL used, was selected to be tested in the extraction and concentration ($CF = 250$) of PSA from human urine samples.

Figure 4.1 represents the macroscopic appearance of the extraction performed with [P₄₄₄₄][CHES] + salt + human urine (150 ng/mL of PSA added). The left side of the figure shows the ABS after being vigorously stirred, while the right side represents the same ABS after being centrifuged for 10 mins (5000 rpm) and being left in equilibrium for 15 minutes at 25° C ($\pm 1^\circ$ C). It is possible to see the formation of a low volume IL-

rich phase in the top of the ABS (the phase in which PSA is concentrated) and a high volume salt rich-phase in the bottom.



Figure 4.1. ABS composed of $[P_{4444}][CHES]$ + salt + human urine (150 ng/mL of PSA added). ABS after being vigorously stirred (on the left) and after being centrifuged for 10 min and left in equilibrium for 15 min (on the right).

By the weighting of the two phases it was observed an increase in the CF, from 250 to 260, in the presence of urine and when compared with the model systems previously investigated. This trend is somehow expected since urine is a more complex matrix rich in other salts that result in stronger salting-out phenomenon. Even so, higher concentration factors are preferable since they will allow an improved detection and quantification of PSA.

The top and the bottom phases were analyzed by SE-HPLC, together with a sample of pure PSA and human urine for terms of comparison. Figure 4.2. depicts the SE-HPLC profile of pure PSA in water, in human urine and in the top and bottom phases of an extraction performed with $[P_{4444}][CHES]$ + salt + human urine.

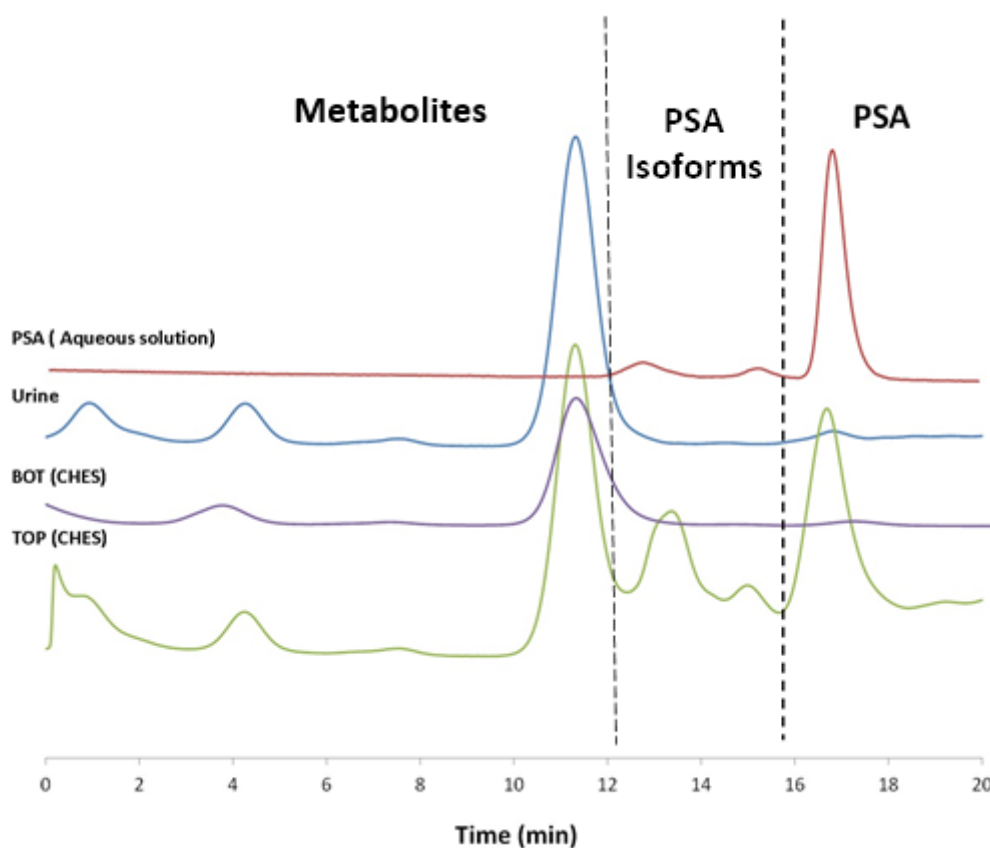


Figure 4.2. SE-HPLC profile of pure PSA in aqueous solution, human urine and in the top and bottom phases of an ABS composed of [P₄₄₄₄][CHES] + salt + human urine (150 ng/mL of PSA added).

The peak of PSA in aqueous solution appearing between 16 and 18 minutes is clearly seen. This peak is also seen in the top phase of the [P₄₄₄₄][CHES]-based ABS and is not found in urine and in the bottom phase of the [P₄₄₄₄][CHES]-based ABS. Therefore, PSA has been extracted to the GB-IL-rich phase and concentrated up to a factor that allows it to be analyzed by a less expensive and less laborious equipment, such as SE-HPLC. Even so, the HPLC profiles reveal that there are two other small peaks between 12 and 16 minutes. PSA is a glycoprotein that can be found in several isoforms with small differences of molecular weight. A previous study already revealed a similar profile of PSA by SE-HPLC where this small band is identified as bPSA (85). In the top phase of the ABS, these peaks have however a higher intensity than the initial aqueous solution of PSA, meaning that PSA isoforms were also concentrated by the system composed of GB-ILs. On the other hand, some of the contaminant metabolites of urine are extracted for the opposite phase of the investigated ABS, “cleaning” therefore the phase in which PSA is concentrated. Both trends can be seen as a window of opportunity to create an even more

accurate PSA test because the PSA isoforms are useful in CaP differential diagnosis (to distinguish between CaP and BPH and to predict the cancer aggressiveness) (5,84,85).

In the urine sample, there are a series of other metabolites (with retention times between 11 and 12 min) that further appear in the bottom and top phases of the investigated ABS. Figure 4.3 - C. depicts the SDS-PAGE of urine where it possible to see a band near 45 kDa. This band is possibly associated to alpha-1-antitrypsin, a protease inhibitor that protect tissues from enzymes of inflammatory cells (150).

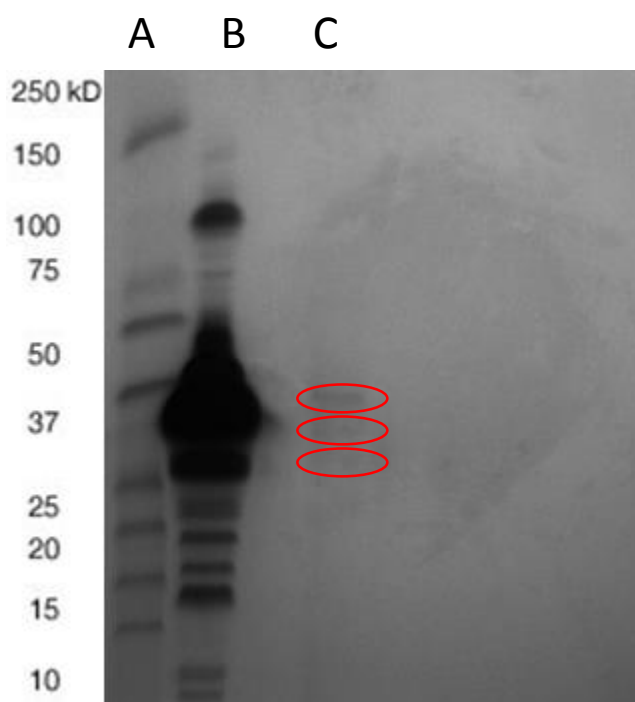


Figure 4.3. SDS-PAGE analyses. A: Molecular Wweight marker; B: Pure human serum; C: Pure human urine.

It is also possible to see two less intense bands between possible alpha-1-antitrypsin and 25 kDa. Thus, these two bands can correspond to proteins or other metabolites between this molecular weight, such as apoprotein A₁ or apha 1 microglobulin that usually appears between this range (150). However, it is just a prediction and more investigation has to be done to clarify these results, using for instance mass spectrometry.

4.4. Conclusions

The objective of this MSc thesis was achieved since a *CF* of 250-fold of PSA from human urine was achieved allowing its quantification by HPLC. It is possible to believe now that a new test for the CaP early detection is closer. However, much more

experiments have to be conducted in order to identify the urine contaminants and whether they are interfering with the protein mass balance. Moreover, these analyses should be combined with urine samples of a large range of healthy volunteers and CaP patients to see if exists a growing trend in the peak intensity according to the disease status.

5. Final remarks and future work

The results obtained in this work lead us to foresee a possible revolution in the early-stage detection of CaP. The gathered data show that it is possible to completely extract PSA to the IL-rich phase, in a single step, and to concentrate it up to 250-fold from urine samples. This work also shows that PSA can be identified and quantified by SE-HPLC, meaning that urine (non-invasive sampling) can be used in the future for CaP diagnosis using less laborious and less expensive equipment, although much more work is still needed to correlate the PSA levels in urine and the probability of CaP occurrence. In this work, a calibration curve for PSA by SE-HPLC is still in need and should be performed in the near future in order to test the quantitative approach. It is also of crucial importance to analyze a broad number of urine samples from healthy volunteers and CaP patients in different stages of the disease to validate the hypothesis that our test is useful for CaP early detection. We also believe that it is possible to increase the sensibility of our test for the selective and concomitant extraction of PSA and prostatic acid phosphatase (an additional CaP biomarker). In summary, much more investigation is still required, but the promising preliminary results obtained lead us to believe that in a short/medium period it will be possible to develop a new KIT for CaP early-stage detection.

A market-study was finally conducted aiming at our possible competitors in the market. In fact, 4 possible competitors have been identified: (i) an academic study being carried out by Dr. Goreti Sales, from University of Porto, Portugal, that is developing a biosensor for detecting some types of cancer in a cheap, painless and quick way; (ii) the PRIMA[®] company which introduced in the market a simple sensor which uses a drop of blood performing an immunoassay (151). Nevertheless, this test has led to a large level of reported false positive results; (iii) the Craig Medical Distributions Inc. which offered a semi-quantitative immunoassay to be carried out at the patient's homes. This advantage can also be seen as a disadvantageous factor because once the test is performed at the patient's home, some limitations in what concerns sample loss, contamination and preservation can be addressed (152). In addition, a unit of this test costs more than 40 €.

In summary, our biggest competitor is the PSA blood test from PRIMA[®]. This is the most used test for CaP early detection due to its high accuracy and reliability. However, it is a time consuming test that requires sample blood collection and specific and highly expensive equipment (specific antibodies and immunoassays). In Portugal, a PSA blood test costs approximately 20.91 €. Competitively, our test will cost

approximately 2.92 €. Moreover, we are proposing the use of urine samples instead of blood, representing also a non-invasive approach. Finally, we suggest the use of HPLC for PSA quantification instead of immunoassays allowing the broadening of this technique to a larger number of clinical laboratories.

In Portugal, there are no available statistics for the number of PSA blood tests performed *per* year. However, based on an estimation suggested by Dr. Pereira B., an urologist from *Centro Hospitalar Cova da Beira*, Portugal, the 50-75 years old male population in Portugal do a PSA analysis in each year. There are 1440,351 males in Portugal with that age range (153). In this context, the substitution of the current PSA blood test by our approach would result in a money saving of 25 M€ (only in Portugal). If we apply this type of calculation to a largest country, such as USA, where more than 25 million tests are done *per* year (154), there will be a reduction of 450 M€ associated to the PSA screening *per* year. Those are huge amounts of money that can be used by the National Health Associations to provide better conditions to their patients or even, in a large term and optimized perspective, to be invested in cancer research.

6. References

- (1) World Health Organization. (2012) Prostate Cancer Estimated Incidence, Mortality and Prevalence Worldwide in 2012. Accessed on October 5, 2015; Available from: http://globocan.iarc.fr/Pages/fact_sheets_cancer.aspx.
- (2) Ilic, D., Neuberger, M. M., Djulbegovic, M., and Dahm, P. (2013) Screening for prostate cancer. *The Cochrane Database of Systematic Reviews* 1, 1–76.
- (3) Drevin, L., Carlsson, S., Garmo, H., Bill-axelson, A., and Loeb, S. (2014) Nationwide Population Based Study of Infections after Transrectal Ultrasound Guided Prostate Biopsy. *Journal of urology* 192, 1116 – 1122.
- (4) National Cancer Institute at the National Institutes of Health. (2012) Tumor Markers. Accessed on November 15, 2014; Available from: <http://www.cancer.gov/cancertopics/factsheet/detection/tumor-markers>.
- (5) Stephan, C., Ralla, B., and Jung, K. (2014) Prostate-specific antigen and other serum and urine markers in prostate cancer. *Biochimica et Biophysica Acta* 1846, 99–112.
- (6) Fortin, T., Salvador, A., Charrier, J. P., Lenz, C., Lacoux, X., Morla, A., Choquet-Kastylevsky, G., and Lemoine, J. (2009) Clinical quantitation of prostate-specific antigen biomarker in the low nanogram/milliliter range by conventional bore liquid chromatography-tandem mass spectrometry (multiple reaction monitoring) coupling and correlation with ELISA tests. *Molecular & Cellular Proteomics: MCP* 8, 1006–1015.
- (7) Acevedo, B., Perera, Y., Ruiz, M., Rojas, G., Benítez, J., Ayala, M., and Gavilondo, J. (2002) Development and validation of a quantitative ELISA for the measurement of PSA concentration. *Clinica Chimica Acta* 317, 55–63.
- (8) Adel Ahmed, H., and Azzazy, H. M. E. (2013) Power-free chip enzyme immunoassay for detection of prostate specific antigen (PSA) in serum. *Biosensors & bioelectronics* 49, 478–484.
- (9) Freire, M. G., Cláudio, A. F. M., Araújo, J. M. M., Coutinho, J. A. P., Marrucho, I. M., Canongia Lopes, J. N., and Rebelo, L. P. N. (2012) Aqueous biphasic systems: a boost brought about by using ionic liquids. *Chemical Society reviews* 41, 4966–4995.
- (10) Bubalo, M. C., Radošević, K., Redovniković, I. R., Halambek, J., and Srček, V. G. (2014) A brief overview of the potential environmental hazards of ionic liquids. *Ecotoxicology and Environmental Safety* 99, 1–12.
- (11) Hou, X.-D., Liu, Q.-P., Smith, T. J., Li, N., and Zong, M.-H. (2013) Evaluation of toxicity and biodegradability of cholinium amino acids ionic liquids. *PLoS one* 8, 1–7.
- (12) International Agency for Research on Cancer. (2012) World Cancer Factsheet. Accessed on November 15, 2014; Available from: http://publications.cancerresearchuk.org/downloads/product/CS_REPORT_WORLD.pdf.
- (13) American Cancer Society (2015) Cancer facts and figures. Accessed on July 14, 2015; Available from: <http://www.cancer.org/acs/groups/content/@editorial/documents/document/acspc-044552.pdf>.
- (14) Direção Geral de Saúde. (2013) Portugal: Doenças Oncológicas em Números. Accessed on November 15, 2014; Available from: <http://www.rorcentro.com.pt/Data/RORCentro/241/i019431.pdf>.
- (15) International Agency for research on cancer (2012) Prostate Cancer mortality. Accessed on July 14, 2015; Available from: <http://globocan.iarc.fr/ia/world/atlas.html>.

- (16) International Agency for Research on Cancer. (2008) Mechanisms of Carcinogenesis 3. Accessed on November 17, 2014; Available from: http://www.iarc.fr/en/publications/pdfs-online/wcr/2008/wcr_2008_5.pdf.
- (17) World Health Organization. (2013) International Classification of Diseases for Oncology (ICDO).
- (18) Oliveira, P. A., Colaço, A., Chaves, R., and Guedes-Pinto, H. (2007) Chemical carcinogenesis. *Anais da Academia Brasileira de Ciência* 79, 593–616.
- (19) Trosko, J. E. (2003) The Role of Stem Cells and Gap Junctional Intercellular Communication in Carcinogenesis. *Journal of Biochemistry and Molecular Biology* 36, 43–48.
- (20) Thomas, R. K., Baker, A. C., DeBiasi, R. M., Winckler, W., Laframboise, T., Lin, W. M., Wang, M., Feng, W., Zander, T., MacConaill, L., Macconnaill, L. E., Lee, J. C., Nicoletti, R., Hatton, C., Goyette, M., Girard, L., Majmudar, K., Ziaugra, L., Wong, K.-K., Gabriel, S., Beroukhim, R., Peyton, M., Barretina, J., Dutt, A., Emery, C., Greulich, H., Shah, K., Sasaki, H., Gazdar, A., Minna, J., Armstrong, S. a, Mellinghoff, I. K., Hodi, F. S., Dranoff, G., Mischel, P. S., Cloughesy, T. F., Nelson, S. F., Liau, L. M., Mertz, K., Rubin, M. a, Moch, H., Loda, M., Catalona, W., Fletcher, J., Signoretti, S., Kaye, F., Anderson, K. C., Demetri, G. D., Dummer, R., Wagner, S., Herlyn, M., Sellers, W. R., Meyerson, M., and Garraway, L. a. (2007) High-throughput oncogene mutation profiling in human cancer. *Nature genetics* 39, 347–351.
- (21) Heisterkamp, N., Stam, K., and Groffen, J. (1985) Structural organization of the bcr gene and its role in Ph¹ translocation. *Nature publish group* 315, 758–761.
- (22) Berenblum, I., and Shubik, P. (1974) The role of croton oil applications, associated with a single painting of a carcinogen, in tumor induction of the mouse's skin. *British Journal Cancer* 1, 379–382.
- (23) Colburn, N. H., Matrisian, L., Walker, C., and Trosko, J. E. (2001) Commentary: Is the Concept of Tumor Promotion' a Useful Paradigm? *Wiley-Liss Journals: Molecular Carcinogenesis* 30, 131–137.
- (24) Macleod, K. (2000) Tumor suppressor genes. *Current Opinion in Genetics & Development* 10, 81–93.
- (25) Levine, A. J. (1997) p53, the Cellular Gatekeeper for Growth and Division. *Cell* 88, 323–331.
- (26) Williams, G. M. (2001) Mechanisms of chemical carcinogenesis and application to human cancer risk assessment. *Toxicology* 166, 3–10.
- (27) Vincent, T. L., and Gatenby, R. A. (2008) An evolutionary model for initiation, promotion, and progression in carcinogenesis. *International Journal of Oncology* 32, 729–737.
- (28) Knudson, A. G. (1971) Mutation and Cancer: Statistical Study of Retinoblastoma. *Proceedings of the National Academy of Sciences* 68, 820–823.
- (29) Chau, B. N., and Wang, J. Y. J. (2003) Coordinated regulation of life and death by RB. *Nature reviews. Cancer* 3, 130–138.
- (30) Nagy, R., Sweet, K., and Eng, C. (2004) Highly penetrant hereditary cancer syndromes. *Nature publish group* 23, 6445–6470.
- (31) Jasperson, K. W., Tuohy, T. M., Neklason, D. W., and Burt, R. W. (2010) Hereditary and familial colon cancer. *Gastroenterology* 138, 2044–2058.
- (32) Hoeijmakers, J. H. J. (2009) DNA damage, aging, and cancer. *The New England journal of medicine* 361, 1475–1485.
- (33) Vasto, S., Carruba, G., Lio, D., Colonna-Romano, G., Di Bona, D., Candore, G., and Caruso, C. (2009) Inflammation, ageing and cancer. *Mechanisms of ageing and development* 130, 40–45.

- (34) Zane, L., Sharma, V., and Misteli, T. (2014) Common features of chromatin in aging and cancer: cause or coincidence? *Cell Press:trends in cell Biology* 24, 686–694.
- (35) Takai, D., and Jones, P. A. (2002) Comprehensive analysis of CpG islands in human chromosomes 21 and 22. *Proceedings of the National Academy of Sciences of the United States of America* 99, 3740–3745.
- (36) Herman, J. G., Latif, F., Weng, Y., Lerman, M. I., Zbar, B., Liu, S. U. E., Samidii, D., Duan, D. R., Gnarrat, J. R., Linehan, W. M., and Baylin, S. B. (1994) Silencing of the VHL tumor-suppressor gene by DNA methylation in renal carcinoma. *Proceedings of the National Academy of Sciences* 91, 9700–9704.
- (37) Prentice, R. L., Caan, B., Chlebowski, R. T., Ockene, J. K., Karen, L., Limacher, M. C., Manson, J. E., Linda, M., Paskett, E., Phillips, L., Robbins, J., Rossouw, J. E., Gloria, E., Shikany, J. M., Stefanick, M. L., Cynthia, A., Horn, L. Van, Vitolins, M. Z., Wallace, R. B., Anderson, G. L., Annlouise, R., Beresford, S. A. A., Black, H. R., Robert, L., Brzyski, R. G., Hays, J., Heber, D., Hsia, J., Hubbell, F. A., Jackson, R. D., Karen, C., Kotchen, J. M., Lacroix, A. Z., Dorothy, S., and Langer, R. D. (2006) Low-Fat Dietary Pattern and Risk of Invasive Breast Cancer. *American Medical Association* 295, 629–642.
- (38) Gammal, E. B., and Carrol, K. K. (1991) Dietary fats. *The American Journal of Clinical Nutrition* 53, 1064–1068.
- (39) Chong, C., Emenaker, N., Indorato, D., and Jones, J. M. (2002) Position of the American Dietetic Association: Health implications of dietary fiber. *The American Dietetic Association* 102, 993–1000.
- (40) World Health Organization–International Agency for Research on Cancer. (2010) Alcohol Consumption and Ethyl Carbamate, in *IARC Monographs on the Evaluation of Carcinogenic Risks to Humans*, p Vol. 96.
- (41) Hogervorst, J. G., Schouten, L. J., Konings, E. J., Brandt, P. A. van den, and Goldbohm, R. A. (2008) Dietary acrylamide intake and the risk of renal cell, bladder, and prostate cancer. *The American Journal of Clinical Nutrition* 87, 1428–1438.
- (42) Jaga, K., and Brosius, D. (1999) Pesticide exposure: human cancers on the horizon. *Reviews on environmental health* 14, 39–50.
- (43) Cross, A. J., and Sinha, R. (2004) Meat-related mutagens/carcinogens in the etiology of colorectal cancer. *Environmental and molecular mutagenesis* 44, 44–55.
- (44) Narayanan, D. L., Saladi, R. N., and Fox, J. L. (2010) Ultraviolet radiation and skin cancer. *International journal of dermatology* 49, 978–986.
- (45) World Health Organization. (2007) Smokeless Tobacco and Some Tobacco-specific N -Nitrosamines, in *IARC Monographs on the Evaluation of Carcinogenic Risks to Humans*, pp 55–60.
- (46) Bianchini, F., Kaaks, R., and Vainio, H. (2002) Weight control and physical activity in cancer prevention. *Obesity Reviews* 3, 5–8.
- (47) Kusters, J. G., van Vliet, A. H. M., and Kuipers, E. J. (2006) Pathogenesis of Helicobacter pylori infection. *Clinical microbiology reviews* 19, 449–490.
- (48) Hariri, S., Unger, E. R., Sternberg, M., Dunne, E. F., Swan, D., Patel, S., and Markowitz, L. E. (2011) Prevalence of genital human papillomavirus among females in the United States, the National Health And Nutrition Examination Survey, 2003–2006. *The Journal of infectious diseases* 204, 566–573.
- (49) National Cancer Institute at the National Institutes of Health (2012) Biomarkers. Accessed on November 17, 2014; Available from: <http://www.cancer.gov/publications/dictionaries/cancer-terms?cdrid=45618>.

- (50) Stavridis, S., Saidi, S., Lj, L., Dohcev, S., and Spasovski, G. (2010) Screening for prostate cancer: a controversy or fact. *Hippokratia* 14, 170–175.
- (51) National Cancer Institute at the National Institutes of Health. (2012) Tumor Markers. Accessed on November 15, 2015; Available from: <http://www.cancer.gov/cancertopics/factsheet/detection/tumor-markers>.
- (52) Bostwick, D. G., Burke, H. B., Djakiew, D., Euling, S., Ho, S., Landolph, J., Morrison, H., Sonawane, B., Shifflett, T., Waters, D. J., and Timms, B. (2004) Human prostate cancer risk factors. *Cancer* 101, 2371–2490.
- (53) Dasgupta, S., Srinidhi, S., and Vishwanatha, J. K. (2012) Oncogenic activation in prostate cancer progression and metastasis: Molecular insights and future challenges. *Journal of carcinogenesis* 11, 1–18.
- (54) Tammela, T. L. J., Ciatto, S., Nelen, V., Kwiatkowski, M., Lujan, M., Lilja, H., Zappa, M., Ph, D., Denis, L. J., Recker, F., Berenguer, A., Määttänen, L., Bangma, C. H., Aus, G., Villers, A., Rebillard, X., Kwast, T. Van Der, Blijenberg, B. G., Moss, S. M., Koning, H. J. De, Auvinen, A., and Investigators, E. (2009) Screening and Prostate-Cancer Mortality in a Randomized European Study. *The New England journal of medicine* 360, 1320–1328.
- (55) Nam, R. K., Saskin, R., Lee, Y., Liu, Y., Law, C., Klotz, L. H., Loblaw, D. A., Trachtenberg, J., Stanimirovic, A., Simor, A. E., Seth, A., Urbach, D. R., and Narod, S. a. (2010) Increasing hospital admission rates for urological complications after transrectal ultrasound guided prostate biopsy. *The Journal of urology* 183, 963–968.
- (56) Reiner, A., Cheng, G., Sugiyama, N., Alonso-magdalena, P., Bro, C., Warner, M., and Gustafsson, J.-åke. (2009) A role for epithelial-mesenchymal transition in the etiology of benign prostatic hyperplasia. *Proceedings of the National Academy of Sciences* 106, 2859–2863.
- (57) Catalona, W. J. (2012) The “True” History of the Discovery of Prostate-specific Antigen. *The ASCO Post* 3, 98–99.
- (58) Alexander B. Gutman. (1968) The development of the acid phosphate test for prostatic carcinoma. *The New York Academy of Medicine* 44, 63–76.
- (59) Yam, L. T., Winkler, C. F., Janckila, A. J., Li, C. Y., and Lam, K. W. (1983) Prostatic Cancer Presenting as Metastatic Adenocarcinoma of Undetermined Origin. *Cancer* 51, 283–287.
- (60) Graddis, T. J., McMahan, C. J., Tamman, J., Page, K. J., and Trager, J. B. (2011) Prostatic acid phosphatase expression in human tissues. *International journal of clinical and experimental pathology* 4, 295–306.
- (61) Flocks, R., Urich, V., Patel, C., and Opitz, J. (1960) Studies on antigenic proprieties of prostatic tissue. *Journal of urology* 84, 134–143.
- (62) Flocks, R., Bandhaur, K., Patel, C., and Begley, B. (1962) Studies on spermagglutinating antibodies in Antihuman prostate sera. *Journal of Urology* 87, 475–478.
- (63) Hara, M., Koyanagi, Y., Inoue, T., and Fukuyama, T. (1971) Some physico-chemical characteristics of “-semipoprotein”, an antigenic component specific for human seminal plasma. Forensic immunological study of body fluids and secretion. *The japanese journal of legal medicine* 25, 322–324.
- (64) Rao, A. R., Motiwala, H. G., and Karim, O. M. (2008) The discovery of prostate-specific antigen. *BJU international* 101, 5–10.
- (65) Wang, M. C., Valenzuela, L. A., Murphy, G. P., and Chu, T. M. (2002) Purification of a Human Prostate Specific Antigen. *The Journal of Urology* 167, 1226–1230.

- (66) Stamey, T. A., Hay, A. R., McNeal, J. E., Freiha, F. S., and Redwine, E. (1987) Prostate-specific antigen as a serum marker for adenocarcinoma of the prostate. *The New England Journal of Medicine* 317, 909 – 916.
- (67) Catalona, W. J., Smith, D. S., Doods, K. M., Coplen, D. E., Petros, J. A., and Andriole, G. L. (1991) Measurement of prostate-specific antigen in serum as a screening test for prostate cancer. *The New England Journal of Medicine* 324, 1156–1161.
- (68) Bolduc, S., Lacombe, L., Naud, A., Grégoire, M., Fradet, Y., and Tremblay, R. R. (2007) Urinary PSA: a potential useful marker when serum PSA is between 2.5 ng/mL and 10 ng/mL. *Canadian Urological Association Journal* 1, 377–381.
- (69) Aprikian, A. (2007) PSA for prostate cancer detection: In serum, in urine or both? *Canadian Urological Association Journal* 1, 382–382.
- (70) Heidenreich, A., Bastian, P. J., Bellmunt, J., Bolla, M., Joniau, S., van der Kwast, T., Mason, M., Matveev, V., Wiegel, T., Zattoni, F., and Mottet, N. (2014) EAU guidelines on prostate cancer. Part 1: Screening, Diagnosis, and Local Treatment with Curative Intent - Update 2013. *European Association of Urology* 65, 124–137.
- (71) Luboldt, H.-J., Schindler, J. F., and Rübber, H. (2007) Age-Specific Reference Ranges for Prostate-Specific Antigen as a Marker for Prostate Cancer. *European Association of Urology* 5, 38–48.
- (72) Gretzer, M. B., and Partin, A. W. (2002) PSA Levels and the Probability of Prostate Cancer on Biopsy. *European Urology Supplements* 1, 21–27.
- (73) Pierorazio, P. M., Walsh, P. C., Partin, A. W., and Epstein, J. I. (2014) Prognostic Gleason grade groupin: data based on the modified Gleason scoring system. *British Journal of Urology* 111, 753–760.
- (74) Linton, K. D., and Catto, J. W. F. (2013) Prostate cancer. *Renal and Urological Surgery II* 31, 516–522.
- (75) Richardson, T. D., Wojno, K. J., England, B. G., Henricks, W. H., and Giacherio, A. (1996) Half-life determination of serum free prostate-specific antigen following radical retropubic prostatectomy. *Urology* 48, 40–44.
- (76) Thorek, D. L. J., Evans, M. J., Carlsson, S. V, Ulmert, D., and Lilja, H. (2013) Prostate-specific kallikrein-related peptidases and their relation to prostate cancer biology and detection. Established relevance and emerging roles. *Thrombosis and haemostasis* 110, 484–492.
- (77) Balk, S. P., Ko, Y.-J., and Bubley, G. J. (2003) Biology of Prostate-Specific Antigen. *Journal of Clinical Oncology* 21, 383–391.
- (78) Lilja, H. (2003) Biology of prostate-specific antigen. *Urology* 62, 27–33.
- (79) Ménez, R., Michel, S., Muller, B. H., Bossus, M., Ducancel, F., Jolivet-Reynaud, C., and Stura, E. A. (2008) Crystal structure of a ternary complex between Human prostate-specific antigen, its Substrate Acyl Intermediate and an Activating Antibody. *Journal of Molecular Biology* 376, 1021–1033.
- (80) Velonas, V. M., Woo, H. H., Remedios, C. G. Dos, and Assinder, S. J. (2013) Current Status of Biomarkers for Prostate Cancer. *International Journal of Molecular Sciences* 14, 11034–11060.
- (81) Parracino, A., Neves-Petersen, M. T., di Gennaro, A. K., Pettersson, K., Lövgren, T., and Petersen, S. B. (2010) Arraying prostate specific antigen PSA and Fab anti-PSA using light-assisted molecular immobilization technology. *Protein science: a publication of the Protein Society* 19, 1751–1759.

- (82) Lilja, H., Ulmert, D., and Vickers, A. J. (2008) Prostate-specific antigen and prostate cancer: prediction, detection and monitoring. *Nature reviews. Cancer* 8, 268–278.
- (83) Factor-binding, G., Papa, M. Z., Pariente, C., and Goldwasser, B. (1993) Serum Insulin-Like Growth Factor-Binding Protein-2 (IGFBP-2) Is Increased and IGFBP-3 is Decreased in Patients with Prostate Cancer: Correlation with Serum Prostate-Specific Antigen. *Journal of Clinical Endocrinology and Metabolism* 77, 229–233.
- (84) Christensson, A., Laurell, C.-B., and Lilja, H. (1990) Enzymatic activity of prostate-specific antigen and its reactions with extracellular serine proteinase inhibitors. *European Journal of Biochemistry* 194, 755–763.
- (85) Mikolajczyk, S. D., Millar, L. S., Wang, T. J., Rittenhouse, H. G., Wolfert, R. L., Marks, L. S., Song, W., Wheeler, T. M., and Slawin, K. M. (2000) “BPSA”, a specific molecular form of free prostate-specific antigen, is found predominantly in the transition zone of patients with nodular benign prostatic hyperplasia. *Adult urology* 4295, 41–45.
- (86) Stephan, C., Vincendeau, S., Houlgatte, A., Cammann, H., Jung, K., and Semjonow, A. (2013) Multicenter Evaluation of [-2]Prostate-Specific Antigen and the Prostate Health Index for Detecting Prostate Cancer. *Clinica Chimica Acta* 59, 306–314.
- (87) Woodrum, D. L., Brawer, M. K., Partin, A. W., Catalona, W. J., and Southwick, P. C. (1998) Interpretation of Free Prostate Specific Antigen Clinical research studies for the detection of Prostate Cancer. *The Journal of Urology* 159, 5–12.
- (88) Arcangeli, C. G., Smith, D. S., Ratliff, T. L., and Catalona, W. J. (1997) Stability of Serum total and Free Prostate Specific Antigen under varying storage intervals and temperature. *The Journal of urology* 158, 2182 – 2187.
- (89) Reed, A. B., Ankerst, D. P., Leach, R. J., Vipraio, G., Thompson, I. M., and Parekh, D. J. (2008) Total Prostate Specific Antigen stability confirmed after long-term storage of serum at -80 °C. *The Journal of Urology* 180, 534–538.
- (90) Ledge, J. J. C., Son, D. T., Ril, H. V. E. R., Son, P. C. L., and Ley, I. E. (1999) The stability of free and bound prostate-specific antigen. *British Journal of Urology* 84, 810–814.
- (91) Sumi, S., Arai, K., and Yoshida, K. (2001) Separation methods applicable to prostate cancer diagnosis and monitoring therapy. *Journal of Chromatography B: Biomedical Sciences and Applications* 764, 445–455.
- (92) Kalyvas, M., Zammit, S., and Chem, C. (1996) Ultrasensitive detection of prostate-specific antigen by a time-resolved immunofluorometric assay and the Immulite immunochemiluminescent third-generation assay: potential applications in prostate and breast cancers. *Clinical Chemistry* 42, 675–684.
- (93) Tang, L., Dong, C., and Ren, J. (2010) Highly sensitive homogenous immunoassay of cancer biomarker using silver nanoparticles enhanced fluorescence correlation spectroscopy. *Talanta* 81, 1560–1567.
- (94) Uludag, Y., and Tothill, I. E. (2012) Cancer Biomarker Detection in Serum Samples Using Surface Plasmon Resonance and Quartz Crystal Microbalance Sensors with Nanoparticle Signal Amplification. *Analytical Chemistry-American Cancer Society* 84, 5898–5904.
- (95) Oh, S. W., Kim, Y. M., Kim, H. J., Kim, S. J., Cho, J.-S., and Choi, E. Y. (2009) Point-of-care fluorescence immunoassay for prostate specific antigen. *Clinica chimica acta; international journal of clinical chemistry* 406, 18–22.

- (96) Poon, C.-Y., Chan, H.-M., and Li, H.-W. (2014) Direct detection of prostate specific antigen by darkfield microscopy using single immunotargeting silver nanoparticle. *Sensors and Actuators B: Chemical* 190, 737–744.
- (97) Peter, J., Unverzagt, C., Lenz, H., and Hoesel, W. (1999) Purification of prostate-specific antigen from human serum by indirect immunosorption and elution with a haptin. *Analytical biochemistry* 273, 98–104.
- (98) Kawinski, E., Levine, E., and Chadha, K. (2002) Thiophilic interaction chromatography facilitates detection of various molecular complexes of prostate-specific antigen in biological fluids. *The Prostate* 50, 145–153.
- (99) Soukka, T., Antonen, K., Ha, H., and Pelkkikangas, A. (2003) Highly sensitive immunoassay of free prostate-specific antigen in serum using europium(III) nanoparticle label technology. *Clinica Chimica Acta* 328, 45–58.
- (100) Satheesh Babu, a K., Vijayalakshmi, M. a, Smith, G. J., and Chadha, K. C. (2008) Thiophilic-interaction chromatography of enzymatically active tissue prostate-specific antigen (T-PSA) and its modulation by zinc ions. *Journal of chromatography B* 861, 227–235.
- (101) Kumar, V., Hassan, M. I., Singh, A. K., Dey, S., Singh, T. P., and Yadav, S. (2009) Strategy for sensitive and specific detection of molecular forms of PSA based on 2DE and kinetic analysis: a step towards diagnosis of prostate cancer. *Clinica chimica acta; international journal of clinical chemistry* 403, 17–22.
- (102) Zhang, W., Leinonen, J., Kalkkinen, N., Dowell, B., and Stenman, U.-H. (1995) Purification and Characterization of Different Molecular Forms of Prostate-Specific Antigen in Human Seminal Fluid. *Clinical Chemistry - Enzymes and Protein Markers* 41, 1567–1573.
- (103) Järås, K., Adler, B., Tojo, A., Malm, J., Marko-Varga, G., Lilja, H., and Laurell, T. (2012) Porous silicon antibody microarrays for quantitative analysis: measurement of free and total PSA in clinical plasma samples. *Clinica chimica acta; international journal of clinical chemistry* 414, 76–84.
- (104) Freire, M. G., Pereira, J. F. B., Francisco, M., Rodríguez, H., Rebelo, L. P. N., Rogers, R. D., and Coutinho, J. A. P. (2012) Insight into the interactions that control the phase behaviour of new aqueous biphasic systems composed of polyethylene glycol polymers and ionic liquids. *Chemistry (Weinheim an der Bergstrasse, Germany)* 18, 1831–1839.
- (105) Albertsson, P.-A. (1958) Particle fractionation in liquid two-phase systems: The composition of some phase systems and the behaviour of some model particles in them application to the isolation of cell walls from microorganisms. *Biochimica et Biophysica Acta* 27, 378–395.
- (106) Naganagouda, K., and Mulimani, V. H. (2008) Aqueous two-phase extraction (ATPE): An attractive and economically viable technology for downstream processing of *Aspergillus oryzae* α -galactosidase. *Process Biochemistry* 43, 1293–1299.
- (107) Ventura, S. P. M., de Barros, R. L. F., de Pinho Barbosa, J. M., Soares, C. M. F., Lima, Á. S., and Coutinho, J. A. P. (2012) Production and purification of an extracellular lipolytic enzyme using ionic liquid-based aqueous two-phase systems. *Green Chemistry* 14, 734–740.
- (108) Dreyer, S., Salim, P., and Kragl, U. (2009) Driving forces of protein partitioning in an ionic liquid-based aqueous two-phase system. *Biochemical Engineering Journal* 46, 176–185.
- (109) Deive, F. J., Rodríguez, A., Rebelo, L. P. N., and Marrucho, I. M. (2012) Extraction of *Candida antarctica* lipase A from aqueous solutions using imidazolium-based ionic liquids. *Separation and Purification Technology* 97, 205–210.

- (110) Deive, F. J., Rodríguez, A., Pereiro, A. B., Araújo, J. M. M., Longo, M. A., Coelho, M. A. Z., Lopes, J. N. C., Esperança, J. M. S. S., Rebelo, L. P. N., and Marrucho, I. M. (2011) Ionic liquid-based aqueous biphasic system for lipase extraction. *Green Chemistry* 13, 390–396.
- (111) Ruiz-Angel, M. J., Pino, V., Carda-Broch, S., and Berthod, A. (2007) Solvent systems for countercurrent chromatography: an aqueous two phase liquid system based on a room temperature ionic liquid. *Journal of Chromatography A* 1151, 65–73.
- (112) Walden, P. (1914) Molecular weights and electrical conductivity of several fused salts. *Bulletin of the Russian Academy of Sciences* 405–422.
- (113) Graenecher, C., and Sallmann, R., (1939) Cellulose solutions and process of making same. US 2179181 A, submitted on April 1, 1937, published on November 7, 1939. Accessed on November 10, 2014. Available from: <http://www.google.com/patents/US2179181>.
- (114) Ventura, S. P. M., Gonçalves, A. M. M., Sintra, T., Pereira, J. L., Gonçalves, F., and Coutinho, J. A. P. (2013) Designing ionic liquids: the chemical structure role in the toxicity. *Ecotoxicology (London, England)* 22, 1–12.
- (115) Zafarani-Moattar, M. T., Hamzehzadeh, S., and Nasiri, S. (2011) A new aqueous biphasic system containing polypropylene glycol and a water-miscible ionic liquid. *Biotechnology Progress* 28, 146–156.
- (116) Du, Z., Yu, Y.-L., and Wang, J.-H. (2007) Extraction of proteins from biological fluids by use of an ionic liquid/aqueous two-phase system. *Chemistry (Weinheim an der Bergstrasse, Germany)* 13, 2130–2137.
- (117) Sigma-Aldrich (2005) Enabling Technologies Ionic Liquids. Accessed on November 23, 2014; Available from: https://www.sigmaaldrich.com/content/dam/sigmaaldrich/docs/Aldrich/Brochure/al_chemfile_v5_n6.pdf.
- (118) Manzer, L. E., and Parshall, G. W. (1976) Lewis acid adducts of trans-hydrocyanobis(triethylphosphine)platinum. *Inorganic Chemistry Journal* 15, 3114–3116.
- (119) Fraser, K. J., and MacFarlane, D. R. (2009) Phosphonium-Based Ionic Liquids: An Overview. *Australian Journal of Chemistry* 62, 309–321.
- (120) Bradaric, C. J., Downard, A., Kennedy, C., Robertson, A. J., and Zhou, Y. (2003) Industrial preparation of phosphonium ionic liquids. *Green Chemistry* 5, 143–152.
- (121) Chowdhury, S., Mohan, R. S., and Scott, J. L. (2007) Reactivity of ionic liquids. *Tetrahedron* 63, 2363–2389.
- (122) Gutowski, K. E., Broker, G. A., Willauer, H. D., Huddleston, J. G., Swatloski, R. P., Holbrey, J. D., and Rogers, R. D. (2003) Controlling the aqueous miscibility of ionic liquids: aqueous biphasic systems of water-miscible ionic liquids and water-structuring salts for recycle, metathesis, and separations. *Journal of the American Chemical Society* 125, 6632–6633.
- (123) Pereira, M. M., Pedro, S. N., Quental, M. V., Lima, Á. S., Coutinho, J. A. P., and Freire, M. G. (2015) Enhanced extraction of bovine serum albumin with aqueous biphasic systems of phosphonium- and ammonium-based ionic liquids. *Journal of Biotechnology* 206, 17–25.
- (124) Gupta, B. S., Taha, M., and Lee, M.-J. (2013) Interactions of bovine serum albumin with biological buffers, TES, TAPS, and TAPSO in aqueous solutions. *Process Biochemistry* 48, 1686–1696.
- (125) Ferguson, W. J., Braunschweiger, K. I., Braunschweiger, W. R., Smith, J. R., McCormick, J. J., Wasmann, C. C., Jarvis, N. P., Bell, D. H., and Good, N. E. (1980) Hydrogen ion buffers for biological research. *Analytical Biochemistry* 104, 300–310.

- (126) Lee, D., Redfern, O., and Orengo, C. (2007) Predicting protein function from sequence and structure. *Nature Reviews. Molecular Cell Biology* 8, 995–1005.
- (127) Patel, R., Kumari, M., and Khan, A. B. (2014) Recent advances in the applications of ionic liquids in protein stability and activity: A review. *Applied Biochemistry and Biotechnology* 172, 3701–3720.
- (128) Ward, W., and Swiatek, G. (2009) Protein Purification. *Current Analytical Chemistry* 5, 85–105.
- (129) Aguilar, O., Albitar, V., Serrano-Carreón, L., and Rito-Palomares, M. (2006) Direct comparison between ion-exchange chromatography and aqueous two-phase processes for the partial purification of penicillin acylase produced by *E. coli*. *Journal of Chromatography B: Analytical Technologies in the Biomedical and Life Sciences* 835, 77–83.
- (130) Domínguez-Pérez, M., Tomé, L. I. N., Freire, M. G., Marrucho, I. M., Cabeza, O., and Coutinho, J. A. P. (2010) (Extraction of biomolecules using) aqueous biphasic systems formed by ionic liquids and aminoacids. *Separation and Purification Technology* 72, 85–91.
- (131) Taha, M., e Silva, F. A., Quental, M. V., Ventura, S. P. M., Freire, M. G., and Coutinho, J. A. P. (2014) Good's buffers as a basis for developing self-buffering and biocompatible ionic liquids for biological research. *Green Chemistry* 16, 3149–3159.
- (132) Quental, M. V. (2014) Application of ionic liquids in the concentration of cancer biomarkers. Chemistry Department - University of Aveiro.
- (133) Mourão, T., Cláudio, A. F. M., Boal-Palheiros, I., Freire, M. G., and Coutinho, J. A. P. (2012) Evaluation of the impact of phosphate salts on the formation of ionic-liquid-based aqueous biphasic systems. *Journal of Chemical Thermodynamics* 54, 398–405.
- (134) Merchuk, J. C., Andrews, B. A., and Asenjo, J. A. (1998) Aqueous two-phase systems for protein separation. Studies on phase inversion. *Journal of Chromatography B: Biomedical Sciences and Applications* 711, 285–293.
- (135) Ivanisenko, V. A., Demenkov, P. S., Ivanisenko, T. V., and Kolchanov, N. A. (2011) Protein Structure Discovery: A Software Package to Computer Proteomics Tasks (Review). *Russian Journal of Bioorganic Chemistry* 37, 17–29.
- (136) Pegram, L. M., and Record, M. T. (2007) Hofmeister salt effects on surface tension arise from partitioning of anions and cations between bulk water and the air-water interface. *Journal of Physical Chemistry B* 111, 5411–5417.
- (137) Bridges, N. J., Gutowski, K. E., and Rogers, R. D. (2007) Investigation of aqueous biphasic systems formed from solutions of chaotropic salts with kosmotropic salts (salt-salt ABS). *Green Chemistry* 9, 177–183.
- (138) Ventura, S. P. M., Neves, C. M. S. S., Freire, M. G., Marrucho, I. M., Oliveira, J., and Coutinho, J. A. P. (2009) Evaluation of Anion Influence on the Formation and Extraction Capability of Ionic-Liquid-Based Aqueous Biphasic Systems. *Journal of Physical Chemistry* 113, 9304–9310.
- (139) Pei, Y., Wang, J., Wu, K., Xuan, X., and Lu, X. (2009) Ionic liquid-based aqueous two-phase extraction of selected proteins. *Separation and Purification Technology* 64, 288–295.
- (140) Taha, M., Quental, M. V., Correia, I., Freire, M. G., and Coutinho, J. A. P. (2015) Extraction and stability of bovine serum albumin (BSA) using cholinium-based Good's buffers ionic liquids. *Process Biochemistry* 50, 1158–1166.
- (141) Taylor, P., Fedotoff, O., Mikheeva, L. M., Chait, A., Uversky, V. N., and Boris, Y. (2012) Influence of Serum Proteins on Conformation of Prostate-Specific Antigen Influence of Serum Proteins on

Conformation of Prostate-Specific Antigen. *Journal of Biomolecular Structure and Dynamics* 29, 1051–1064.

(142) Healy, D. A., Hayes, C. J., Leonard, P., McKenna, L., and O’Kennedy, R. (2007) Biosensor developments: application to prostate-specific antigen detection. *Trends in Biotechnology* 25, 125–131.

(143) Passos, H., Sousa, A. C. A., Pastorinho, M. R., Nogueira, A. J. A., Rebelo, L. P. N., Coutinho, J. A. P., and Freire, M. G. (2012) Ionic-liquid-based aqueous biphasic systems for improved detection of bisphenol A in human fluids. *Analytical Methods* 4, 2664–2667.

(144) Rodrigues, G., Warde, P., Pickles, T., Crook, J., Brundage, M., Souhami, L., and Lukka, H. (2012) Pre-treatment risk stratification of prostate cancer patients: A critical reviews. *Canadian Urological Association Journal* 6, 121–127.

(145) Su, S.-B., Chuen, T., Poon, W., and Thongboonkerd, V. (2013) Human Body Fluid. *BioMed Research International* 2013, 2–4.

(146) Porstmann, B., Jung, K., Schmechta, H., Evers, U., Pergande, M., Porstmann, T., Kramm, H. J., and Krause, H. (1989) Measurement of lysozyme in human body fluids: comparison of various enzyme immunoassay techniques and their diagnostic application. *Clinical biochemistry* 22, 349–355.

(147) Comabella, M., and Montalban, X. (2014) Body fluid biomarkers in multiple sclerosis. *The Lancet Neurology* 13, 113–126.

(148) Selvin, E., Steffes, M. W., Zhu, H., Matsushita, K., Wagenknecht, L., Pankow, J., Coresh, J., and Brancati, F. L. (2010) Glycated hemoglobin, diabetes, and cardiovascular risk in nondiabetic adults. *The New England journal of Medicine* 362, 800–811.

(149) Taylor, E. N., and Curhan, G. C. (2006) Body Size and 24-Hour Urine Composition. *American Journal of Kidney Diseases* 48, 905–915.

(150) Kshirsagar, B., and Wiggins, R. C. (1986) A map of urine proteins based on one-dimensional SDS-polyacrylamide gel electrophoresis and Western blotting using one microliter of unconcentrated urine. *International journal of clinical chemistry* 158, 13–22.

(151) PRIMA (2013) Prostate test - PSA. Accessed on July 1, 2015; Available from: <https://primahometest.com/prostate-test>.

(152) Craig Medical distribution INC (2012) Drug testing and screening. Accessed on July 1, 2014; Available from: [http://www.craigmedical.com/products.htm#NEW...The\(PSA\)](http://www.craigmedical.com/products.htm#NEW...The(PSA)).

(153) Saúde, I. N. de. (2011) Censos 2011-População por grupo estário.

(154) Constantinou, J., and Feneley, M. R. (2006) PSA testing: an evolving relationship with prostate cancer screening. *Prostate cancer and prostatic diseases* 9, 6–13.

Appendix A

BLitz® Pro system calibration curve

A.1. BLItz Pro® system calibration curve for PSA

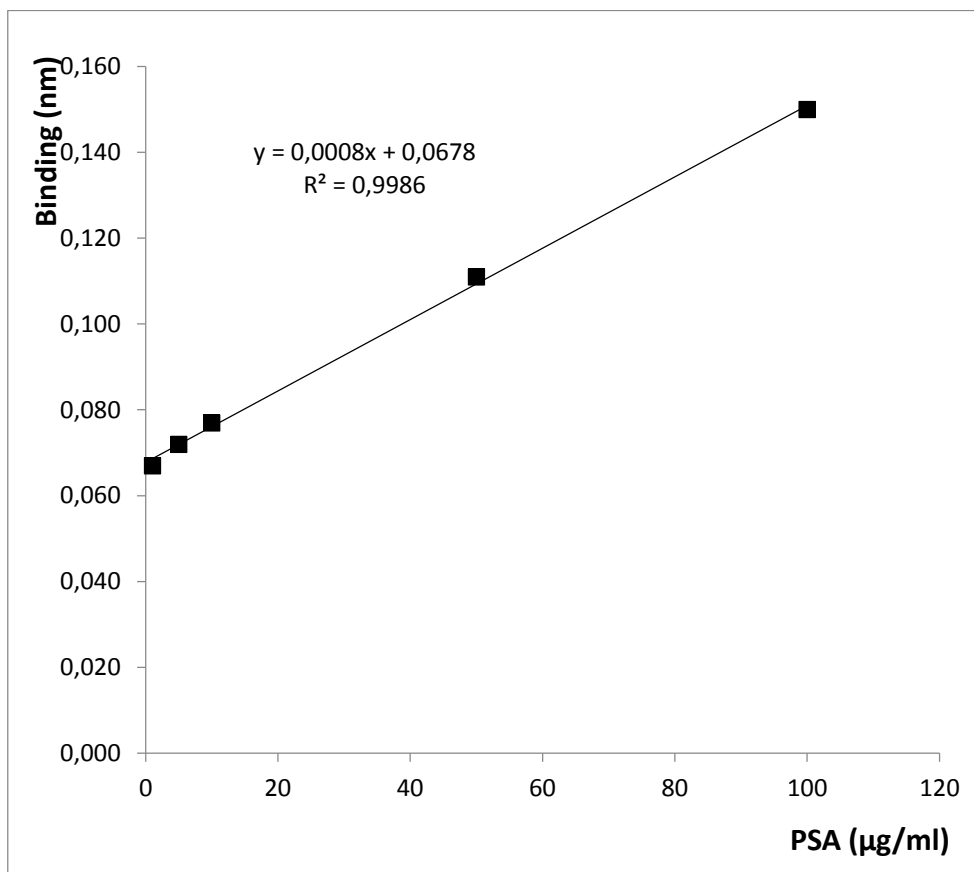


Figure A.1. Calibration curve for PSA in aqueous solution.

Appendix B

Experimental binodal data

B.1. Experimental Binodal Data for the Systems Composed of IL + salt + H₂O.

Table B.1.4. Experimental weight fraction data for the binodal curve of the systems composed of [P₄₄₄₄][GB] (1) + K₃C₆H₅O₇ (2) at (25 ± 1) °C

[P ₄₄₄₄][TES] <i>M_w</i> = 487.69 g.mol ⁻¹		[P ₄₄₄₄][MES] <i>M_w</i> = 453.66 g.mol ⁻¹		[P ₄₄₄₄][HEPES] <i>M_w</i> = 496.72 g.mol ⁻¹	
100 <i>w</i> ₁	100 <i>w</i> ₂	100 <i>w</i> ₁	100 <i>w</i> ₂	100 <i>w</i> ₁	100 <i>w</i> ₂
76.7069	0.9602	62.3717	1.9534	79.0463	1.2140
70.8659	1.3572	55.0746	3.0687	57.3815	3.8233
68.2725	2.1660	46.1457	5.2053	54.3893	4.3607
65.1872	2.4366	38.9888	7.5466	52.9863	4.8784
61.7348	2.9165	35.5324	9.4461	51.0045	5.2142
59.3491	3.8172	32.1736	10.4337	49.7780	5.7866
57.4007	4.3772	29.2351	12.1770	48.5506	6.4546
55.1249	4.6711	25.0058	14.2196	46.8489	6.7966
51.1784	5.6150	24.3730	14.9448	45.8407	7.2063
48.0776	6.7585	23.4465	15.5913	44.9174	7.5423
45.4535	7.5826	22.7324	15.9857	43.9395	8.0321
44.3554	8.0084	22.1010	16.2701	43.0836	8.3337
43.2974	8.3144	21.0463	17.2067	42.2405	8.6264
41.4746	9.2730	20.1913	17.4856	41.0589	9.4620
39.3799	10.1176	19.8753	17.7077	40.2864	9.7631
37.7142	10.7034	19.2960	18.0770	39.6085	9.9950
36.7566	11.0932	18.8178	18.3213	38.7789	10.4148
35.7102	11.6940	18.4771	18.7802	38.0856	10.7895
34.4566	12.4919	17.9601	19.0542	37.1480	11.5128
33.1800	12.8464	17.5589	19.3400	36.5145	11.8715
32.2965	13.2737	17.1589	19.5134	35.9247	12.1013
31.3356	13.8476	16.7271	19.9010	35.0893	12.6849
30.8074	13.9839	16.3047	20.0070	34.5783	12.8815
29.8842	14.5095	15.9311	20.2144	33.9887	13.0928
29.4592	14.5563	15.7730	20.5767	33.2017	13.6317
28.6566	14.9631	15.0549	21.1613	32.7173	13.8141
27.9593	15.3925	14.7790	21.3413	31.9773	14.3907
27.2225	15.8238	14.4682	21.4879	31.5401	14.5988

26.4220	15.9225	14.0210	21.8603	31.0895	14.7894
25.5657	16.3281	13.5973	22.2147	30.4952	15.2897
24.2081	16.8379	13.3496	22.4360	30.0682	15.4687
23.8472	16.9281	13.1172	22.5457	29.4377	15.9744
23.2970	17.3304	12.8557	22.7482	29.0323	16.1842
22.9946	17.3495	12.6174	22.8941	28.4782	16.6043
22.3836	17.7987	12.3314	23.0981	28.1064	16.7660
21.6036	18.2128	12.1281	23.2549	27.5444	17.2465
21.3292	18.2571	11.9372	23.4139	27.1562	17.4312
20.8961	18.5831	11.6437	23.7911	26.7717	17.6314
20.4677	18.8857	11.4069	23.8702	26.2562	18.0963
20.2223	18.8879	11.1862	24.1448	25.9124	18.2348
19.7738	19.1910	10.8123	24.4067	25.5547	18.4400
19.2462	19.3739	10.6356	24.5665	25.0862	18.8429
18.9256	19.5577	10.2575	25.3191	24.7562	19.0434
18.6499	19.7752	10.0548	25.3267	24.4325	19.1928
18.2835	20.0163	9.9013	25.4396	24.1295	19.3462
17.6456	20.3441	9.7624	25.5814	23.8514	19.4689
17.4407	20.3563	9.4916	25.9226	23.5605	19.6638
17.1177	20.6181	9.3455	26.1029	23.1424	20.0931
16.9670	20.7616			22.8762	20.2151
16.5536	21.1438			22.5964	20.4074
16.1634	21.2496			22.3685	20.5117
15.9537	21.3318			22.0924	20.6744
15.7829	21.3693			21.7425	21.0080
15.5580	21.3169			21.4919	21.1585
15.1395	21.5924			21.2324	21.3295
14.9734	21.6647			20.9928	21.5054
14.6763	21.9494			20.7564	21.6458
14.3540	22.0933			20.5049	21.8034
14.2098	22.1238			20.1739	22.1712
14.0587	22.1748			19.9540	22.3240
13.8147	22.4282			19.7418	22.4395
13.4649	22.6969			19.5269	22.5751
13.3046	22.7489			19.3328	22.6994

13.0039	23.1101	19.1294	22.8101
12.8723	23.1770	18.9272	22.9416
12.6612	23.3747	18.7374	23.0451
12.3640	23.5577	18.5586	23.1337
12.1186	23.6864	18.3699	23.2760
11.8639	23.8066	18.1792	23.3980
11.6571	23.9221	17.9884	23.5619
11.4390	24.0440	17.8004	23.7110
11.1471	24.3031	17.6390	23.8141
10.9409	24.3849	17.4725	23.8990
10.6828	24.5823	17.3051	23.9930
10.4964	24.6401	17.0633	24.2733
10.2787	24.7997	16.9135	24.3400
9.9800	25.0353	16.7573	24.4280
		16.6179	24.4931
		16.4627	24.5548
		16.3114	24.6708
		16.1609	24.8339
		16.0083	24.9827
		15.8933	25.0836
		15.7494	25.1729
		15.6078	25.2723
		15.4442	25.3540
		15.2482	25.4261
		14.9644	25.5705
		14.7844	25.5726
		14.6638	25.6354
		14.5404	25.7313
		14.4274	25.7960
		14.3273	25.8698
		14.2180	25.9580
		14.1053	26.0754
		14.0054	26.1412
		13.9034	26.2410
		13.6752	26.4403

13.4380	26.5215
13.3321	26.6150
13.1223	26.9538
13.0212	27.0392
12.9296	27.0986
12.8243	27.1788
12.7332	27.2597
12.6435	27.3055
12.5550	27.3834
12.4512	27.4816
12.3510	27.5601
12.2638	27.6426
12.1809	27.7100
12.0351	27.5498
11.9108	27.5261
11.8294	27.6381
11.7417	27.7355
11.6583	27.7854
11.5681	27.7946
11.4415	27.9978
11.3621	28.0604
11.2111	28.1925
11.1332	28.2368
11.0554	28.3165
10.9783	28.3645
10.9028	28.4271
10.8242	28.4983
10.7550	28.5507
10.6903	28.5929
10.5568	28.6798
10.4514	28.8405
10.3869	28.8751
10.3099	28.9227
10.1744	29.0601
10.1046	29.1099

9.9960	29.2017
9.9331	29.2384
9.8652	29.2873
9.7744	29.4242
9.7142	29.4694
9.6508	29.5226
9.5954	29.5549
9.5060	29.7251
9.3880	29.7914
9.2867	29.8751
9.1271	29.8189
9.0140	29.8419

Table B.1.2 Experimental weight fraction data for the binodal curve of the systems composed of [P₄₄₄₄][GB] (1) + K₃C₆H₅O₇ (2) at (25 ± 1) °C.

[P ₄₄₄₄][CHES]		[P ₄₄₄₄][Tricine]	
<i>M_w</i> = 465.71 g.mol ⁻¹		<i>M_w</i> = 437.59 g.mol ⁻¹	
100 <i>w</i> ₁	100 <i>w</i> ₂	100 <i>w</i> ₁	100 <i>w</i> ₂
44.7594	3.9161	77.5111	1.3976
41.7133	4.7445	69.0398	3.2813
39.3281	5.3443	60.3936	4.6040
37.5478	5.8334	45.3106	10.9072
36.2173	6.3403	43.2973	12.0387
34.4777	6.6717	41.7906	12.7137
33.4844	7.0417	40.7737	13.4039
32.3207	7.4695	39.4115	13.8630
30.9793	7.8335	38.4819	14.5159
29.7327	8.1674	37.5246	15.0688
28.7294	8.3923	36.6356	15.6331
27.9449	8.7909	35.8293	16.1561
27.3862	9.1807	35.0777	16.6438
26.6892	9.5276	34.3202	17.1529
25.8564	9.6746	33.6512	17.6142
25.2516	10.0156	32.9250	18.0855
24.5309	10.2402	32.2737	18.5240
23.9560	10.6026	31.5877	18.9671
23.3246	10.7184	30.9769	19.3892
22.7933	10.8318	30.4459	19.6828
22.4552	11.1649	29.8602	20.0574
21.9599	11.2770	29.3288	20.4102
21.4739	11.4556	28.7964	20.7798
21.0590	11.7289	27.9689	21.6115
20.5271	11.9246	27.5021	21.9881
20.0348	12.0460	27.0526	22.2898
19.6862	12.2523	26.6139	22.5766
19.2679	12.3565	26.1790	22.8039
18.9461	12.5667	25.5152	23.4747
18.5846	12.6653	25.1113	23.7524
18.2738	12.8611	24.7146	23.9830

17.9125	12.9048	24.2941	24.1475
17.6078	13.1377	23.9505	24.3704
17.2418	13.1908	23.4108	24.9376
16.9497	13.3802	23.0802	25.1276
16.5959	13.5326	22.7777	25.3079
16.2658	13.6967	21.9759	25.9534
15.9372	13.8345	21.6897	26.1745
15.6394	13.9743	21.2422	26.6289
15.3494	14.1216	20.9856	26.7786
15.0804	14.1880	20.7143	26.9484
14.8653	14.1273	20.2641	27.4060
14.6160	14.1969	20.0440	27.4713
14.3627	14.2270	19.6646	27.8548
14.1691	14.4094	19.4356	28.0177
13.9297	14.5667	19.2146	28.1671
13.7059	14.6082	18.8964	28.4463
13.4937	14.7288	18.6063	28.7423
13.3214	14.8631	18.3036	29.0215
13.0987	14.9625	18.1074	29.1358
12.8854	15.0692	17.7775	29.4780
12.6897	15.1054	17.5843	29.5748
12.5331	15.2312	17.4062	29.7475
12.3603	15.2814	17.1936	29.8764
12.1796	15.4112	16.9327	30.1473
11.9638	15.3512	16.6746	30.3763
11.8745	15.5212	16.5059	30.5192
11.7315	15.6061	16.2517	30.7703
11.6065	15.7144	16.0879	30.8671
11.4715	15.7766	15.8639	31.0559
11.3333	15.8107	15.6137	31.2773
11.2234	15.8936	15.3613	31.5346
11.1094	15.9354	15.2180	31.5846
11.0086	16.0450	14.9933	31.7975
10.8894	16.0704	14.7745	31.9996
10.7829	16.1802	14.5414	32.2434

10.5886	16.1623	14.2661	32.4125
10.4981	16.2169	14.0897	32.6000
10.3988	16.3194	13.9659	32.6448
10.3033	16.3790	13.7769	32.8457
10.1787	16.4264	13.6422	32.9745
10.0473	16.6499	13.4665	33.1494
9.9031	16.6303	13.2741	33.2291
9.8062	16.6971	13.0964	33.4211
9.7334	16.7589	12.8799	33.7079
9.6460	16.8281	12.7729	33.7572
9.5454	16.8790	12.4852	33.9822
9.4609	16.9587	12.0250	34.0183
9.3665	16.9371	11.8725	34.1810
9.2806	17.0041	11.7110	34.3599
9.1653	17.1692	11.5823	34.4851
9.0362	17.3527	11.4282	34.6641
8.8758	17.4518	11.3124	34.7944
		11.1593	34.8316
		11.0294	35.0037
		10.8889	35.1658
		10.8121	35.1672
		10.7023	35.3094
		10.4568	35.5745

Appendix C

Experimental data for CF

C.1. Experimental data for the concentration factors in ABS composed of IL + salt + H₂O.

Table C.1.5. Experimental data for the CF of the systems composed of [P₄₄₄₄][GB] + K₃C₆H₅O₇ + water at (25 ± 1) °C

[P ₄₄₄₄][MES]							
Theoretical <i>CF</i>	5	20	50	100	150	200	250
w IL / g	0.1538	0.8746	0.9034	0.4669	0.608	0.3206	0.2578
w Salt/ g	0.4907	11.1844	28.8004	29.0330	58.2693	40.8537	40.8927
w H ₂ O/ g	0.3556	7.9404	20.3765	20.5313	41.1231	28.8267	28.8521
w Top/ g	0.0783	0.4023	0.4108	0.2064	0.2603	0.1476	0.1166
w Bottom/ g	0.8099	18.7884	48.9843	46.2209	98.9366	69.2375	69.1359
Real <i>CF</i>	4.54	19.74	49.60	99.47	157.98	195.30	247.45

[P ₄₄₄₄][CHES]							
Theoretical <i>CF</i>	5	20	50	100	150	200	250
w IL / g	0.1546	0.8718	0.896	0.4543	0.3079	0.317	0.2541
w Salt/ g	0.4918	11.2273	28.8647	29.1384	29.2327	40.9848	41.0242
w H ₂ O/ g	0.3553	7.9012	20.2728	20.4156	20.4793	28.7043	28.7221
w Top/ g	0.0855	0.4322	0.3842	0.2101	0.1319	0.1406	0.1174
w Bottom/ g	0.8246	17.8944	48.8542	49.2884	49.1391	68.4552	69.6864
Real <i>CF</i>	4.16	18.28	52.77	97.17	155.26	204.16	244.65

[P ₄₄₄₄][HEPES]							
Theoretical <i>CF</i>	5	20	50	100	150	200	250
w IL / g	0.1590	0.8554	0.8861	0.4548	0.6189	0.3307	0.2691
w Salt/ g	0.4999	11.3395	29.164	29.4442	57.0792	41.4222	41.4620
w H ₂ O/ g	0.3530	7.8059	19.95	20.1002	40.3018	28.2491	28.273
w Top/ g	0.0730	0.4038	0.3922	0.2042	0.264	0.142	0.1119
w Bottom/ g	0.7998	18.8912	48.7235	49.3160	98.9670	68.8742	69.4209
Real <i>CF</i>	4.84	19.33	50.87	98.43	152.66	198.94	252.66

[P ₄₄₄₄][TES]							
Theoretical <i>CF</i>	5	20	50	100	150	200	250
w IL / g	0.1565	0.6673	0.9148	0.4615	0.3091	0.3267	0.2603
w Salt/ g	0.4839	8.2646	28.3289	28.6225	28.7143	40.266	40.3037
w H ₂ O/ g	0.3588	6.0672	20.7886	20.9159	20.9797	29.413	29.4364
w Top/ g	0.0801	0.3159	0.4201	0.2118	0.1394	0.1438	0.115
w Bottom/ g	0.7982	14.2206	48.4881	49.3160	49.1121	67.8044	69.5518
Real <i>CF</i>	4.48	19.21	49.48	98.75	150.50	204.54	255.97

	[P ₄₄₄₄][Tricine]						
Theoretical <i>CF</i>	5	20	50	100	150	200	250
w IL / g	0.1582	0.9758	1.1577	0.7204	0.5731		
w Salt/ g	0.4862	11.1054	28.575	28.8193	28.0000		
w H ₂ O/ g	0.3542	7.931	20.3498	20.4447	20.5376		
w Top/ g	0.0800	0.4147	0.4138	0.2111	0.1426		
w Bottom/ g	0.7948	19.4130	49.1102	49.3373	49.3575		
Real <i>CF</i>	4.43	19.12	49.18	96.85	144.02		

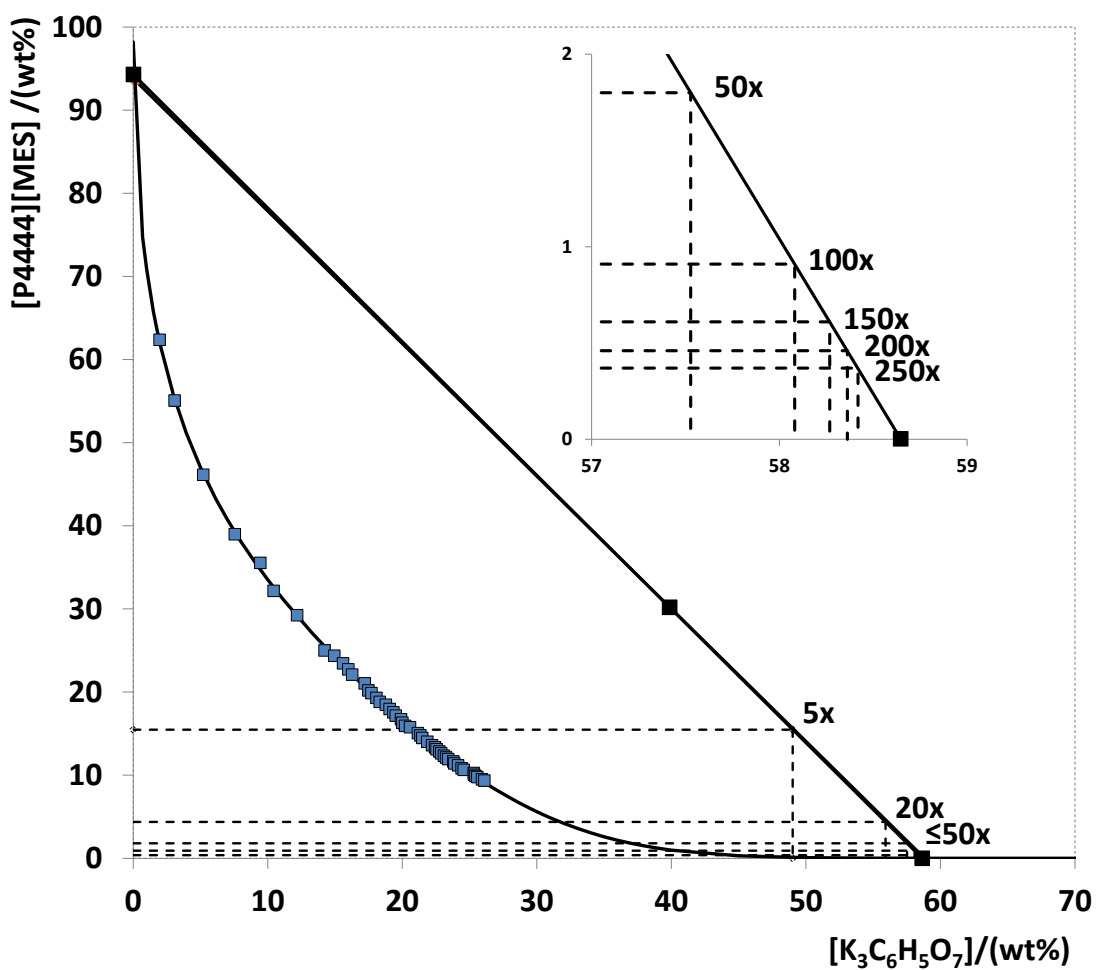


Figure C.1.6. Experimental data for *CF* of the systems composed of [P₄₄₄₄][GB] + K₃C₆H₅O₇ + water at (25 ± 1) °C

